Characterizing the Duck NLRP3 Inflammasome

by

Michelle Lee

A thesis submitted in partial fulfillment of the requirements for the degree of

Master of Science

in

Physiology, Cell, and Developmental Biology

Department of Biological Sciences
University of Alberta

Abstract

Ducks, as the natural reservoir host of influenza A virus (IAV), do not exhibit the same detrimental symptoms when infected by IAV as other susceptible host species, such as chickens and humans. A dysregulated NLRP3 inflammasome response activated by IAV has been linked to severe host outcomes, potentially leading to death. It is not known whether dampening of the NLRP3 inflammasome is a mechanism by which ducks avoid damage due to IAV. Here, I have cloned the duck NLRP3 inflammasome components, assessed their function, and examined their expression in duck tissues following an IAV infection. I cloned and expressed recombinant proteins of the duck NLRP3 inflammasome to examine their interactions *in vitro* using confocal microscopy and immunoprecipitation. I created expression constructs for NLRP3, Caspase-1, and Interleukin-1beta. I was unable to identify ASC, the adaptor molecule apoptosis-associated speck-like protein containing a CARD, one component of the inflammasome, suggesting that the NLRP3 inflammasome may be incomplete in ducks. To activate the duck NLRP3 inflammasome and examine whether the proteins interacted, I used polyinosinic: polycytidylic acid (poly I:C) and nigericin, a known NLRP3 inflammasome agonist. qPCR and RNA-seq were used to investigate the priming step of the duck NLRP3 inflammasome and how it differed from the priming responses of other species. I found little evidence that the TLR3 transcriptional priming pathway that is activated by poly I:C triggered the downstream NLRP3 inflammasome. This suggests that a lower level of activity is exhibited by the NLRP3 inflammasome during an IAV infection in ducks. This may be a mechanism by which the natural reservoir host of IAV could avoid detrimental damage induced by hyper-inflammation and cytokine storms.

Acknowledgments

I would like to first thank my supervisor, Dr. Katharine Magor, for all her support and guidance throughout the years. Thank you, Kathy, for providing me with all the tools that would allow me to succeed. I would also like to thank you for igniting my interest in immunology and virology all those years ago when I was in your Immunology 200 class during my undergrad degree. Your virology section for that class was easily one of my favourite sections of classes that I have taken. I have been able to develop both my research skills as well as professional skills during my time in your lab and found that I took great enjoyment in working in the lab. Thank you for allowing me the opportunity to develop more and discover more, both as a person and a scientist.

Thank you to my committee members, Dr. James Stafford, and Dr. Patrick Hannington for all of your time and constructive feedback. Thank you for providing me with suggestions and advice and answering my questions. Both of you have been endlessly helpful and supportive and I am immensely grateful.

Thank you to all the members of the Magor lab, for without your friendship and support, this entire process would have been significantly less fun and much more difficult. Thank you to Ximena for teaching me many of the things I know, as well as learning many new things alongside me, and being a never-ending source of joy in the lab. Thank you to Danyel, for getting me started in the lab and giving me my first real taste of what it was to work in a lab setting as well as imparting many of your good lab habits on me. Thank you to Lee, for being incredibly patient with me and helping me with so many different things like the transcriptome and confocal imaging. Thank you to Eric, Dexter, Adam, Doaa, Aradana, Yemaya, and anyone

else that I may have missed, who made my experience these last few years as a graduate student infinitely more enjoyable.

Thank you to my funding sources, I was supported financially by the Department of Biological Sciences, GSA, FGSR, and CIHR during the course of this degree.

Lastly, thank you to my family. My parents who have been endlessly supportive of me pursuing a degree in the sciences, thank you for encouraging me to do whatever I wanted with my degree and academic career. Thank you, Clara, for all your editing help and time listening to my presentations. Thank you, Lucy, the best dog that anyone could ever ask for who made sure I would leave the house at semi-regular intervals daily for my wellbeing. I could not have done this without any of the people mentioned here and I hope that I have made all of you proud. Thank you for your support.

Table of Contents

List of Tables

List of Figures

Abbreviations

A549	Adenocarcinoma human alveolar basal epithelial cells
AIM2	Absent in melanoma
ASC	Apoptosis-associated speck-like protein containing a CARD
BIR	Baculovirus inhibitor of apoptosis protein repeats
BLAST	Basic local alignment search tool
BMDM	Bone marrow-derived macrophages
BSA	Bovine serum albumin
CARD	Caspase activation and recruitment domain
CASP1	Caspase-1
CIITA	Class II major histocompatibility complex transactivator
CpG	5′-C-phosphate-G-3′
DAMP	Damage associated molecular pattern
DEF	Duck embryonic fibroblasts
DF-1	Douglas Foster-1 immortalized chicken embryonic fibroblasts derived from an East Lansing line
DMEM	Dulbecco's modified eagle medium
dsDNA	Double-stranded DNA

dsRNA	Double-stranded RNA
FBS	Fetal bovine serum
FIIND	Function to find domain
FITC	Fluorescein isothiocyanate
GAPDH	Glyceraldehyde-3-phosphate dehydrogenase
GSDMD	Gasdermin-D
GSDME	Gasdermin-E
GST	Glutathione-S transferase
HEK293T	Immortalized human embryonic kidney cells with a large SV40 T antigen
HeLa	Human cervical cancer cell line
HIN	Hematopoietic expression, interferon-inducible nature, and nuclear localization
HPAI	Highly pathogenic avian influenza
IAV	Influenza A virus
IBDV	Infectious bursal disease virus
IFI16	Gamma interferon-inducible protein 16
IFIT5	Interferon-induced protein with tetratricopeptide repeats 5
IFN	Interferon

IL	Interleukin
IPAF	ICE-protease activating factor
IRF1	Interferon regulatory factor 1
JNK1	c-Jun N-terminal kinase 1
LeTx	Lethal toxin
LGP2	Laboratory of genetics and physiology 2
LPS	Lipopolysaccharide
LRR	Leucine rich repeat
MDA5	Melanoma differentiation-associated protein 5
MDP	Muramyl dipeptide
Meso-DAP	Meso-diaminopimelic acid
MOI	Multiplicity of infection
mtDNA	Mitochondrial DNA
MyD88	Myeloid differentiation factor 88
NAIP	NLR family, apoptosis inhibitory protein
NDV	Newcastle disease virus
NF-κB	nuclear factor kappa light chain enhancer of activated B cells

NK cell	Natural killer cell
NLR	NOD-like receptor
NLRC4	NLR family CARD domain-containing protein 4
NLRC5	NLR family CARD domain-containing protein 5
NLRP1	NLR family pyrin domain containing 1
NLRP3	NLR family pyrin domain containing 3
NLRP6	NLR family pyrin domain containing 6
NOD	Nucleotide oligomerization domain
NOD1	Nucleotide-binding oligomerization domain-containing protein 1
NOD2	Nucleotide-binding oligomerization domain-containing protein 2
ox-mtDNA	Oxidated mitochondrial DNA
P2X7	P2X purinoceptor 7
PAMP	Pathogen associated molecular patterns
PCR	Polymerase chain reaction
PFA	Paraformaldehyde
Poly I:C	Polyinosinic: polycytidylic acid
PRR	Pattern recognition receptor

PYHIN	Pyrin and HIN domain
qPCR	Quantitative polymerase chain reaction
RIG-I	Retinoic acid-inducible gene I
RLR	RIG-I like receptor
SARS	Severe acute respiratory syndrome
SDS-PAGE	SDS polyacrylamide gel electrophoresis
ssDNA	Single-stranded DNA
ssRNA	Single-stranded RNA
T3SS	Type III secretion system
Th1	T helper cell type 1
Th2	T helper cell type 2
TLR	Toll-like receptor
WCL	Whole cell lysate

Chapter 1. Introduction

1.1 Innate Immunity

Host survival depends on an effective immune system that recognizes pathogens and effectively eliminates threats that could otherwise lead to adverse effects or fatal outcomes. The host's survival is dependent on the innate immune response to control the spread of the pathogen during the first few days of infection until the adaptive immune system is effectively recruited. Pathogens that can bypass physical barriers, like the skin or mucous membranes, and enter the host are met with a barrage of innate immune receptors found on a multitude of immune cells like macrophages as well as non-immune cells like fibroblasts. These innate immune receptors are called pattern recognition receptors (PRRs) and recognize specific Pathogen Associated Molecular Patterns (PAMPs) (reviewed by Mogensen, 2009). There are many different types of PRRs, from toll-like receptors (TLRs), RIG-I-like receptors (RLRs), and NOD-like receptors (NLRs). These PRRs have been evolutionarily selected to recognize PAMPs, which exist on all pathogens. After recognition and subsequent binding of these PAMPs, a quick response by the innate immune system occurs that is both general and nonspecific but still tailored to that specific PAMP and pathogen. Infection with a pathogen can trigger inflammation, the production of different cytokines or interferons, recruitment of immune cells to the area of infection, or even cell death.

In addition to detecting exogenous signals from PAMPs, the innate immune system is also capable of detecting endogenous signals in the form of Damage Associated Molecular Patterns (DAMPs). These DAMPs activate the innate immune system in response to damaged or

dying cells by binding to PRRs. DAMPs can be intracellular components like heat-shock proteins, cellular DNA, or histones, or they can be extracellular components like fibrinogen, hyaluronan, uric acid, or ATP (Mariathasan et al. 2006; Martinon et al. 2006; Muruve et al. 2008). Like PAMPs, the response to a DAMP is dictated by the PRR that recognizes it and is in turn activated.

1.1.1 Toll-like receptors

Toll-like receptors are integral membrane glycoproteins, present on the cell surface of many different cells as well as on the membrane of intracellular compartments within the cell. The N-terminal region of the TLR contains many leucine-rich repeats and is responsible for binding to the ligand-specific to each PRR while the C-terminal region is responsible for signaling (Bell et al. 2003). Due to widespread selective pressures, the TLR families are well conserved regardless of their diversified ligand recognizing motifs. For example, TLR2 binds lipopeptides, TLR3 binds double-stranded RNA (dsRNA), TLR4 binds lipopolysaccharides (LPS), TLR5 binds flagellin, and TLR7 through TLR9 bind nucleic acids. While there are species-specific variations, most vertebrates will have one TLR orthologue for each of these mentioned TLR families.

In a mammalian system, activation of a TLR by its ligand will trigger one of two known pathways: the MyD88-dependent pathway or the TRIF-dependent pathway. The TRIF-dependent pathway is used only by TLR3, TLR4. and TLR7-9. MyD88 and TRIF are both adaptor molecules that associate with activated TLR complexes and the ensuing signal cascade will activate the transcription factor NF-κB. NF-κB upregulates cellular processes that ultimately,

result in the synthesis and release of cytokines and chemokines. These chemokines and cytokines recruit immune cells like macrophages or neutrophils to the region of infection or damage to further the innate immune response (reviewed in Kawasaki and Kawai, 2014).

TLR2 is responsible for detecting lipoproteins and will complex with other TLRs (i.e., TLR1 or TLR6) to bind different types of lipoproteins (Aliprantis, 1999; Brightbill, 1999; Jin et al. 2007; Kang et al. 2009). Meanwhile, TLR4 binds LPS, and TLR5 binds flagellin (Hayashi et al. 2001; Kim et al. 2007). These TLRs are usually found on the cell surface, located optimally to detect the exogenous pathogens associated with these PAMPs. TLR3 which binds dsRNA (Liu et al. 2008), TLR7 and TLR8, both of which bind single-stranded RNA (ssRNA) (Heil et al. 2004; Hemmi et al. 2002), and TLR9 which binds unmethylated CpG sequences in DNA, are found within intracellular compartments (Bauer et al. 2001). They are positioned to ensure the detection of aberrant genetic material within a cell that would not be exposed in the extracellular environment.

Within avian species, there are differences when comparing their TLRs to mammalian TLRs. Among the different bird species that have been widely researched, TLR15 appears to be specific to birds. TLR15 recognizes structures from yeast and fungi but is distinct from the TLR2 family (Boyd et al. 2012). Another difference in the TLR system in many currently well-studied bird species is the deletion of TLR9 and in some species, like chickens and ducks, the gene for TLR8 has also been disrupted and is no longer functional (MacDonald et al. 2007; Philbin et al. 2005). TLR9 is important for detecting unmethylated CpG DNA and its loss in an organism could prove fatal. However, chicken TLR21 responds to unmethylated CpG DNA like that of TLR9 (Keestra et al. 2010). Based on amino acid sequences, TLR21 has low sequence similarity to mammalian TLR9, indicating that it is not evolutionary related but rather a functional

analogue. Additionally, TLR3 has been identified in many birds and can recognize RNA as well as poly I:C which can induce strong responses in ducks (M. Zhang et al. 2015; Karpala, Lowenthal, and Bean 2008). In ducks, the activity of TLR3 has been linked to antiviral responses (Pal, Pal, and Baviskar 2020; Zhang et al. 2015).

1.1.2 RIG-I-like receptors

RIG-I-like receptors (RLRs) are important cytosolic sensors of RNA. RLRs are RNA helicases that respond to viral RNA inside a cell (reviewed by Rehwinkel and Gack, 2020). Within this family of receptors, there are three different proteins: retinoic acid-inducible gene I (RIG-I), which the family is named after, melanoma differentiation-associated protein 5 (MDA5), and laboratory of genetics and physiology 2 (LGP2). Activation of the RLRs induces the expression of host antiviral genes as well as the production of type I interferons (IFNs) (reviewed by Onoguchi et al. 2011). IFNs create an antiviral state that inhibits viral replication within the infected cell as well as neighbouring cells. Generally, RLRs contain a DECH box helicase domain which binds to dsRNA and hydrolyzes ATP, and a carboxy-terminal domain which also assists in binding to RNA. Overall, these receptors can detect viral RNA. RIG-I and MDA5 both have two N-terminal caspase activation and recruitment domains (CARDs) which can induce further downstream signals. Meanwhile, LGP2, which does not have the CARD domains, is believed to serve regulatory functions instead (Saito et al. 2007).

RIG-I is a receptor that recognizes short pieces of RNA with a 5′ triphosphate group and a panhandle structure that is formed as a result of the 5′ and 3′ ends of the viral RNA base pairing with itself. MDA5 recognizes longer pieces of dsRNA and upon recognizing its ligand, forms

long RNA-associated filaments. Studies on LGP2, the lone RLR without an N-terminal CARD domain, have come to different conclusions on its function. Satoh *et al.* (2010) found that LGP2 positively regulated the activities of RIG-I and MDA5 while Venkataraman *et al.* (2007) suggested that LGP2 negatively regulated the activities of RIG-I and MDA5. LGP2 has also been shown to inhibit DICER, an endoribonuclease, so that RNA cannot be processed into small RNA and micro-RNA (van der Veen et al. 2018). Despite these disparate findings, it is evident that LGP2 plays a role in the induction of RLR responses.

In species with RLRs, these proteins are present universally in nearly every cell type. Most avian species retain all of their RLR genes. However, it appears that chickens and other Galliformes have lost the *RIG-I* gene (Barber et al. 2010; Zheng & Satta, 2018). Instead, MDA5 in chickens appears to functionally compensate for their lack of RIG-I (Karpala et al. 2011; Liniger et al. 2012). Unlike chickens, ducks have retained RIG-I. Barber *et al.* (2010) also showed that chicken cells that are overexpressing duck RIG-I can recognize RIG-I ligands and induce an upregulation in IFNβ response.

1.1.3 NOD-like receptors

NOD-like receptors, like RLRs, are cytosolic sensors that respond to a wide variety of pathogens and immune challenges. Not only do NLRs detect PAMPs, but they can also detect DAMPs and other forms of cellular disruption which would indicate that something is awry with regular cell functions (reviewed by Franchi et al. 2009). NLRs share a similar tripartite structure and usually follow the same organization of protein domains: a C-terminal LRR, a central NACHT domain that binds to nucleotides, and then a variable N-terminal region which is

considered the effector region and interacts with other proteins (Figure 1). The C-terminal LRRs are believed to be the domain responsible for ligand binding. However, this may be the exception rather than the rule for the NLRs. For example, NLRP1 is activated by proteolytic cleavage of its FIIND domain (Finger et al. 2012), and NLRP3 is activated by K+ efflux (Katsnelson et al. 2015). Currently, the NLRs divide into five subfamilies based on the type of domain present at the N-terminal: NLRA, NLRB, NLRC, NLRP, and NLRX.

NLRA consists of one member, CIITA, which has an N-terminal acidic transactivating domain. NLRB has an N-terminal Baculovirus inhibitor of apoptosis protein repeat (BIR) and also has one member: NAIP. NLRC has an N-terminal CARD domain and consists of NOD1, NOD2, NLRC3, NLRC4, and NLRC5. NLRP has an N-terminal PYRIN domain, and its members include NLRP1 through to NLRP14. NLRX has only one member, NLRX1, and its N-terminal domain bears no homology to any other N-terminal domain (as reviewed in Y. Zhong et al. 2013).

Upon recognition of their ligand, the NLR will oligomerize through their NACHT domains and use their variable N-terminal domains to mediate the signal. This mediation can happen as CARD-CARD interactions or PYRIN-PYRIN interactions, depending on the NLR and its associated proteins. Only a few NLRs are known to bind to specific ligands and some of them also associate with an accessory protein.

CIITA, the only member of the NLRA family, has no known ligand in humans but is a transcriptional coactivator important in the mediation of adaptive immunity because of its ability to regulate the expression of the major histocompatibility complex (MHC) (Singer & Devaiah, 2013). NAIP, NOD1, NOD2, NLRC4, and NLRP1 are known to recognize bacterial structures. NAIP responds to flagellin (Kortmann et al. 2015), NOD1 is specific for meso-diaminopimelic

acid (meso-DAP) (Chamaillard et al. 2003; Girardin, 2003), while NOD2 recognizes muramyl dipeptide (MDP) (Girardin et al. 2003). Similar to NAIP, NLRC4 also recognizes flagellin, sometimes in complex with NAIP (Kofoed & Vance, 2011). On its own, NAIP seems to only respond to the flagellin of specific bacteria while NLRC4 does not show the same preference (Yang et al. 2013). NLRP1 will respond to the lethal toxin from *Bacillus anthracis* (Chavarría-Smith & Vance, 2013), MDP (Chavarría-Smith et al. 2016), even double-stranded RNA (Bauernfried et al. 2021). NLRC5 has a regulatory role in the inflammatory response in the absence of any direct association with a ligand (Lian et al. 2012). It also plays a regulatory role for MHC I genes (Kobayashi & van den Elsen, 2012). NLRP3 is the most controversial NLR when it comes to what ligand it binds to but also the most well-known due to its role in the very well-studied NLRP3 inflammasome. NLRP3 is activated in response to many different stimuli and upon activation, will form the NLRP3 inflammasome to mediate the inflammatory cascade (reviewed by Schroder et al. 2010). NLRP6 plays a role in detecting and repairing damage in the gastrointestinal system (Seregin et al. 2017). The functions of the other members of the NLRP family have yet to be identified. Finally, NLRX1 is much like CIITA and does not recognize a ligand but rather acts as an inhibitor of INFβ (Moore et al. 2008).

There has been some research into avian NLRs. Chickens have NOD1 but lack NOD2 (Boyle et al. 2013). A recent study by Wang *et al.* (2021) indicates that chickens are still capable of responding to MDP, the NOD2 ligand, suggesting that other NLRs (like NOD1) could be assuming the function of the missing NOD2. Ducks also have NOD1 and respond to stimulation by peptidoglycans (H. Li et al. 2017). They have also been shown to express NLRC5 (Lian et al. 2012) which exhibits pro-viral activities in chickens infected with IAV (Chothe et al. 2020).

Both chickens and ducks have NLRP3 (R. Li et al. 2018; Ye et al. 2015). Currently, the presence of the other NLRs known in other species and their functions has still yet to be determined.

1.2 Inflammation

Inflammation is a major component of the innate immune response. Acute inflammation is an immediate, fast-acting, generalized response mounted against any insult. Different inflammatory signals cause fluid and immune cells to infiltrate into the local area where the insult is located, allowing immediate defense in a localized fashion (reviewed by Ryan and Majno, 1977). Classically, inflammation is associated with redness, swelling, heat, pain, and even loss of function. In a viral infection, virally infected cells, or cells that have undergone virally induced necrosis, can release the necessary signals for immune cells to infiltrate into the local tissue. However, there is a fine balance between sufficient inflammation to clear the infection and an overactive inflammatory response which can lead to immunopathology. This is often seen as a cytokine storm coupled with excessive movement of immune cells and fluid into the region of infection. There is no consensus as to what a cytokine storm consists of. However, it is generally accepted that there are increased levels of pro-inflammatory cytokines like IL-1α, IL-1β, IL-6, IL-12, IL-18, and tumor necrotic factor (as reviewed in Tisoncik et al. 2012; Fajgenbaum and June 2020) For example, in many cases of influenza A infection, especially involving highly pathogenic strains of H5N1 or the 1918 strain of H1N1, the resulting immunopathology often takes the form of lung consolidation. In humans infected with H5N1, this has been seen as severe viral pneumonia (Yuen et al. 1998). In macaques infected with the 1918 strain of H1N1, this is seen as lesions on the lung, lung edema, and alveolar damage

(Kobasa et al. 2007). Perrone et al. (2008) found that mice infected with highly pathogenic H5N1 or the 1918 strain of H1N1 had increased immune cell infiltration in their lungs compared to mice infected with low pathogenic strains of H5N1 or H1N1. Although the mice which were infected with the highly pathogenic viral strain had increased inflammation and increased immune cell infiltration, their viral titers were much greater when compared to their respective low pathogenic conditions, indicating that the increased immune response of the highly pathogenic conditions was unable to clear the virus (Perrone et al. 2008). These studies suggest that reducing the number of inflammatory cytokines would alleviate the immunopathological damage by influenza A infections. However, Allen *et al*. (2009) found that inflammation is crucial for the survival of the host organism following an influenza A viral challenge. They ablated the NLRP3 inflammasome, a major player in the induction of inflammatory response. In mice deficient in the *Asc* gene or *Casp1* gene to ablate the NLRP3 inflammasome, reduced airway inflammation and also significantly higher mortality was observed after an influenza A infection (Allen et al. 2009).

Inflammation is a crucial part of the innate immune response. However, uncontrolled inflammation caused by an overactive innate immune response can result in serious tissue damage and potentially fatal outcomes for the infected host. The host immune system must balance the inflammatory response to clear the infection while limiting damage to its tissues.

1.2.1 Inflammasomes

Inflammasomes are large multi-protein complexes. These oligomerized structures usually consist of a detector protein, an adaptor protein, and an effector protein. The organization of the

NLRP3 inflammasome is seen in many other inflammasomes (Figure 2). Although there are some inflammasome-specific differences, usually the detector protein binds to a complementary domain on the adaptor protein via its N-terminal effector domain. ASC is the adaptor protein that binds to the PYRIN domain of the activated detector protein with its PYRIN domain and acts as a bridge to link the sensor protein to the effector protein, caspase-1 (CASP1). The CARD domain of ASC binds to the CARD domain of CASP1. This binding enables CASP1 to be proteolytically cleaved into its active form, consisting of the p10 and p20 enzymatic subunits. Activated CASP1 then homodimerizes and cleaves pro-IL-1β and pro-IL-18 into active IL-1β and active IL-18, respectively.

Active IL-1β is responsible for the induction of the inflammatory response, signaling the rapid recruitment of immune cells to the area of inflammation and the production of more cytokines. Additionally, active IL-1β also increases adhesion molecule expression on endothelial cells, further promoting the entrance of immune cells into inflamed extravascular areas (X. Wang et al. 1995). Active IL-18, on the other hand, stimulates the production of IFNγ as well as priming natural killer (NK) cell responses (Okamura et al. 1995). Additionally, IL-18, in conjunction with IL-12, can help modulate the T helper cell type 1 (Th1) and T helper cell type 2 (Th2) responses (Nakanishi et al. 2001).

Activation of the inflammasome also leads to a pyroptotic response. Pyroptosis is a cellular process much like apoptosis, but instead of keeping all of the intracellular materials contained like apoptosis does, pyroptosis results in the release of intracellular components into the extracellular milieu (reviewed by Bergsbaken et al. 2009). This causes a cascading activation of inflammatory responses by neighbouring cells which detect the intracellular components as DAMPs or if there is any intracellular pathogens present, PAMPS (reviewed by Jorgensen and

Miao, 2015). Pyroptosis occurs when activated CASP1 cleaves Gasdermin-D (GSDMD) into its active form (Martinon et al. 2002; Shi et al. 2015). There is some evidence that Gasdermin-E (GSDME) also plays a role in NLRP3 inflammasome activation as well, performing similar functions as GSDMD with different kinetics but in an additive manner (Zhou & Abbott, 2021).

1.2.1.1 NLRP1 inflammasome

The NLRP1 inflammasome was the first to be identified. NLRP1 is the detector protein of the NLRP1 inflammasome and does not follow the typical domain organization of the NLRs. In addition to typical NLR domains, it also has a function-to-find domain (FIIND) followed by a CARD domain on the C-terminal end (Martinon et al. 2002). It was originally thought that NLRP1 would be more efficient because it has two effector domains, a CARD domain, and a PYRIN domain. NLRP1 could bind to the CARD domain of CASP1 using its endogenous CARD domain, and also bind to ASC to activate a second CASP1 using its PYRIN domain (Martinon et al. 2002). However, in 2012, Finger et al., using mutant NLRP1 found that the PYRIN domain was not necessary for the interaction between NLRP1 and ASC. Mutants that lack the PYRIN domain show no significant change in activation of IL-1β compared to the full-length protein. Meanwhile, mutants that lack the CARD domain are, however, unable to activate IL-1β (Finger et al. 2012).

The NLRP1 unique domain, FIIND, is needed for a process termed functional degradation. The degradation of the FIIND domain activates NLRP1. A FIIND domain deletion mutant resulted in lowered IL- 1β activation (Finger et al. 2012). The FIIND domain is composed of two parts: ZU5 and UPA. NLRP1 also has auto-proteolytic capabilities which are

mediated by the FIIND domain and cleave NLRP1 into two non-covalently associated but distinct subunits. The N-terminal end contains ZU5 and the C-terminal end contains UPA (Finger et al. 2012). This self-cleavage results in proteasomal degradation of the N-terminal end of the protein, allowing the active C-terminal domains to self-associate or associate with ASC to form a signaling platform for the activation of CASP1 and further downstream inflammatory responses (Chui et al. 2019; Sandstrom et al. 2019; Wickliffe et al. 2008). However, NLRP1 is not only activated by self-cleavage but can also be activated by exogenous factors cleaving the FIIND domain. Murine NLRP1b was also found to be activated by the exogenous proteolytic effect of the Lethal Toxin (LeTx) of *Bacillus anthracis* (Boyden & Dietrich, 2006; Chavarría-Smith & Vance, 2013).

Chavarría-Smith *et al.* (2016) have also found that proteolytic cleavage, using an altered cleavage site recognized by the Tobacco Etch virus, can activate the other murine NLRP1 isoforms as well as the human NLRP1. Additionally, Liao and Mogridge (2013) showed that the NLRP1 inflammasome can be activated by a depletion in cytosolic ATP, suggesting that functional degradation is not the only mechanism of activation. However, this is not well understood, and it is possible that lowered cytosolic ATP could indirectly lead to functional degradation. Interestingly, Bauernfried *et al.* (2021) also found that NLRP1 was detected, and was subsequently activated by, long pieces of dsRNA. How the mechanism of activation differs between recognition of long dsRNA compared to functional degradation, or whether recognition of long dsRNA could lead to functional degradation is still unknown. Taken together, this suggests that the NLRP1 inflammasome is activated by the NLRP1 protein detecting cleavage of itself by pathogens or other processes that lead to its degradation. Functional degradation seems

to be unique to the NLRP1 inflammasome- it is the only inflammasome inhibited by proteasome inhibitors (Sandstrom et al. 2019; Wickliffe et al. 2008).

1.2.1.2 NLRC4 inflammasome

Formerly known as ICE-Protease Activating Factor (IPAF), the NLRC4 inflammasome is one of the most well-characterized and its activation is more in line with the classical ligand binding and activation of the TLRs. NLRC4 activates CASP1 and induces the activation of IL-1β and IL-18 (Poyet et al. 2001). It responds to enteric pathogens like *Salmonella typhimurium* (Franchi et al. 2006)*, S. flexneri* (Suzuki et al. 2014; Suzuki et al. 2007)*, Pseudomonas aeruginosa* (Franchi et al. 2007)*,* and *Legionella pneumophila* (Amer et al. 2006). It is composed of four protein components instead of the classical three protein components found in other inflammasomes. In addition to using ASC and CASP1 as the adaptor and effector proteins respectively, the NLRC4 inflammasome has NLR family Apoptosis Inhibitory Proteins (NAIP) as its sensor protein and NLRC4 as the nucleator protein.

NAIP detects specific ligands in the cytosol and then associates with NLRC4 to induce NLRC4 inflammasome activation (Kofoed & Vance, 2011; Zhao et al. 2011). Mice have separate NAIP proteins with different specificities for ligands, allowing NLRC4 inflammasome to be activated by different ligands. NAIP2 is needed to detect bacterial inner rod protein PrgJ, and NAIP5 is responsible for the activation of the NLC4 inflammasome in response to bacterial flagellin (Kofoed & Vance, 2011). Both of these NAIP proteins are specific to their proteins and show no response when stimulated with the ligand of the other NAIP protein. Meanwhile, humans have only one NAIP protein that binds to the type III secretion system (T3SS) rod and

needle protein from bacteria. However, a spliced variant of human NAIP shows 68% similarity to murine NAIP5 and some specificity for flagella (Kortmann et al. 2015).

NLRC4 also lacks the N-terminal PYRIN domain that is typically found in NLRs but has a CARD domain in its place. This allows it to directly associate with CASP1. However, NLRC4 can still associate with ASC, which enhances the efficacy of NLRC4 activation of CASP1. Without a PYRIN domain, NLRC4 associates with ASC using their respective CARD domains instead. ASC self-associates through its PYRIN domains to form the large telltale ASC specks and activate CASP1.

1.2.1.3 PYHIN inflammasome

PYHIN proteins are proteins that contain a PYRIN domain and one or two HIN domains. Of these proteins, absent in melanoma 2 (AIM2) and interferon-inducible protein 16 (IFI16) acts as the sensor proteins to form inflammasome complexes. AIM2 has an N-terminal PYRIN domain and a single HIN domain at the C-terminal end. IFI16 is similarly organized but contains two HIN domains instead of one. Unlike the other inflammasome-forming proteins, AIM2 and IFI16 bind directly to dsDNA through their HIN domains. The PYRIN domain is then used to bind to ASC for downstream activation of CASP1 as part of the inflammasome. AIM2 binds to cytosolic dsDNA from intracellular pathogens like bacteria or viruses (Bürckstümmer et al. 2009; Hornung et al. 2009). AIM2 can also bind to self-DNA, but this seems to be largely prevented by its presence only in the cytosol and not in the nucleus. IFI16 has also been shown to detect foreign DNA in the cytoplasm (Unterholzner et al. 2010). However, unlike AIM2, it can detect foreign DNA from Epstein-Barr virus and Kaposi's sarcoma-associated herpesvirus in

the nucleus of infected cells, recruiting ASC to the nucleus for inflammasome formation when activated (Ansari et al. 2013; Kerur et al. 2011). Recent studies have shown that IFI16 is activated in response to viral DNA synthesis in the nucleus of infected cells (Merkl and Knipe, 2019).

1.2.1.4 RIG-I inflammasome

Similar to the PYHIN inflammasome, RIG-I is capable of nucleating an inflammasome despite not being an NLR. After recognition of the 5′ triphosphate nucleoside of double-stranded RNA, RIG-I is activated (Hornung et al. 2006). RIG-I is capable of upregulating the production of pro-IL-1β through the NF-κB pathway (Poeck et al. 2010). This is a necessary step to ensure that enough pro-IL-1β is present in the cell for inflammasome activation. Using its CARD domain, RIG-I interacts with ASC which binds to and activates CASP1 to induce IL-1β activation (Poeck et al. 2010; Pothlichet et al. 2013). However, the RIG-I inflammasome appears to be redundant during infection with RNA viruses, like vesicular stomatitis virus or encephalomyocarditis virus, and the absence of RIG-I did not affect IL-1β activation (Poeck et al. 2010).

1.2.1.5 NLRP3 inflammasome

The NLRP3 inflammasome is a multi-protein oligomeric complex that forms a spoke-like structure (Schroder et al. 2012) (Figure 2). Its function is to induce inflammation through the activation and eventual secretion of the pro-inflammatory cytokines, IL-1β and IL-18. It consists

of NLRP3, ASC, and CASP1. NLRP3 is the sensor protein of the inflammasome complex, and activation of this protein will ultimately cause inflammasome formation and activation. The NLRP3 protein, known by many different names over the years— cryopyrin, Pypaf1, Nalp3, has three different functional domains: an N-terminal PYRIN domain, a NACHT domain, and a C-terminal LRR domain. Activation of the NLRP3 inflammasome has been associated with a range of different pathogens and diseases ranging from viruses (Allen et al. 2009; Kanneganti et al. 2006), bacteria and fungi (Kankkunen et al. 2010) to autoimmune conditions (Inoue & Shinohara, 2013; Masters et al. 2010). With such a broad range of activators, the current hypothesis of activation for the NLRP3 inflammasome is that NLRP3 does not bind to specific ligands- the range of ligands would be too diverse, but rather detects cellular stressors common to many different types of immune challenges.

Macrophages are well studied in regard to the NLRP3 inflammasome (Kortmann et al. 2015; Z. Zhong et al. 2013). As an immune cell that is broadly circulating in peripheral tissues, they are often among the first to come into contact with pathogens and potential activating signals of the NLRP3 inflammasome. However, the NLRP3 inflammasome can also be activated in epithelial cells as well as different fibroblasts, indicating that the NLRP3 inflammasome is not specific to just one cell type but offers a more general line of innate defense (He et al. 2021; Kawaguchi et al. 2011; Wei et al. 2021).

There are two steps in the activation of the NLRP3 inflammasome. The first step is the priming step, which consists of the activation of other immune receptors like TLRs, NOD1, NOD2, or other cytokine receptors (Bauernfeind et al. 2009). The activation of these other immune receptors leads to the activation of the transcription factor NF-κB and the synthesis of more NLRP3 and pro-IL-1β proteins (Bauernfeind et al. 2009). The transcription-dependent

priming step is needed only to synthesize adequate numbers of all three proteins to mount an effective immune response (Bauernfeind et al. 2009; Franchi et al. 2009). At rest, NLRP3 is expressed in low concentrations and pro-IL-1β is not detected within the cytosol.

NF-κB is not the only transcriptional factor that is needed during the priming step of the NLRP3 inflammasome. Interferon regulatory factor 1 (IRF1) is a transcription factor located downstream of the TLRs and MyD88 signaling pathways and is important for priming the NLRP3 inflammasome (Zhong et al. 2018). One of the necessary factors in NLRP3 inflammasome activation is the oxidation of mitochondrial DNA (ox-mtDNA) and its release into the cytosol (Nakahira et al. 2011; Z. Zhong et al. 2016). IRF1 is crucial in the synthesis of *de novo* mitochondrial DNA (mtDNA) that can be oxidized. Without IRF1, a lack of mtDNA synthesis results in a lack of ox-mtDNA being formed when the mitochondria become damaged by the actions of different NLRP3 agonists, leading to an inhibition of NLRP3 inflammasome activation (Zhong et al. 2018).

Though the priming step is often understood as the upregulation of the expression of NLRP3 and pro-IL-1β, recent studies show that the priming step also functions in preparing the NLRP3 protein for activation, independent of transcription. One of the hypotheses for transcription-independent priming is that the priming step induces a post-translational modification or cellular relocalization of the components of the NLRP3 inflammasome. For effective activation of the NLRP3 inflammasome, NLRP3 needs to be deubiquitinated. Acute priming of NLRP3 with LPS for even just 10 minutes is sufficient to partially deubiquitinate the protein, successfully priming the NLRP3 inflammasome independent of the NF-κB pathway (Juliana et al. 2012; Schroder et al. 2012). Phosphorylation of serine-198 by JNK1 also occurs within 15 minutes of priming as part of the priming step (Song et al. 2017). This phosphorylation

allows the oligomerization of the NLRP3 proteins- the basis of the NLRP3 inflammasome formation.

Activation of the NLRP3 inflammasome has been attributed to a few different cellular changes. One of the most commonly accepted mechanisms of activation of NLRP3 is through cellular K^+ efflux (Katsnelson et al. 2015; Muñoz-Planillo et al. 2013). The activation of active IL-1β through the activation of the NLRP3 inflammasome is to be dependent on K^+ efflux (Mariathasan et al. 2006; Perregaux & Gabel, 1994; Pétrilli et al. 2007; Walev et al. 1995, 2000). Inhibition of the movement of K^+ across the cell membrane or high concentrations of K^+ in the extracellular milieu is sufficient to inhibit NLRP3 inflammasome activation and subsequent IL-1β activation (Perregaux and Gabel, 1994; Pétrilli et al. 2007). ATP and nigericin are two well-established NLRP3 inflammasome agonists that activate the NLRP3 inflammasome using K^+ efflux (Perregaux & Gabel, 1994). ATP binds to the P2X7 receptor, a ligand-gated ion channel (Surprenant et al. 1996). Activation of P2X7 induces the formation of non-selective pores, leading to K^+ efflux and disruption of cell homeostasis (Coutinho-Silva et al. 2001). In addition to K^+ efflux, the P2X7 receptor can also allow ATP to leave the cell either through these non-selective pores or through the activity of pannexin-1 (Pelegrin & Surprenant, 2006). However, in an experiment with pannexin-1 knockout mice, Qu et al. (2011) demonstrated that *Pnx1*$^{-/-}$ bone marrow-derived macrophages were still capable of activating the NLRP3 inflammasome when stimulated with ATP or nigericin after LPS priming for 4 hours. This result suggests that pannexin-1 has a redundant role in the activation of NLRP3 inflammasome and is in fact dispensable.

Additionally, the release of ATP into the extracellular milieu further propagates inflammatory responses as neighbouring cells detect the released ATP as a DAMP.

Nigericin has a slightly different mechanism to induce K^+ efflux. Nigericin is an antibiotic produced by *Streptomyces hygroscopicus* (Benedict, 1953). It is a potassium ionophore and exchanges K^+ for H^+, culminating in a net reduction of K^+ and an accumulation of H^+ in the cell (Perregaux & Gabel, 1994). The net reduction of intracellular K^+ through the action of nigericin is sufficient to activate the NLRP3 inflammasome. However, despite the effect of K^+ efflux on the NLRP3 inflammasome being well documented, the mechanisms behind the actual detection of the change in K^+ concentration are still unclear.

While the NLRP3 inflammasome is crucial to the clearance of viral infections, the overactivation of this inflammasome also leads to detrimental outcomes for the host. Overactivation of the NLRP3 inflammasome leads to a hyperactive inflammatory response called a cytokine storm (Chousterman et al. 2017; Lin et al. 2019; Tisoncik et al. 2012). This results in an uncontrolled increase in recruited immune cells and fluid to the area of infection, potentially causing fatal outcomes for the host. It is this dysregulated overactivation of the NLRP3 inflammasome during severe infections that suggests that it would be a good therapeutic target.

1.3 NLRP3 inflammasome of other species

1.3.1 Pig NLRP3 inflammasome

Pigs have a functional NLRP3 inflammasome with activity that resembles that of the human and the mouse NLRP3 inflammasomes (Kim et al. 2014). The pig NLRP3 inflammasome consists of NLRP3, ASC, and CASP1 and could be activated by ATP as well as nigericin after priming with LPS. Interestingly, Kim *et al.* (2014) found that the pig NLRP3 inflammasome was

more sensitive to these two NLRP3 inflammasome activators than the mouse NLRP3 inflammasome. The pig NLRP3 inflammasome could also be inhibited in the same manner as the mouse NLRP3 inflammasome. Inhibition of ROS levels, as well as CASP1 activity, similarly abrogated IL-1β activation between the mouse NLRP3 inflammasome and the pig NLRP3 inflammasome (Kim et al. 2014). The NLRP3 inflammasome in pigs is also activated by viral infections like IAV (Park et al. 2018) and porcine reproductive and respiratory syndrome virus (Bi et al. 2014), as well as bacterial infections like *Haemophilus parasuis* (Fu et al. 2018) and *Escherichia coli* (Zou et al. 2020).

1.3.2 Bat NLRP3 inflammasome

The bat NLRP3 inflammasome is of note due to recent research that has shown that bats have a highly inhibited NLRP3 inflammasome-induced inflammatory response. Bats have also been recognized as crucial reservoir hosts of different viruses— many of which have been able to spill over into other species like humans, resulting in severe implications on the health and wellbeing of humans (Calisher et al. 2006). Like ducks, bats can be asymptomatic even when hosting viruses such as severe acute respiratory syndrome (SARS) coronavirus and Ebola virus, that would otherwise prove fatal to other hosts (Leroy et al. 2005; Li et al. 2005).

One of the explanations as to why bats remain asymptomatic when infected with these viruses is that the bat NLRP3 inflammasome has dampened activation in the face of viral infections (Ahn et al. 2019). More specifically, Ahn *et al.* (2019) found that the bats had a reduced response to transcriptional priming of the NLRP3 inflammasome that is independent of which TLR is activated. Bauernfeind *et al.* (2021) showed that, by inhibiting the priming step by

blocking *de novo* translation, activation of the NLRP3 inflammasome is inhibited. The bat NLRP3 inflammasome also has reduced ASC speck formation and IL-1β cleavage compared to human NLRP3 inflammasome (Ahn et al. 2019). Furthermore, bat NLRP3 has a splice variant that is expressed 60% of the time in tissues and has reduced activity compared to the other splice variants further contributing to the reduction in inflammation caused by the NLRP3 inflammasome (Ahn et al. 2019).

However, bat NLRP3 is not the only component of the NLRP3 inflammasome that has reduced activity. Goh *et al.* (2020) found that bat CASP1 had lower activity compared to human CASP1 and also activated bat CASP1 activated less IL-1β. It would appear that the bat NLRP3 inflammasome has several different mechanisms to decrease activation and thus reducing the amount of inflammation seen in the host. This is a crucial feature of the bat innate immune system, which has evolved alongside the many different viruses that bats are a host to and allowing them to remain asymptomatic.

1.3.3 Fish NLRP3 inflammasome

Several species of fish have functioning NLRP3 inflammasomes capable of activating fish IL-1β homologs and inducing pyroptosis (H. Chen et al. 2020; Li et al. 2020). Y. Li *et al.* (2018) characterized ASC of *Danio rerio*, successfully creating crystal structures of ASC and showing that the protein was capable of forming specks on its own when overexpressed. Zebrafish ASC could also interact with human NLRP3 and human CASP1 to induce activation of human IL-1β after treatment with nigericin (Y. Li et al. 2018). Li *et al.*(2020) characterized NLRP3 and GSDME in zebrafish and showed that zebrafish NLRP3 was capable of interacting

with zebrafish ASC to induce ASC speck formation, caspase activation, and subsequent zebrafish IL-1β activation as well. Furthermore, Chen *et al.* (2020) examined Japanese flounder NLRP3 inflammasome, finding that it was capable of restricting *Edwardsiella piscicida* in Japanese flounder by inducing a robust inflammatory response through IL-1β activation and pyroptosis. Though there are not many studies on fish NLRP3 inflammasomes, based on the few that are currently available, it appears that the fish NLRP3 inflammasome is activated in a manner that is similar to mammalian NLRP3 inflammasomes.

1.3.4 Avian NLRP3 inflammasome

There has been some research on the avian NLRP3 inflammasome. Studies have been performed on chickens and ducks, investigating the effects of various immune challenges and the response of the avian NLRP3 inflammasome. Li *et al.* (2018) observed that NLRP3 was found in every tissue tested in Cherry Valley ducks, indicating that NLRP3 could be involved in a widespread immune response. They also found that upregulation of NLRP3 affects antibacterial innate immune responses in live ducks, reducing the level of *E. coli* in duck tissues (R. Li et al. 2018). The NLRP3 inflammasome also plays a role in antiviral innate responses. He *et al.* (2021) found that chicken embryonic fibroblasts, when their NLRP3 inflammasome was knocked down, had higher infectious bursal disease virus (IBDV) replication. These chicken embryonic fibroblasts also exhibited increased cell death at earlier stages of IBDV infection than control, suggesting that the NLRP3 inflammasome is activated as a mechanism of reducing viral replication in chicken cells (He et al. 2021). The avian NLRP3 inflammasome has been implicated in responding to heavy metal toxicity. Wei *et al.* (2021) examined the effects of

cadmium on duck renal tubular epithelial cells and found that there was transcriptional upregulation of the components of the duck NLRP3 inflammasome as well as increased pyroptosis after treatment with cadmium. Most studies investigating avian inflammasomes examine the upregulation of NLRP3 and IL-1β. Avian CASP1 and ASC interactions and upregulation in the context of the avian NLRP3 inflammasome often go ignored.

1.4 Experimental aims and results

With a long evolutionary history with the influenza A virus (IAV), ducks, and other waterfowl are considered to be the natural reservoir host of IAV (Taubenberger & Kash, 2010; Webster et al. 1992). They have a propensity to survive IAV infections with little to no symptoms or other detrimental side effects (Cornelissen et al. 2013; van den Brand et al. 2018), unlike other hosts of this virus, for example, humans (Chotpitayasunondh et al. 2005; de Jong et al. 2006) or Galliform poultry like chickens (Cornelissen et al. 2013; Kuchipudi et al. 2014). Commonly observed with severe IAV infections, susceptible hosts show a dysregulated increase in inflammation and activation of pro-inflammatory cytokines, often referred to as a cytokine storm, in the area of infection (Peiris et al. 2010; To et al. 2010). The duck inflammatory response is of interest because ducks do not show the same hyper-inflammation and cytokine response when they are infected with strains of highly pathogenic avian influenza (HPAI) that kill other hosts (Kuchipudi et al. 2014).

The main objective of this thesis was to characterize the duck NLRP3 inflammasome. Previous work done in our lab has observed that ducks infected with influenza A viruses of different pathogenicities exhibit robust antiviral response which includes the upregulation of

interferons, and other interferon-stimulated genes like *IFIT5, MX1, PKR,* and *OASL* (Saito et al. 2018; Fleming-Canepa et al. 2019). In comparison, pro-inflammatory cytokines like *IL1B, IL6,* and *IL18* were only observed to have a moderate upregulation in the same IAV infected ducks (Saito et al. 2018). The NLRP3 inflammasome is a powerful activator of IL-1β and subsequent inflammatory response in many other species. Due to the lack of detrimental hyper-inflammatory symptoms by ducks when infected by IAV strains that would lead to severe outcomes for other susceptible hosts (Kida et al. 1980; Kuchipudi et al. 2014) and the moderate upregulation of the pro-inflammatory cytokines that our lab previously observed in ducks infected with IAV (Saito et al. 2018), I hypothesized that the duck NLRP3 inflammasome may respond to infections in a manner that would allow the host to avoid detrimental effects while mounting a sufficient immune response to combat infections. Here, I cloned the sequences of duck NLRP3, CASP1, and IL-1β from cDNA. We have not been able to locate ASC in the duck genome or transcriptome, suggesting that ducks may lack a functional ASC. Additionally, transcriptional priming of the duck NLRP3 inflammasome in duck embryonic fibroblasts does not induce transcriptional upregulation of NLRP3 or IL-1β. These results suggest that the activity of the duck NLRP3 inflammasome is dampened, potentially contributing to why they do not exhibit hyper-inflammatory responses during IAV infection.

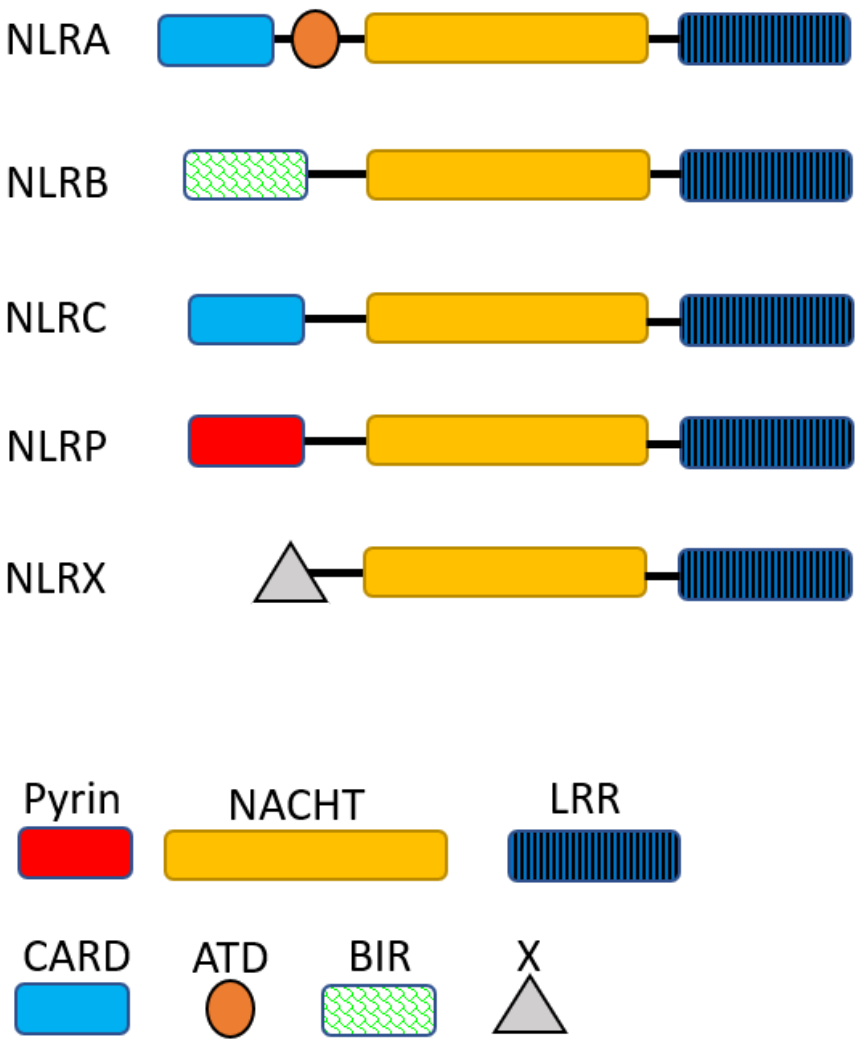

Figure 1. Organization of the protein domains of the different NLR families. NLRA consists of a CARD domain, acidic transactivating domain, NACHT domain, and LRRs. NLRB consists of Baculovirus inhibitor of apoptosis protein repeats, NACHT, and LRRs. NLRC consists of a CARD domain, NACHT, and LRRs. NLRP consists of a pyrin domain, NACHT, and LRRs. NLRX consists of an X domain, NACHT, and LRRs.

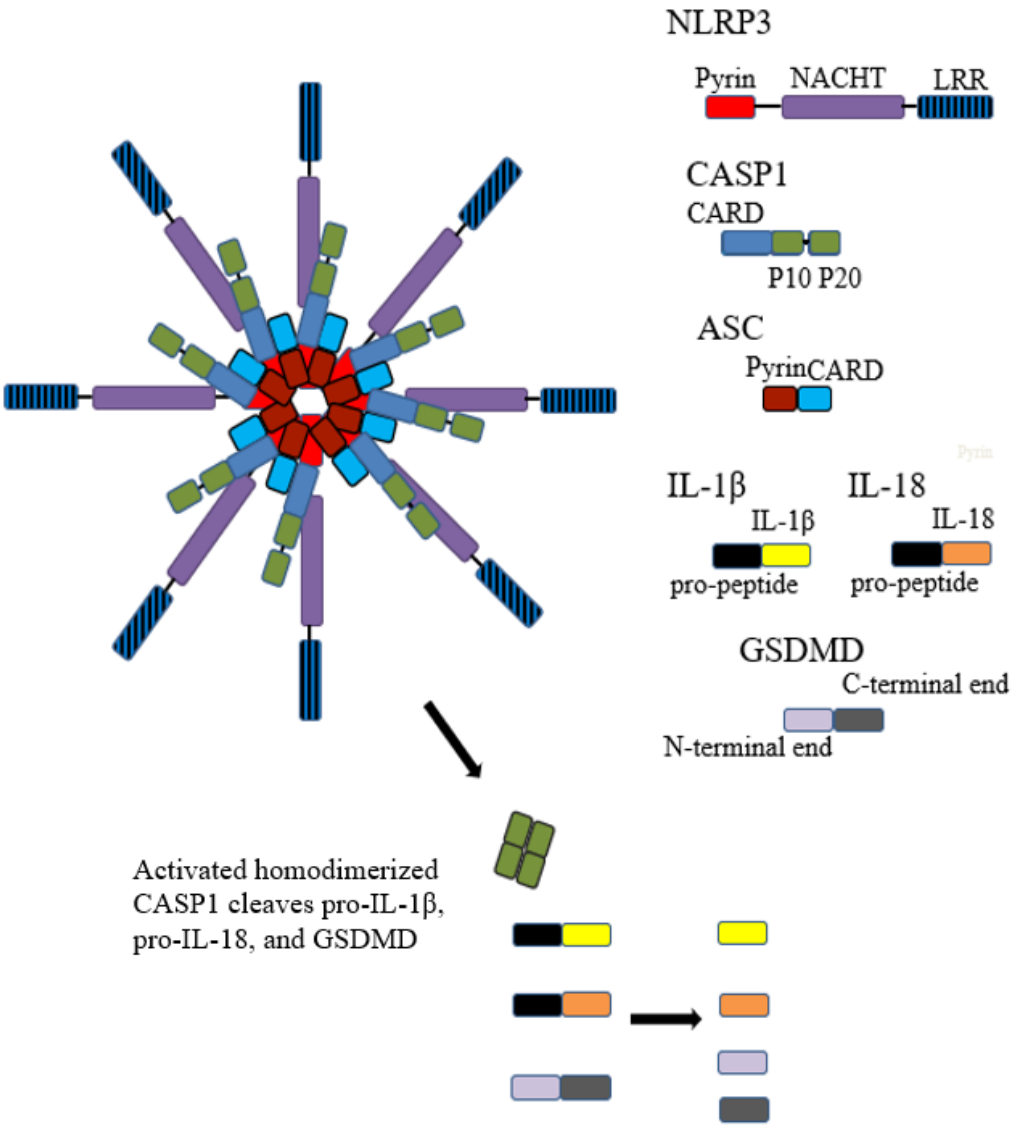

Figure 2. NLRP3 inflammasome forms spoke-like specks when activated. NLRP3 is the sensor protein that activates in response to changes in cell homeostasis induced by infection or cellular stress. ASC acts as a link between NLRP3 and the effector protein, CASP1. The CARD domain is cleaved from activated CASP1, leaving only the enzymatic P10 and P20 subunits. Activated CASP1 will homodimerize to cleave pro-IL-1β into activated IL-1β, pro-IL-18 into activated IL-18, and GSDMD into its N-terminal and C-terminal subunits. IL-1β and IL-18 are pro-inflammatory cytokines. The cleaved -terminal end of GSDMD induces pyroptosis.

Chapter 2. Methods and Materials

2.1 Duck NLRP3

The duck NLRP3 coding sequence was identified by Sai Mao and cloned into a pCR®2.1-TOPO vector (Invitrogen). This sequence was confirmed using sequencing with the primers listed in Table 2 and aligned with a published duck NLRP3 sequence from Li *et al.* (2018) (Accession number: MH373356). After confirmation, I PCR amplified duck NLRP3 from this construct and using PCR, attached a 2xFLAG epitope tag followed by an XhoI restriction site to the C-terminus and a BamHI restriction site to the N-terminus. Phusion®High-Fidelity DNA Polymerase (New England BioLabs) was used for all PCR cloning. Duck NLRP3-2xFLAG and the added restriction sites were cloned into the pCR®2.1-TOPO TA kit vector (Invitrogen) and sequenced with the primers listed in Table 1 to confirm the successful addition of the epitope tag and restriction sites to the duck NLRP3 coding sequence. I then cloned duck NLRP3-FLAG into pcDNA3.1/Hygro+ (Invitrogen) using a Gibson Assembly® (New England BioLabs) approach. The vector backbone was generated from a double digest of pcDNA3.1/Hygro+ (Invitrogen) using BamHI and XhoI restriction sites. Duck NLRP3-2xFLAG was amplified, by PCR, from the duck NLRP3-2xFLAG TOPO construct, and additional regions of homology for pcDNA 3.1 Hygro+ (Invitrogen) were added to the 5′ and 3′ ends of the duck NLRP3-2xFLAG sequence using primers in Table 1. The sequence of NLRP3-FLAG pcDNA 3.1/ Hygro+ was confirmed using sequencing with the primers in Table 2.

Primers were designed to amplify intron 1 from gDNA. The forward primer binds to a segment in exon 1 while the reverse primer binds to a segment in exon 2. Genomic DNA

(gDNA) and cDNA were from Pekin ducks and used as templates for the PCR. The amplified sequences were cloned into pCR®2.1-TOPO TA kit vector (Invitrogen) and then sent for sequencing using the primers in Table 2.

Analysis of the duck NLPR3 promoter was done using JASPAR 2020 online database ((http://jaspar.genereg.net/). 4kb of 5′-UTR of duck NLRP3 was analyzed and transcription factor binding sites were predicted.

2.2 Duck CASP1

Duck CASP1 coding sequence was identified by Lee Campbell *in silico* using transcriptomic analysis. Based on this sequence, duck CASP1 was amplified in two fragments and then joined together using overlap PCR and the primers in Table 1. I added the Myc epitope tag to the C-terminus of CASP1 followed by an XhoI restriction site and an EcoRV restriction site on the N-terminus. The coding sequence and epitope tag were cloned into the pCR®2.1-TOPO vector (Invitrogen) using the Invitrogen™ TOPO™ TA Cloning™ Kit and sequenced with the primers listed in Table 2 to confirm the successful addition of the epitope tag and restriction sites to the duck CASP1 coding sequence. I then cloned duck CASP1-Myc into the pcDNA3.1/Hygro+ (Invitrogen) vector using T4 DNA ligase (Invitrogen). The sequence of CASP1-Myc pcDNA 3.1/ Hygro+ was confirmed using sequencing with the primers in Table 2.

2.3 Duck IL-1β

The duck IL-1β coding sequence was identified by submitting the chicken IL-1β (XP_015152955) protein sequence into the tBLASTn tool on *Ensembl* against the *Anas platyrhynchos* genome CAU_duck1.0 assembly available on *Ensembl* release v95 (January 2019). The unannotated gene ENSAPLG00000025615 showed high homology with the chicken IL-1β protein sequence with an E-value of $3e^{-99}$ and percent identity of 57.10. The duck IL-1β coding sequence was cloned using duck cDNA using primers in Table 1 and a glutathione S-transferase (GST) epitope tag was attached to the C-terminus of the protein using overlap extension PCR and the primers listed in Table 1. mVenus fluorescent tag was also attached to the C-terminal end of duck IL-1β using the primers listed in Table 1 and was a gift from Steven Vogel (Addgene plasmid # 27794; http://n2t.net/addgene:27794; RRID:Addgene_27794). Additional homology for pcDNA 3.1 Hygro+ (Invitrogen) was added to the 5′ and 3′ ends of the duck NLRP3-FLAG sequence using primers in Table 1 for both IL-1β- GST and IL-1β- mVenus. I then cloned duck IL-1β- mVenus into pcDNA3.1/Hygro+ (Invitrogen) using a Gibson Assembly® (New England BioLabs) approach. The vector backbone was generated from a double digest of pcDNA3.1/Hygro+ (Invitrogen) using BamHI and XhoI restriction sites.

2.4 Duck ASC

The predicted coding sequence of ASC from *Anser cygnoides* (XM_013201308) was used to try to identify the duck ASC by searching for the protein and coding sequence using the tBLASTn and BLASTn tools respectively, against the *A. platyrhynchos* genome CAU_duck1.0 assembly. The unannotated gene, ENSAPLG00000026622 was a match with the highest score, an e-value of $4e^{-46}$ and a 72.81 percent identity score. Another grad student in the lab, Lee K.

Campbell, identified a putative ASC sequence using the transcriptome generated with RNA-sequencing (experiment described in 2.5) using HMMER and the ASC sequences from other species: human ASC (NP_075747), mouse ASC (NP_075747, cow ASC (NP_777155), pig ASC (BAV13623), zebrafish ASC (NP_571570), mainland tiger snake ASC (XP_026539257), king cobra ASC (ETE61892.1), eastern brown snake ASC (XP_026580032), and the putative ASC from *A. cygnoides* (XM_013201308). I searched the duck genome on *Ensembl* with this identified sequence and found that it matched with ENSAPLG00000026622 as well as ENSAPLG00000021492. I designed a forward primer that would bind with the 5′-UTR of ENSAPLG00000021492 and a reverse primer that would bind with the 3′-UTR of ENSAPLG00000026622. These primers, referred to as ASC primers and listed in Table 1, were used to PCR amplify putative duck ASC from cDNA. This sequence was cloned into pCR®2.1-TOPO vector (Invitrogen) using the Invitrogen™ TOPO™ TA Cloning™ Kit and then sent for sequencing using the primers listed in Table 2. I used the program, SMART, to analyze the protein domains of the protein sequence and found that there was a FIIND domain in the middle of the protein sequence, a domain characteristic of NLRP1 proteins.

2.5 RNA Sequencing

Pekin duck embryonic fibroblasts (DEFs) were seeded onto a 6 well plate at a concentration of $1.0x10^6$ cells per well in Dulbecco's modified eagle medium (Gibco) with 10% fetal bovine serum (FBS) (Sigma Aldrich) and allowed to recover at 39°C with 5% CO_2 overnight. They were transfected with 1 µg of polyinosinic: polycytidylic acid (poly I:C) for three hours with Lipofectamine™ LTX reagent at a ratio of 1µg DNA to 1µL of Lipofectamine

to 0.5 µL PLUS™ Reagent to 1 µL of FuGene. After three hours, three of the transfected wells were washed with warm 1x phosphate-buffered saline (PBS) and then treated with 20 µM of nigericin (Sigma Aldrich) in 2 mL of DMEM + 10% FBS. RNA from the DEFs was collected and extracted using the PuroSPIN™ Total RNA Purification Kit (Luna Nanotech). The quantity of the RNA was assessed using Qubit (Invitrogen) and the RNA quality was assessed using a Bioanalyzer 2100 (Agilent). 1µg of RNA from each of the control DEFs and of the poly I:C and nigericin treated DEFs that passed the RNA quality test was sent to LC Sciences (https://www.lcsciences.com/) for poly-adenylated RNA sequencing. About 40 million reads per sample were obtained.

2.6 Brightfield microscopy

Pekin DEFs were grown in DMEM plus 10% FBS at 39°C with 5% CO_2. Cells were seeded at a concentration of 1.0 x 10^6 cells/ well in 6 well plates for 24 hours. The cells were either primed with poly I:C only, primed with poly I:C and treated with nigericin, or left untreated as previously described. One set of cells was primed with poly I:C for three hours and then treated with nigericin for 24 hours before imaging. Images were taken on a Zeiss Axio Observer A1 inverted microscope at 100x and analyzed using the ImageJ program.

2.7 Pull-down assay and Western blotting

Immortalized chicken embryonic fibroblasts (DF-1) derived from an East Lansing line embryo were grown in DMEM plus 10% FBS at 39°C with 5% CO_2 (Schaefer-Klein et al. 1998).

Immortalized human embryonic kidney cells with large SV40 T antigen (HEK293T) were grown in DMEM plus 10% FBS at 37 ℃ with 5% CO_2. Cells were seeded at a concentration of 1.0 x 10^6 cells/ well in 6 well plates and transfected immediately with 1 µg DNA of each expression construct along with empty pcDNA 3.1 Hygro+ (Invitrogen) for a total of 4µg of DNA transfected per well. Lipofectamine 2000® reagent (Invitrogen) was used for all DF-1 and HEK293T transfections at a ratio of 1µg DNA to 1 µL Lipofectamine 2000®. 16 hours post-transfection, cells were washed gently with warm PBS and then lysed with 1000 µL of lysis buffer (50 mM TRIS pH 7.2, 150 mM NaCl, 1% [vol/vol] Triton X-100, protease inhibitor cocktail [Roche]). The lysate was then sonicated twice for 10 seconds each time, resting on ice in between each sonication. Whole-cell lysates (WCL) were collected after sonication and boiled with 1x Laemmli buffer for 10 minutes. The remainder of the sonicated lysates were centrifuged at 4℃ at 22000 x g for 15 minutes. Supernatants were added to 50 µL of Glutathione Sepharose 4B resin (GE Healthcare), which was equilibrated with 1000 µL lysis buffer. This mix was incubated overnight at 4°C while rotating. The GST-pulldown was then washed three times with ice-cold PBS plus 0.1% TWEEN® 20 (Sigma Aldrich). The beads were resuspended in 30 µL of ice-cold lysis buffer and 10 µL 8x Laemmli buffer, and then boiled in Laemmli buffer for 10 minutes. For Western blotting, the WCL and immunoprecipitated proteins were separated using 12% SDS polyacrylamide gel electrophoresis (SDS-PAGE) and then transferred to a nitrocellulose membrane using the wet transfer method. Immunoblotting was performed using either a primary mouse M2 anti-FLAG monoclonal antibody at 1:5000 (F3165; Sigma-Aldrich), a primary mouse anti-Myc monoclonal antibody at 1:2500 (9E10; Invitrogen), and a rabbit anti-GST polyclonal at 1:5000 (G7781; Sigma-Aldrich). Visualization was performed using

chemiluminescence on a ChemiDoc imager (Bio-Rad) using Pierce® ECL Western blotting substrate (Thermo Scientific).

2.8 Quantitative Polymerase Chain Reaction

Pekin DEFs and A549 were seeded at a concentration of 1.0 x 10^6 cells/ well in 6 well plates for 24 hours. DEFs in the poly I:C and poly I:C then nigericin conditions were transfected with 1µg of poly I:C per well using Lipofectamine™ LTX reagent as previously described. Cells were also treated with 20 µM nigericin as previously described. After 1 hour of treatment with nigericin, cells were gently washed with 1mLof warm PBS and then collected with 1mL TRIzol (Ambion™), combining three wells per condition, according to the manufacturer's protocols. cDNA was synthesized using 500ng of RNA and Superscript III (Invitrogen) reverse transcriptase and oligo DT. A PCR was performed on the cDNA to amplify Glyceraldehyde-3-Phosphate Dehydrogenase (GAPDH) using Phusion® High-Fidelity DNA polymerase (New England BioLabs) and then visualized on 1% agarose gels to confirm that cDNA synthesis was successful. Quantitative polymerase chain reaction (qPCR) primers and probes for duck *NLRP3*, duck *IL1B*, duck *IL18* were validated against primers and probes for duck *GAPDH* (Table 3). Probes with an efficiency that fell within 10% of the efficiency of the primers and probes for duck GAPDH were considered successfully validated and used for qPCR experiments. *IFIT5* primers and probes were previously made and validated by Ximena Fleming-Canepa. qPCR experiments were performed using QuantStudio™ 3 (Applied Biosystems) and analyzed using QuantStudio™ Design and Analysis software (Applied Biosystems). qPCR reactions were performed in a 10µL reaction which contained 5µL of in-house qPCR probe master mix, 1µL of

10x qPCR primers and probes master mix (Table 3), 1.5µL of nuclease-free water (IDT DNA), and 2.5µL of cDNA. Thermal cycling parameters were: 95℃ for 10 minutes, 40 cycles of 96℃ for 15 seconds, and 60℃ for 1 minute. Each sample was done in triplicate and the expression fold change of each gene was calculated relative to *GAPDH* as a reference gene.

2.9 Confocal immunofluorescent microscopy

DF-1 cells were seeded onto glass coverslips in a 24 well plate at a concentration of 8.0 x 10^5 cells/well for 24 hours and then transfected with 1µg of each expression construct with Lipofectamine 2000 (Invitrogen) at a ratio of 1:2.5 DNA to Lipofectamine 2000. 100 µL of the DNA, Lipofectamine 2000, and optimem was added to each well. After 16 hours, the media was removed, and the coverslips were washed gently with warm PBS. PBS plus 1% paraformaldehyde (PFA) (Sigma Aldrich) was used to fix the cells onto the coverslips. The cells on the coverslips were permeabilized using PBS plus 0.2% Triton X-100 (Sigma Aldrich) then blocked with PBS plus 4% bovine serum albumin (BSA). Duck NLRP3-2xFLAG was stained using an anti-FLAG mouse antibody conjugated to Alexa Fluor 647 (Life Tech). CASP-Myc was detected using an anti-Myc mouse primary monoclonal antibody (9E10; Invitrogen) and then a goat anti-mouse secondary antibody conjugated to Alexa Fluor 549 (Life Tech). IL-1β-GST was stained using an anti-GST mouse antibody conjugated to FITC (Abcam). Cell nuclei were stained with a Hoechst stain 33342 (Molecular Probes™). ImageJ was used to analyze the images. Coloc2 tool in ImageJ was also used to calculate the Pearson's coefficient.

Table 1. Primer sequences for amplification and cloning of duck NLRP3 inflammasome components.

Gene	Primer	Primer Sequence (5′→3′)
NLRP3	Forward	GCAGGTGATTTTCCACATCCTGTG
	Reverse	GTCAGCAGTGGTTTCTGTTGCT
	BamHI Forward	GGATCCATGCGGGGGAAGGGAG
	FLAG Reverse	CTCGAGTCACTTGTCGTCATCGTC
	Gibson Assembly Forward	CTTAAGCTTGGTACCGAGCTCGGATCCATGGCGGGGGA AGGG
	Gibson Assembly Reverse	GTTTAAACGGGCCCTCTAGACTCGAGTCACTTGTCGTCA TCGTC
CASP1	Forward	TGAGCGGCTGCAGGGGG
	Reverse	TGAGGTTGCGGCAGGCAGA
	Internal F1	GATAGAGGAGTCCCTGTGCTGCCTAC
	Internal R1	AGGCTCTCTCCAGTGGTACCCAGT
	EcoRV Forward	GATATCATGGCGGACCAGGAGCTG
	Myc Reverse	CTCGAGTCACAGATCCTCTTCTGAGATGAGTTTTTGTTC GTGGCCTGGGAAGAGATAG
ASC	Forward	GAATCTGGGGCATCAAGAGGCAGT
	Reverse	CCCTGAGTCCTCAAAGTCCTGTGT
IL-1β	Forward	GTTTCCCGTTTGGCGTGGAG
	Reverse	GGTCGGGGTCGGGGTCGGGC
	BamHI Forward	GAGTGGATGGCGTTCGTCCCCGAC
	NotI Reverse	GCGGCCGCTGCGCCCACTCAGCTTG
	GST Forward	CAGCGGCCGCATGGCCCCTATAC
	GST Reverse	CTCGAGTCATTTTGGAGGATGGTCGCCACCAC
	Overlap PCR Forward	GCCACCTACAAGCTGAGTGGGCGCAGCGGCCGC GTTTAAACTTAAGCTTGGTACCGAGCTCGGATCCATGG
	Gibson Assembly Forward	CGTTCG CAGCGGGTTTAAACGGGCCCTCTAGACTCGAGTCATTT
	Gibson Assembly Reverse	TGGAG

Table 2. Primer sequences for sequencing duck NLRP3 inflammasome components.

Gene	Primer	Primer Sequence (5′→3′)
NLRP3	Internal F1	GTTTCCCGTTTGGCGTGGAG
	Internal F2	CTCTGACTGCGCTTCCTTCCAG
	Internal F3	GGTCGGGGTCGGGGTCGGGC
	Internal F4	CACAGACACTGTTTAAACCTG
IL-1β	BGHR	GTTTCCCGTTTGGCGTGGAG
	GST	CAGCGGCCGCATGGCCCCTATAC
Vector	M13 F	GTAAAACGACGGCCAG
	M13R	CAGGAAACAGCTATGAC
	T7-pgem	TAATACGACTCACTATAGGG
	BGHR	GTTTCCCGTTTGGCGTGGAG

Table 3. Primer sequences for quantitative polymerase chain reaction of duck NLRP3 inflammasome components.

Gene	Primer	Primer Sequence (5′→3′)
NLRP3	Forward	GAGAAGGTGAAGGAGTACAA
	Reverse	TTCTTGGTGATGGTCAGG
	Probe	/56-FAM/AAGTACAGA/ZEN/GAGCACGTGGCCAGA/3IABkFQ/
IL-1β	Forward	AGGAGATTTTCGAACCCG
	Reverse	ACTTGTGGTTGATGTCGTAG
	Probe	/56-FAM/TACACCCGC/ZEN/TCCCAGTCCTTCG/3IABkFQ/
IL-18	Forward	TGCTGTGAATTGATGGTTGTG
	Reverse	ACCTGGCTATTTACATTCCG
	Probe	/56-FAM/CAGCCAGTG/ZEN/CCTCAGTTTCCCAG /31ABKFQ/
IFIT5	Forward	GGTGTCACTGTTAAGGCTTTTCTCA
	Reverse	TCCTGCGATATGCTGCTATATTTTAT
	Probe	/56-FAM/CTCCAGTGC/ZEN/CTTGTCCACTTTCCCTTTC/3IABkFQ/
GAPDH	Forward	AAATTGTCAGCAATGCCTCTTG
	Reverse	TGGCATGGACAGTGGTCATAA
	Probe	/56-FAM/ACCACCAAC/ZEN/TGCCTGGCGCC/3IABkFQ/

Table 4. Primer sequences for quantitative polymerase chain reaction of human NLRP3 inflammasome components.

Gene	Primer	Primer Sequence (5'→3')
IL-1β	Forward	AAAGGACATGGAGAACACCA
	Reverse	TGTACGATCACTGAACTGCAC
	Probe	/56-FAM/TCCCTGGAG/ZEN/GTGGAGAGCTTTCA/3IABkFQ/
IL-18	Forward	AATTTCATTGCCACAAAGTTGATG
	Reverse	CAGACCTTCCAGATCGCTTC
	Probe	/56-FAM/TGTCTTCTA/ZEN/CTGGTTCAGCAGCCATC/3IABkFQ/
IFIT5	Forward	TGCTGAGGAGAGAGCGAT
	Reverse	CTCCAACAGAATGGCCTTCA
	Probe	/56-FAM/ATGAGTGTC/ZEN/TTGATCTTATACCCAATGTCAGC/31ABKFQ/
GAPDH	Forward	AGGGTGGTGGACCTCAT
	Reverse	TGAGTGTGGCAGGGACT
	Probe	/56-FAM/CAGCAAGAG/ZEN/CACAAGAGGAAGAGAGA/31ABKFQ/

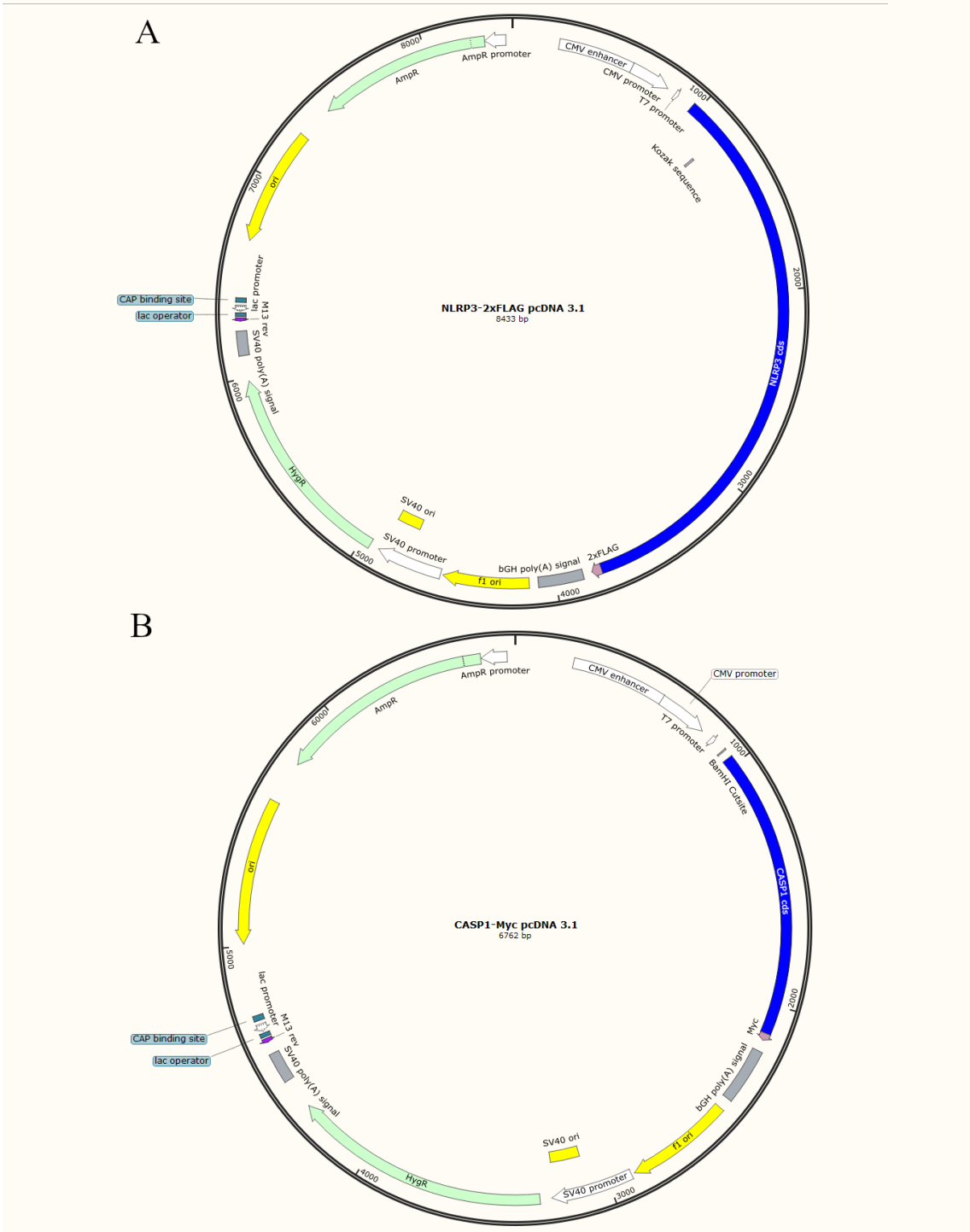
A
NLRP3-2xFLAG pcDNA 3.1
8433 bp
AmpR promoter
AmpR
CMV enhancer
CMV promoter
T7 promoter
Kozak sequence
NLRP3 cds
2xFLAG
bGH poly(A) signal
f1 ori
SV40 promoter
SV40 ori
HygR
SV40 poly(A) signal
M13 rev
lac promoter
lac operator
CAP binding site
ori
8000
1000
2000
3000
4000
5000
6000
7000
B
CASP1-Myc pcDNA 3.1
6762 bp
AmpR promoter
AmpR
CMV enhancer
CMV promoter
T7 promoter
BamHI Cutsite
CASP1 cds
Myc
bGH poly(A) signal
f1 ori
SV40 promoter
SV40 ori
HygR
SV40 poly(A) signal
M13 rev
lac promoter
lac operator
CAP binding site
ori
1000
2000
3000
4000
5000
6000

C

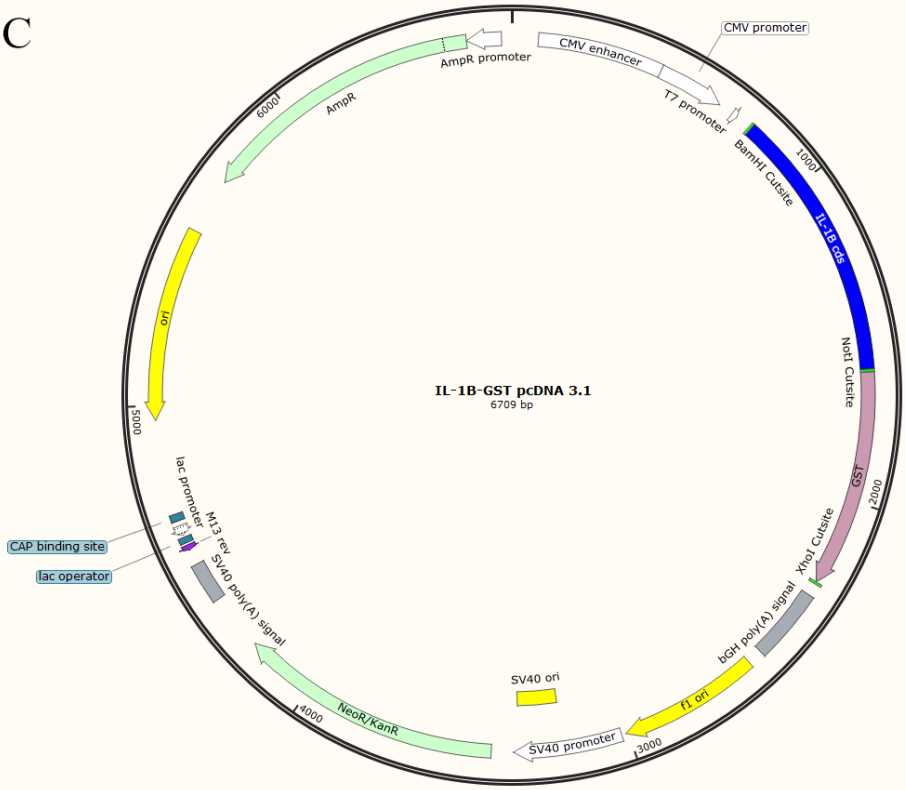
CMV promoter
CMV enhancer
AmpR promoter
T7 promoter
BamHI Cutsite
IL-1B cds
NotI Cutsite
GST
XhoI Cutsite
bGH poly(A) signal
f1 ori
SV40 promoter
SV40 ori
NeoR/KanR
SV40 poly(A) signal
M13 rev
lac promoter
CAP binding site
lac operator
ori
AmpR
IL-1B-GST pcDNA 3.1
6709 bp
1000
2000
3000
4000
5000
6000

D

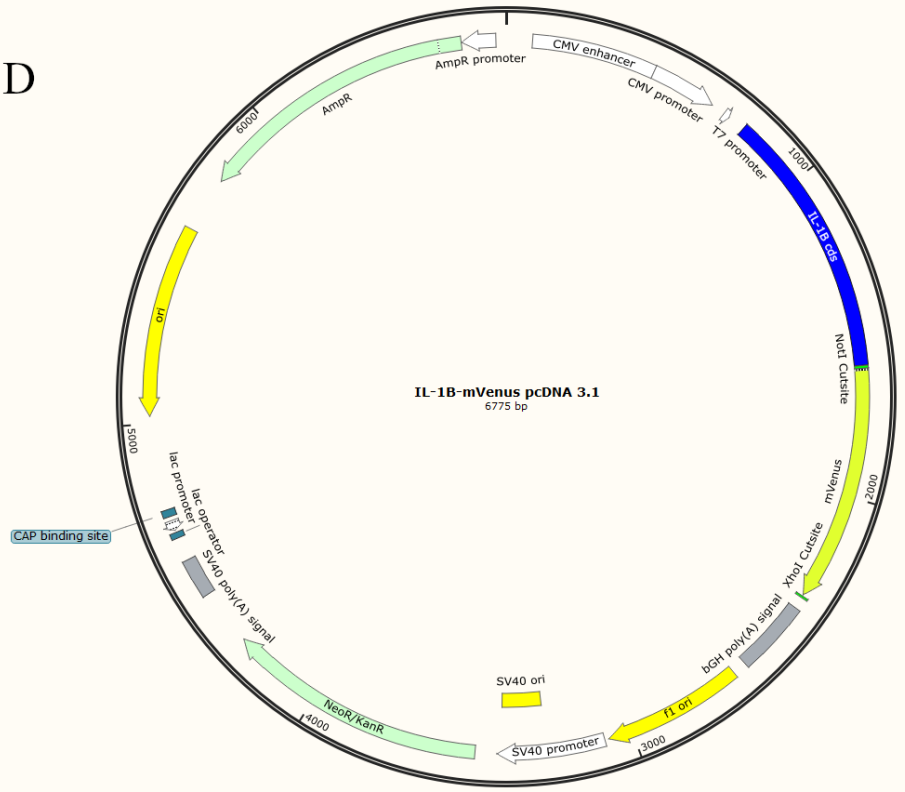
CMV enhancer
CMV promoter
AmpR promoter
T7 promoter
IL-1B cds
NotI Cutsite
mVenus
XhoI Cutsite
bGH poly(A) signal
f1 ori
SV40 promoter
SV40 ori
NeoR/KanR
SV40 poly(A) signal
lac operator
lac promoter
CAP binding site
ori
AmpR
IL-1B-mVenus pcDNA 3.1
6775 bp
1000
2000
3000
4000
5000
6000

Figure 3. Schematic of expression constructs of components of the duck NLRP3 inflammasome. All expression constructs use a pcDNA 3.1 vector backbone. A) Duck NLRP3 is epitope-tagged with 2xFLAG on the 3′ end of the coding sequence. B) Duck CASP1 is epitope-tagged with Myc on the 3′ end of the coding sequence. C) Duck IL-1β is epitope-tagged with GST on the 3′ end of the coding sequence. D) Duck IL-1β is also epitope-tagged with mVenus on the 3′ end of the coding sequence.

Chapter 3. Results

3.1 Cloning the components of the duck NLRP3 inflammasome

To assess the similarity of duck NLRP3 to that of other species, I aligned several vertebrate NLRP3 amino acid sequences (Figure 4A). Examination of the protein sequence of duck NLRP3 that we cloned and sequenced, showed that duck NLRP3 is quite different from mammalian NLRP3, sharing several patches of conserved amino acid residues and lacking other regions. Duck NLRP3 is also missing a small section of amino acid residues in the linker sequence between the PYRIN domain and the NACHT domain. When compared to NLRP3 from mammalian species, duck NLRP3 and chicken NLRP3 showed the greatest similarity to each other (Figure 4) (Table 4). Duck and chicken NLRP3 have a percent identity of 74.66%, which is comparable to the identity between human and mouse NLRP3 of 83.12%. Both avian NLRP3 proteins show a low percentage identity (36-37%) with the mammalian ones (Figure 4). I confirmed the identity of the duck NLRP3 sequence by using the SMART tool to identify the protein domains (Figure 4B). An N-terminal PYRIN domain, followed by a NACHT domain, and C-terminal LRRs were identified by SMART which is consistent with the structure of known NLRP3 proteins in other species. Phylogenetic analysis of the human, mouse, chicken, and duck NLRP3 protein sequences show that the human and the mouse NLRP3 are closely related, while the chicken and the duck NLRP3 are also more closely related (Figure 4C). The mammalian proteins group on the tree while the avian proteins group together on the tree. Furthermore, searching the NLRP3 of other species using BLAST, including human and mouse, against the

Ensembl (CAU1.0) results in an unannotated gene, ENSAPLG00000010090, as the top match. The sequence of the exons from ENSAPLG00000010090 matches my duck NLRP3 sequence.

To address the missing amino acids of duck NLRP3 in the linking section between PYRIN and NACHT domains, I performed a series of PCRs using a forward primer that binds to a segment in exon 1 and a reverse primer that binds to a segment in exon 2. I performed this PCR using both gDNA as the template as well cDNA. The gDNA PCR allowed me to confirm that the sequence of intron 1 identified in ENSAPLG00000010090 was correct and there were not any missing segments. An alignment of the sequence from the cDNA PCR and the gDNA PCR confirmed where intron 1 was removed and exons 1 and 2 were joined together (Figure 5). Taken all together, my duck NLRP3 is complete and the missing segment in the linking section between the PYRIN and NACHT domains is also missing in the genomic DNA.

The CASP1 coding sequence was identified by another graduate student in the lab, Lee K. Campbell, using transcriptomics. Based on this identified, I was able to locate, clone, and sequenced the coding sequence for CASP1. Compared to protein sequences of CASP1 from mammalian species, duck, and chicken CASP1 show the greatest similarity to one another (Figure 6). They have a percent identity of 74.35, which is higher than that of the similarity between human CASP1 and mouse CASP1. Mammalian CASP1 and avian CASP1 only share 44% percent identity. Based on the multiple sequence alignment of the different CASP1 (Figure 6), it would appear that most of the conserved amino acid residues occur in the enzymatic region of the protein as opposed to the CARD domain, which is responsible for interacting with the other components of the NLRP3 inflammasome. In humans, CASP1 is cleaved at D103 and D119 in the interdomain linker segment between the CARD domain and enzymatic subunits as well as at D297, D315, and D316 between the two enzymatic subunits (Thornberry et al. 1992;

Boucher et al. 2018). Analysis of the duck CASP1 sequences shows only D297 is conserved, the other aforementioned residues are not. However, there are other aspartate residues in the interdomain linker regions that may serve the same function. Phylogenetic analysis of human, mouse, chicken, and duck CASP1 proteins show that human and mouse are more related to each other. Chicken and duck CASP1 are more related to each other than to the mammalian CASP1. Like the duck NLRP3, the duck CASP1 protein sequence has low homology compared to the mammalian CASP1 sequences.

To identify the third component of the duck NLRP3 inflammasome, I tried to identify ASC in the duck genome currently available on *Ensembl*. I used human ASC (NP_037390.2), mouse ASC (NP_075747), cow ASC (NP_777155), pig ASC (BAV13623), zebrafish ASC (NP_571570), mainland tiger snake ASC (XP_026539257), king cobra ASC (ETE61892.1), eastern brown snake ASC (XP_026580032), and swan goose ASC (XM_013201308) as the basis for my search for duck ASC in the duck genome. The mammalian sequences align well with each other and likewise, the reptilian sequences align well with other reptile sequences (Figure 7A). The putative ASC sequence of the swan goose does not appear to align well with either the mammalian sequences or the reptilian sequences. The phylogenic tree of the aforementioned ASC sequences shows that the mammalian ASC are more closely related to each other (Figure 7B). The reptilian sequences are also related to each other, and the zebrafish ASC is closer phylogenetically closer to the reptilian sequences than the mammalian ones. The putative swan goose does not cluster with either the mammalian or the reptilian sequences. I searched for duck ASC using the other ASC sequences from all these other species against the duck genome using the BLAST tool on *Ensembl*. The top match for all of these searches was an unannotated gene, ENSAPLG00000026622. Among all the ASC sequences from other species, this gene had the

highest e-value which ranged from $1e^{-15}$ to $5e^{-21}$and percent coverage 38.10% to 50.00%. ENSAPLG00000026622 is located on the reverse strand of Primary assembly PEDO01011179.1: 61,442-66,737, which has not been identified as a part of any of the current organization of duck chromosomes. However, analysis of the amino acid sequence created by this gene using SMART showed only the CARD domain— ASC is composed of an N-terminal PYRIN domain and a C-terminal CARD domain. This lack of a PYRIN domain suggests that ENSAPLG00000026622 is not ASC or perhaps is a part of a full ASC gene.

Alongside my attempts to locate ASC in the genome, we also examined the transcriptome from DEFs treated with poly I:C followed by nigericin for ASC. The transcriptomic analysis was done by Lee K. Campbell, another graduate student in the lab. Using HMMER, amino acid sequences from human ASC (NP_075747), mouse ASC (NP_075747), and a putative ASC from *A. cygnoides* (XM_013201308) were used to search the poly I:C and nigericin treated DEF transcriptome for duck ASC. Only one transcript in the DEF transcriptome of the 40 million reads had high levels of homology with the ASC sequences from the other species. However, this sequence has some major differences compared to the ASC of other species. The average ASC sequence is about 190- 200 amino acids long. The sequence identified in the transcriptome is nearly double, about 400 amino acids. I searched the duck genome on *Ensembl* for this sequence identified from the DEF transcriptome using the BLAST tool. The sequence matched to two unidentified genes that are both located on the reverse strand of Primary assembly PEDO01011179.1: 61,442-66,737: ENSAPLG00000026622 and ENSAPLG00000021492. The predicted PYRIN domain aligned well to ENSAPLG00000021492, and the predicted CARD domain aligned well to ENSAPLG00000026622. To confirm that both parts are from the same gene, and not misassembled from two different genes. I designed primers to PCR amplify this

sequence as one piece. The forward primer is bound to the 5′-UTR of ENSAPLG00000021492, and a reverse primer is bound to the 3′-UTR of ENSAPLG00000026622. I hypothesized that this could still be the missing ASC sequence with the FIIND domain encoding segment in the center being an intron that was erroneously included. If this were the case, then ASC would be composed of the PYRIN domain of ENSAPLG00000021492 and the CARD domain of ENSAPLG00000026622.

Unfortunately, after cloning and sequencing this gene from cDNA, I found that this sequence was 1188 base pairs long with an amino acid sequence of 396 amino acids. Comparison of this sequence with the putative *A. cygnoides* sequence shows that the C-terminal end shows high homology (Figure 8A). Analysis of the identified sequence using SMART shows that this sequence contains an N-terminal PYRIN domain followed by a FIIND domain and then a C-terminal CARD domain (Figure 8B). ASC does not have a FIIND domain. The FIIND domain is characteristic of NLRP1. No duck NLRP1 has currently been identified. When compared to the human NLRP1, the identified duck sequence shows many differences (Figure 8B). This identified duck sequence does not contain a NACHT domain or LRRs, both of which are important parts of NLRP1. For this reason, and ease of discussion, I will refer to this sequence that was identified in the DEF transcriptome that contains the FIIND domain as NLRP1-like (NLRP1-L). Searches for NLRP1 in the duck genome on *Ensembl* using the human NLRP1 amino acid sequences also return ENSAPLG00000021492 and ENSAPLG00000026622 as results. Searches on Genbank using the BLASTp tool with this duck NLRP1-L sequence has the highest match to NLRP1b allele 2-like protein (XP_038027496.1) in the duck with an E-value of 0.0 and percent identity of 84.25%. Other matches include the NLRP1b-like protein from *Cygnus olor* (XP_040398490.1) as well as NLRP1b allele 2-like protein from *Meleagris*

gallopavo (XP_010708651.1). These results suggest that the protein that I have cloned and sequenced is not duck ASC but also not duck NLRP1. Additionally, this duck sequence did not show any differential expression in the transcriptome from the treated DEFs compared to the control. Furthermore, the current state of the duck genome leaves many unscaffolded pieces of gDNA in the *Ensembl* CAU_duck1.0 assembly. As a result, searching for flanking genes around ASC in other species, for example, *FUS*, *PYDC1*, *KAT8, TRIM72,* and *STX4*, in the duck genome to locate ASC was unsuccessful.

To assess the similarity of duck IL-1β with IL-1β from other species, I aligned IL-1β from human (M15330.1), mouse (NM_008361.4), chicken (NM_204524.1), and duck IL-1β that I cloned and sequenced (Figure 9A). A previous study done by Reis *et al.* (2012) examined IL-1β from many different species to assess whether the cleavage sites were conserved across species. They determined that chicken IL-1β was cleaved at aspartate residue 80 (D80), unlike in humans which process IL-1β at D116, and mice, which process at D117 (Reis et al. 2012). Examination of the IL-1β alignment between chicken and ducks shows that D80 is conserved across those species but not conserved in either of the mammalian species (Figure 9A). The avian IL-1β proteins also have low homology to mammalian IL-1β. Phylogenetic analysis of the human, mouse, chicken, and duck IL-1β shows that the human and mouse IL-1β are more closely related while the chicken and the duck IL-1β proteins are more related (Figure 9B). Taken all together, duck IL-1β retains the conserved cleavage site and would appear to be cleavable but shows low homology to mammalian IL-β.

3.2 Examining gene expression of the duck NLRP3 inflammasome

To assess the activity of the duck NLRP3 inflammasome, I examined the gene expression of the duck NLRP3 inflammasome under different stimulatory conditions. The NLRP3 inflammasome needs to be transcriptionally primed by a first signal before it can be activated (Bauernfeind et al. 2009). During this transcriptional priming, more mRNA copies of *NLRP3*, and *IL1B* are created so that sufficient proteins can be synthesized and available in the cell for activation of the NLRP3 inflammasome (Bauernfeind et al. 2009; Zhu & Kannegant, 2017). Priming can occur through the activation of TLRs by their respective ligands. Based on a study performed by Bauernfeind *et al.* (2009) which showed that stimulating TLR3 using poly I:C was able to prime the NLRP3 inflammasome, I used poly I:C as my priming signal before treating with nigericin, an activating signal. I used a concentration of 1µg/mL of poly I:C as the priming signal, similar to Bauernfeind *et al.* (2009. Additionally, based on Mousani *et al.* (2019), I used 20µM of nigericin as the activating signal. The transcriptome was sequenced from RNA collected from DEFs that were treated with poly I:C for 3 hours and nigericin for 1 hour, and untreated DEFs. Because this was an exploratory experiment, only one sample of each condition was submitted for RNA sequencing.

Differential expression analysis of the transcriptome of DEFs treated with poly I:C followed by nigericin showed many interferon-stimulated genes were strongly upregulated by treatment with poly I:C, like *RSAD2* and *IFIT5* (Figure 10). There was also an additional gene signature alongside the genes that are known to be upregulated by poly I:C which suggests that nigericin stimulated the DEFs. However, I saw no upregulation of the components of the duck NLRP3 inflammasome compared to untreated DEFs. Additionally, *CASP1* and *IL1B* did not show any differential expression when compared to the untreated control DEFs. A gene set enrichment analysis performed on genes that had a differential expression greater than 1.5 and

less than -1.5 using WEBGESTALT and the Reactome pathway database showed the immune system and innate immune system pathways were upregulated in response to the poly I:C and nigericin treatment compared to the control while genes in the hemostasis and metabolism were downregulated in those treatments (Figure 11). This indicates that an immune response was induced by treatment of the DEFs with poly I:C and nigericin, however, the NLRP3 inflammasome was not upregulated as a part of that response. However, the RNA-sequencing and subsequent transcriptome analysis were performed on only one sample of poly I:C and nigericin treated DEFs and one sample of untreated DEFs.

To assess whether to perform additional replicates of the RNA-seq experiment on poly I:C and nigericin-treated DEFs, I used qPCR to examine the gene expression of NLRP3 inflammasome genes after stimulation. The qPCR results would also help confirm whether the poly I:C and nigericin treatments were inducing effects on the DEF cells. I performed qPCRs on DEFs treated with only poly I:C for 4 hours or DEFs treated poly I:C for 3 hours then stimulated with nigericin for 1 hour. This would assess how that stimulation of DEFs with poly I:C alone (the priming signal), or poly I:C then followed by nigericin (the priming and activating signals) could differ. I chose to examine the expression of *NLRP3, IL1B, and IL18* after treatment with priming and activating signals because *NLRP3 and IL1B* are upregulated after priming. *IL18,* on the other hand, is not upregulated by priming signals and was used as a control (Bauernfeind et al. 2009). *IFIT5* was used as a positive control because it is an interferon-stimulated gene that is upregulated by poly I:C (Zhang et al. 2013; Vanderven et al. 2012). Examination of the qPCR results shows that the poly I:C treated DEFs, regardless of whether nigericin was present, does not upregulate *NLRP3*, *IL1B*, or *IL18* compared to untreated Pekin DEFs (Figure 12A-C). I found that *IFIT5* was upregulated strongly in Pekin DEFs in response to the treatment, indicating

that the cells do respond to the treatment (Figure 12D). Treatment of A549 with the same poly I:C and poly I:C then nigericin conditions showed that human *IL1B* and *IFIT5* were upregulated in response (Figure 13). However, human *IL18* did not exhibit any upregulation after treatment, further indicating that the upregulation of cytokines in response to treatment with poly I:C had specificity (Figure 13). Interestingly, human *IFIT5* showed a lower fold change than the duck *IFIT5* under the same treatment conditions (Figure 12D, 13C). Based on the qPCR results, we decided against performing additional RNA-seq experiments.

To examine how the duck NLRP3 inflammasome has a dampened transcriptional priming response, I identified the duck NLRP3 promoter. Currently, no NLRP3 promoter has been identified in the duck. Based on the work done by Anderson *et al.* (2008) in identifying the human NLRP3 promoter and previous work done in our lab on the RIG-I promoter by Xiao *et al.* (2018), I analyzed 4kb of genomic sequence upstream of the duck NLRP3 coding sequence with similar methods. Using the JASPAR 2020 database, I was able to find a putative duck NLRP3 promoter in the 5′-UTR (at 1398 bp upstream of the duck NLRP3 translational start site) that included predicted transcription factor binding sites for NF-κB, SP-1, SP-2, IRF1, and STAT1 (Figure 14). The transcription binding sites are the same for SP-1 and SP-2, indicating that this binding site could be a GC-box. There is a putative TATA box at 1398 bp upstream of the translational start site and a sequence (CTATTCC) that starts at 1086 bp upstream that matches a mammalian initiator sequence (YYANWYY) (Yang et al. 2007). Further experiments are needed to confirm whether this putative sequence is the true duck NLRP3 promoter, but preliminary analysis suggests that this would be a reasonable candidate.

3.3 Treatment of Pekin duck embryonic fibroblasts with poly I:C and nigericin induces changes in cell phenotype

To assess whether nigericin affected the DEFs, I examined the DEFs treated with poly I:C, poly I:C, and then nigericin for 1 hour or 24 hours, or untreated DEFs, under a brightfield microscope to assess changes in the cell phenotype. After priming with poly I:C followed by treatment with nigericin, DEFs take on a visually different phenotype compared to the untreated controls and cells given only the priming signal for a similar amount of time (Figure 15). The nigericin-treated DEFs appeared to be larger and more swollen (Figure 15G-I). Also noticeable in the brightfield microscopy images is that the nigericin-treated DEFs have a dotted cytoplasm which looks like cells that are highly vacuolated (Figure 15G-I). A longer treatment of the DEFs with nigericin for 24 hours also does not induce any further changes in the cell phenotype (Figure 15J-L). The change in phenotype of the DEFs between untreated controls, cells that were only primed with poly I:C, and cells that were primed and then treated with nigericin, indicates that nigericin can induce a cellular response from the DEFs.

3.4 Co-transfection of duck NLRP3 inflammasome components in chicken embryonic fibroblasts and human embryonic kidney cells

To determine whether the duck NLRP3 inflammasome proteins can interact with each other to induce IL-1β activation, expression constructs were created of duck NLRP3, duck CASP1, and duck IL-1β. Each of these proteins was epitope-tagged and inserted into a pcDNA 3.1 vector backbone. Duck NLRP3 was tagged with 2xFLAG (Figure 16). Duck CASP1 was

tagged with Myc (Figure 16). Duck IL-1β was tagged with GST as well as mVenus in two separate expression constructs (Figure 16). Overexpression of NLRP3 can form ASC specks without the need for a priming or activating signal (Hoss et al. 2019; Yu et al. 2006). CASP1 and IL-1β activation can also be induced as a result of NLRP3 overexpression (Wang et al. 2020; Yu et al. 2006). Initially, I transfected my duck NLRP3 inflammasome recombinant constructs into primary DEFs. The recombinant proteins would be able to interact with the endogenous duck proteins with certainty. However, I was unable to detect any recombinant protein expression during transfections using primary DEFs. Transfections of single duck constructs into the DEFs were not successful and no protein bands were detected on the Western blot. After several failed transfections using the primary DEFs, I switched to using DF-1 cells. The chicken NLRP3 inflammasome components have high homology with the duck NLRP3 inflammasome components so I hypothesized that endogenous chicken proteins would be able to interact with the recombinant duck proteins. Additionally, the DF-1 cells have a higher transfection efficiency than the primary DEFs which would allow better transfection of the duck constructs. However, I found that co-transfections of duNLRP3-FLAG, duCASP1-Myc, and duIL-1β- GST into DF-1 cells resulted in the decreased recovery of recombinant proteins (Figure 17). Transfections of these constructs on their own showed strong protein bands on Western blots. duNLRP3-2xFLAG was seen at about 100 kDa. duCASP1-Myc was seen at about 45 kDa while activated duCASP1-Myc would be visible at about 12 kDa. duIL-1β- GST was seen at 55kDA while activated duIL-1β-GST would be visible at about 45kDA. Neither activated duck CASP1 nor activated duck IL-1β was detected in the Western blots with lysates from DF-1 cells.

In contrast, co-transfection of duNLRP3, duCASP1, and duIL-1β into HEK293T cells does not exhibit the same decrease in detection as co-transfections in the DF-1 cells (Figure 18).

Protein expression is detectable for duNLRP3-2xFLAG, duCASP1-Myc, and duIL-1β-GST during co-transfections and is also comparable to levels in transfections of these constructs by themselves. This indicates that there is no issue with promoter interference upon co-transfection. The inability to detect the proteins on a Western blot during transfection in DF-1 cells can be attributed to interactions between the duck recombinant proteins and interactions between the duck recombinant proteins and other avian proteins in the avian system. Furthermore, activated duck CASP1 and activated duck IL-1β were not detected on the Western blots with the lysates from HEK293T cells either. Taken together with the Western blots using lysates from DF-1 cells, this lack of a detectable activated CASP1 or IL-1β could suggest that duck CASP1 and duck IL-1β are not activated when my duck NLRP3 recombinant proteins are overexpressed, or I am not able to detect these activated proteins on the Western blots.

3.5 Examination of the duck NLRP3 inflammasome components in DF-1 cells using immunofluorescence.

To determine whether duck NLRP3 inflammasome components interact with each other, I co-transfected the duck NLRP3 inflammasome components into DF-1 cells and stained them with antibodies tagged with fluorescent probes to examine co-localization. Transfection of the duck NLRP3-2xFLAG in DF-1 cells shows that the recombinant protein spreads diffusely throughout the entire cytoplasm (Figure 19). Transfection of duck CASP1-Myc by itself in DF-1 cells shows that this recombinant protein forms punctate structures in the cytoplasm (Figure 20). Transfection of duck IL-1β-mVenus shows localization to the nucleus of the cell (Figure 21). However, I found string-like structures when DF-1 cells transfected with duck IL-1β -mVenus

were stained with the secondary antibodies that I used to stain the other duck NLRP3 inflammasome recombinant proteins (Figure 22). However, I am unable to tell whether duck IL-1β-mVenus is interacting with the primary antibodies that were used or the secondary antibodies. These string-like structures fluoresced in multiple channels on the confocal microscope with such intensity that all other fluorescent signals were washed out and undetectable. This renders any attempts to examine co-transfections of duck NLRP3-2xFLAG, duck CASP1-Myc, and duck IL-1β-mVenus using confocal microscopy impossible. For this reason, I swapped out my duck IL-1β-mVenus construct for the duck IL-1β-GST construct. Transfection of DF-1 cells with duck IL-1 β-GST showed that duck IL-1β-GST, like duck IL-1β-mVenus, is also localized to the nuclei of the cell with some present in the cytoplasm (Figure 23). This also confirms that the localization of duck IL-1β is not induced by the epitope tag attached to it. Confocal images of the untransfected DF-1 cells show very low levels of background staining when treated with the same antibodies used to stain the DF-1 cells transfected with the duck NLRP3 inflammasome components (Figure 29). Staining using the mouse anti-GST antibody conjugated to FITC does show faint fluorescence in the cytoplasm of the cell which could contribute to the detection of duck IL-1β in the cytoplasm of the cell.

I examined the co-localization of duck NLRP3-2xFLAG and duck CASP1-Myc co-transfected in DF-1 cells (Figure 24). Duck NLRP3-2xFLAG remains in the cytoplasm but appears to form more speck-like structures when co-transfected with duck CASP1-Myc than on its own. However, not all specks formed by duck NLRP3-2xFLAG co-localized with duck CASP1-Myc (Figure 24). Analysis of 8 images with the Coloc2 tool on ImageJ determined that NLRP3-2xFLAG and CASP1-Myc had a Pearson's correlation coefficient of 0.69 (Figure 28), indicating that there is moderate colocalization of these two proteins. Co-localization of duck

NLRP3 and duck CASP1 in the cytoplasm suggests that the duck NLRP3 inflammasome formed in the DF-1 cells. Co-transfection of DF-1 cells with duck NLRP3-2xFLAG and IL-1β-GST exhibits no co-localization (Figure 25). NLRP3-2xFLAG remains spread diffusely throughout the cytoplasm and IL-1β GST remains localized to the nucleus of the cell. These two proteins were visible as two distinct populations within the co-transfected DF-1 cells. Similarly, co-transfections of duck L-1β-GST and CASP1-Myc exhibit no co-localization (Figure 26). Duck CASP1-Myc remains as punctate structures in the cytoplasm of the cell while IL-1β-GST is seen in the nucleus of the cell.

Co-transfections of duck NLRP3-2xFLAG, duck CASP1-Myc, and duck IL-1β-GST into DF-1 cells showed some co-localization of the different components (Figure 27). Duck NLRP3-2xFLAG and duck CASP1-Myc remained in the cytoplasm of the cell. The specks formed by duck NLRP3-2xFLAG did co-localize with the punctate structures of duck CASP1-Myc. Analysis of 8 separate images from 1 slide using the Coloc2 tool in ImageJ determined that co-localization between NLRP3-2xFLAG and CASP1-Myc had a Pearson's coefficient of 0.63 (Figure 28). This would indicate that moderate co-localization was occurring between these two proteins and suggested that the duck NLRP3 inflammasome formation occurred. On the other hand, IL-1β-GST remained heavily localized to the nucleus of the cell with some present in the cytoplasm of the cell, possibly background staining from the antibodies (Figure 28). There did appear to be some specks formed by IL-1β-GST in the cytoplasm and the nucleus. The IL-1β-GST specks in the nucleus did co-localize with CASP1-Myc. However, the CASP1-Myc specks were quite faint in the nucleus compared to the ones visible in the same cell in the cytoplasm. The few bright IL-1β-GST specks in the cytoplasm did co-localize with NLR33-2xFLAG and CASP1-Myc specks, further suggesting that. Despite that, the bulk of the IL-1β -GST protein

expression remained localized to the nucleus of the cell. The co-localization of duck NLRP3 and duck CASP1 in DF-1 cells suggests that the duck NLRP3 inflammasome components were able to interact with the endogenous chicken ASC protein and form an inflammasome.

A

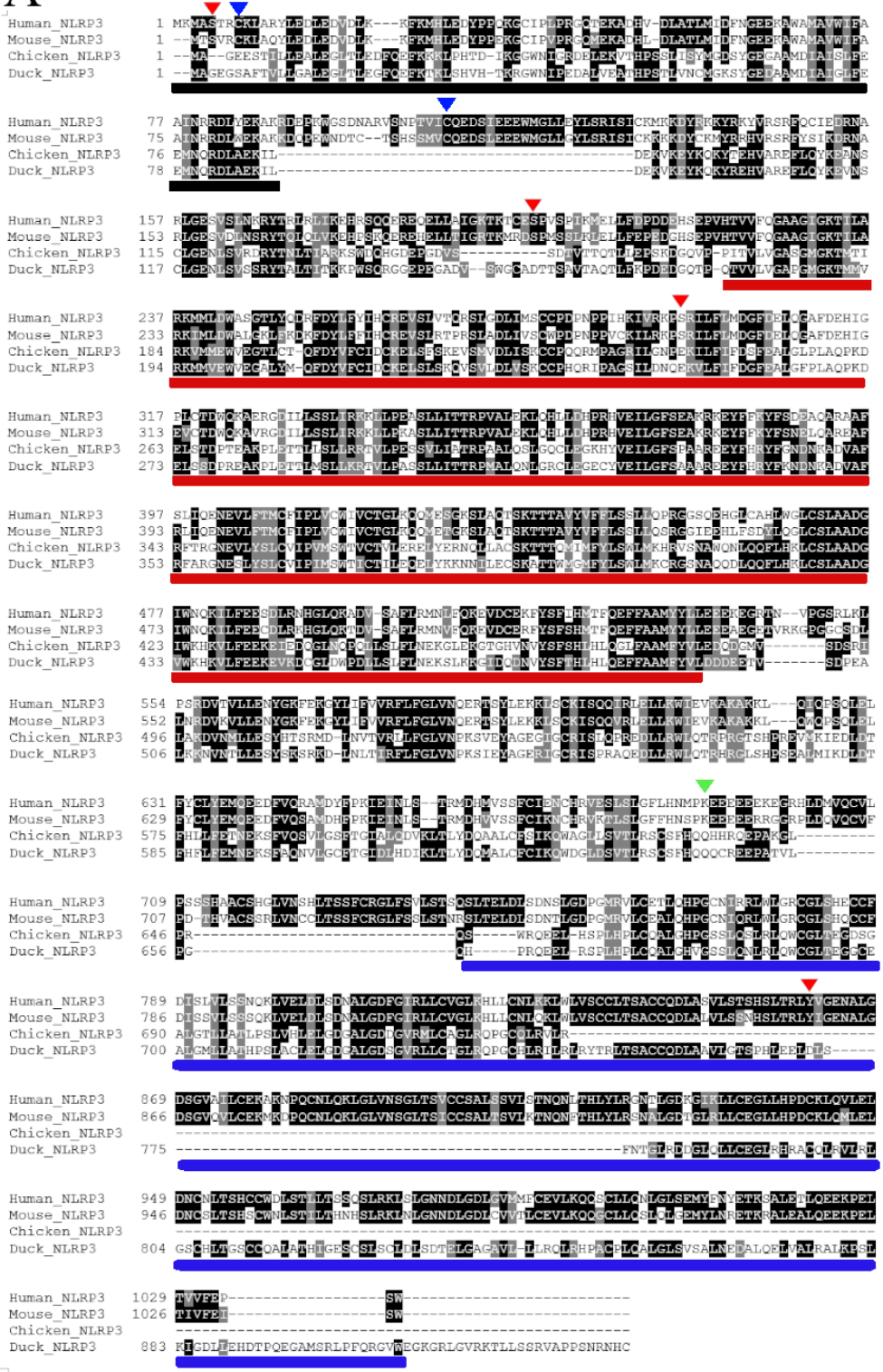
Human_NLRP3
Mouse_NLRP3
Chicken_NLRP3
Duck_NLRP3

B


PYRIN
Pfam
NACHT
LRR
LRR
LRR
LRR
LRR
LRR
0
100
200
300
400
500
600
700
800
900

C

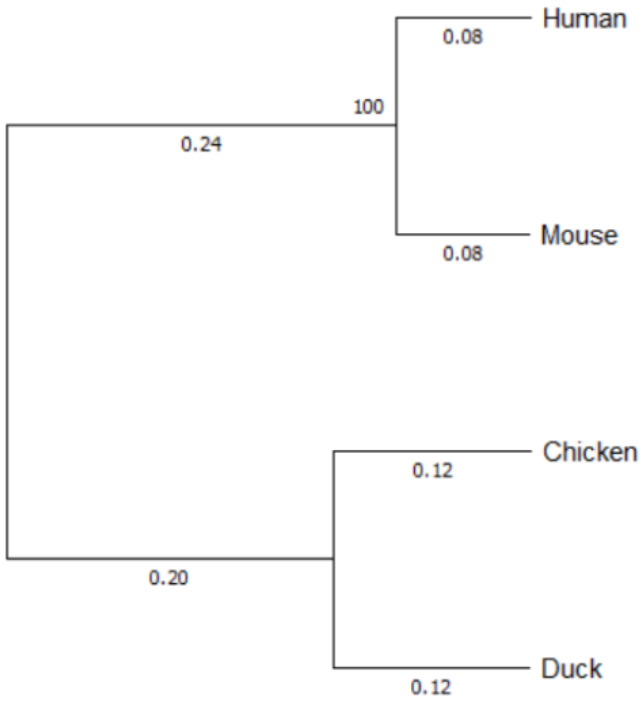

Figure 4. Alignment of human, mouse, chicken, and duck NLRP3. A) Alignment was created using Clustal Omega and edited using Boxshade. Black shading indicates amino acid conservation and grey shading indicates similarity between the amino acid residues. Protein sequences are shown for human NLRP3 (NM_004895), mouse NLRP3 (NM_145827), and chicken NLRP3 (KF318520), and duck NLRP3 that I cloned and sequenced from Pekin ducks. The black underline indicates the start and end amino acid residues of the PYRIN domain in humans and mice. The red underline indicates the start and end amino acid residues of the NACHT domain in humans and mice. The blue underline indicates the start and end amino acid residues of the LRRs in humans and mice. Red arrowheads indicate sites of phosphorylation in

mammalian NLRP3. Blue arrowheads indicate cysteine residues involved in a disulfide bond in mammalian NLRP3. Green arrowheads indicate ubiquitination sites conserved by mammalian NLRP3. B) Analysis of predicted protein domains of duck NLRP3 using SMART. Duck NLRP3 contains PYRIN, NACHT, and LRRs. C) Phylogenetic tree of the aligned sequences was created using MEGA11 with bootstrap analysis (Neighbour-Joining method, 1000 replicates, Poisson mode). Numbers underneath the branches indicate the distance between each node and the number of substitutions per site. Numbers at the node above the branch indicate bootstrap values.

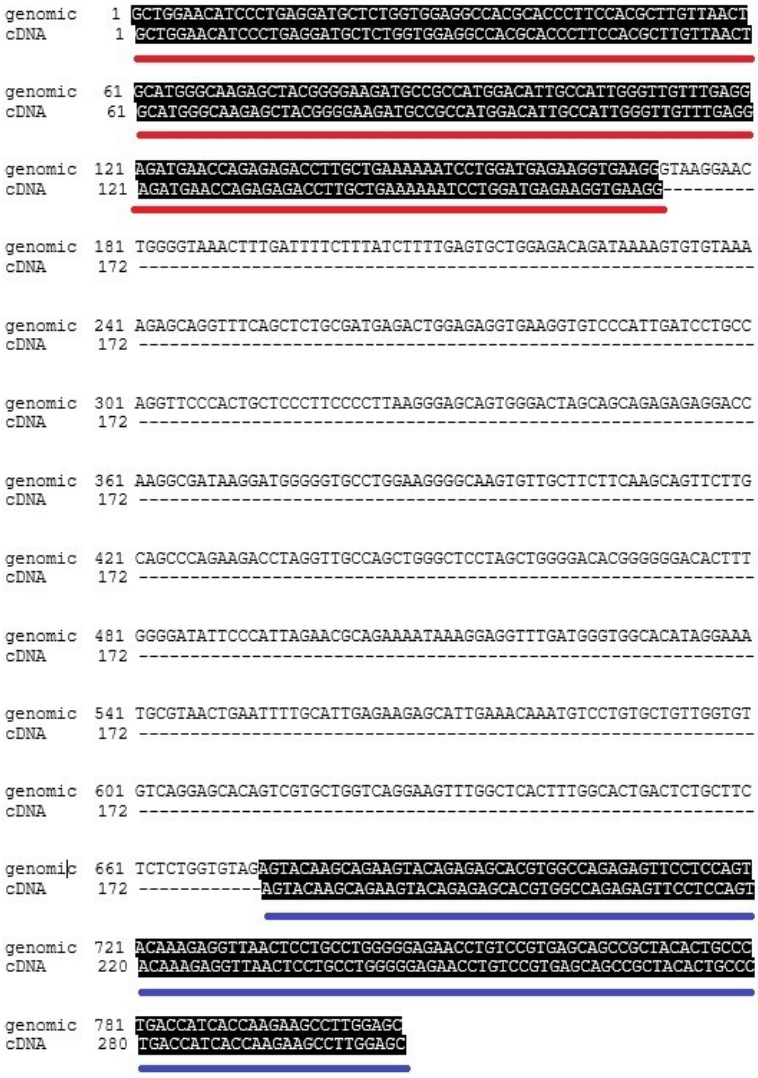

Figure 5. Alignment of duck NLRP3 intron 1. Multiple sequence alignment of duck NLRP3 cDNA sequence and genomic sequence. Alignment was created using T-COFFEE and edited using Boxshade. Black shading indicates amino acid conservation and grey shading indicates similarity between the amino acid residues. The red underline shows the last 173 base pairs of exon 1 of duck NLRP3. The blue underline shows the first 134 base pairs of exon 2 of duck NLRP3. Intron 1 can be seen in the genomic DNA sequence between nucleotides 174 and 649.

Table 5. Similarities between the chicken and duck components of the NLRP3 inflammasome. Percent identity matrix created by Clustal 2.1 comparing the protein sequence of duck NLRP3 and chicken NLRP3 (accession number NP_001335876.1), duck CASP1, and chicken CASP1 (XP_003642432), and duck and chicken IL-1β (NM_204524). Dashes indicate alignments and percent identity analyses were not performed on those pairs of sequences. All duck sequences were from samples that I cloned, sequenced, and translated.

	Duck NLRP3	Chicken NLRP3	Duck CASP1	Chicken CASP1	Duck IL-1β	Chicken IL-1β
Duck NLRP3	100.00	74.24	-	-	-	-
Chicken NLRP3	74.24	100.00	-	-	-	-
Duck CASP1	-	-	100.00	74.35	-	-
Chicken CASP1	-	-	74.35	100.00	-	-
Duck IL-1β	-	-	-	-	100.00	82.40
Chicken IL-1β	-	-	-	-	82.40	100.00

A

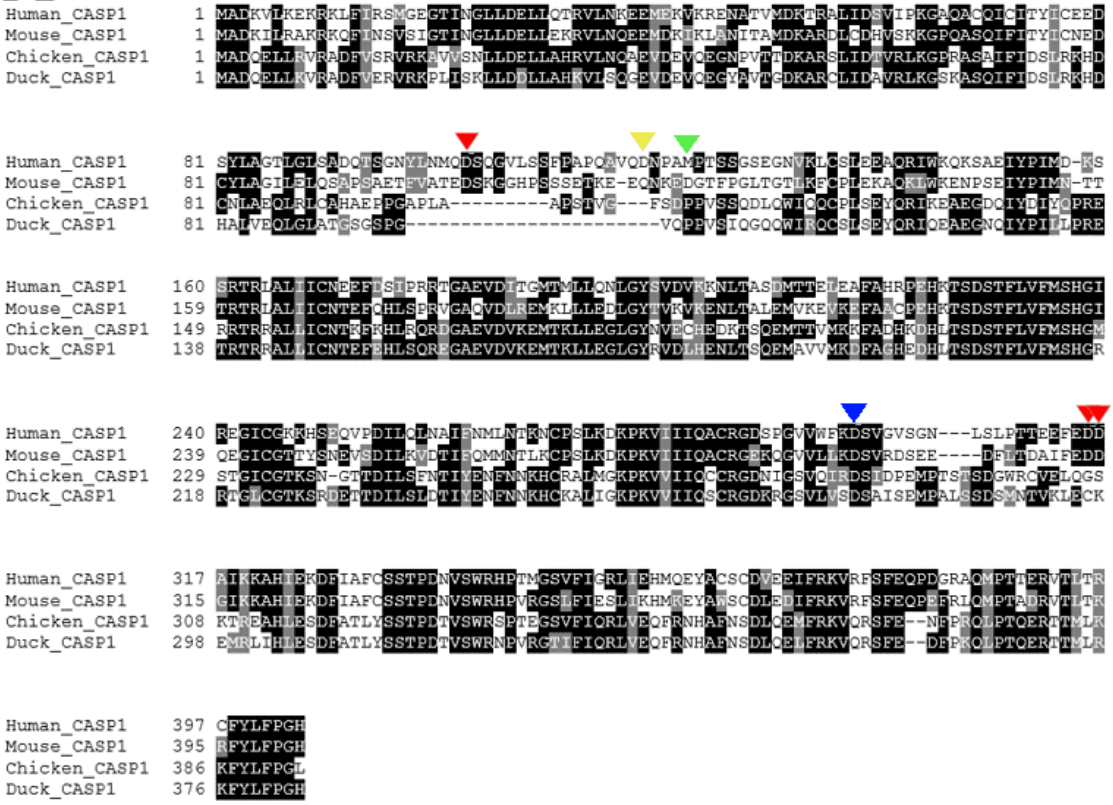
Human_CASP1
Mouse_CASP1
Chicken_CASP1
Duck_CASP1

B

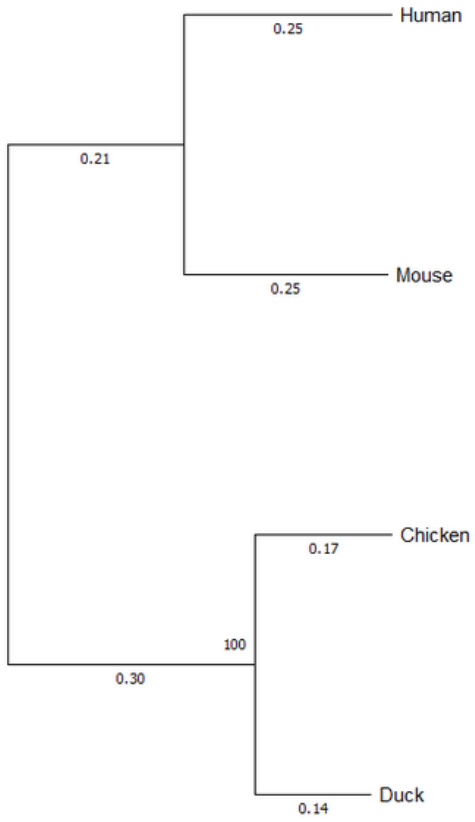
Human
0.25
0.21
Mouse
0.25
Chicken
0.17
100
0.30
Duck
0.14

Figure 6. Alignment of human, mouse, chicken, and duck CASP1. A) Alignment was created using T-COFFEE and edited using Boxshade. Black shading indicates amino acid conservation and grey shading indicates similarity between the amino acid residues. Protein sequences are shown for chicken CASP1 (XM_040687588), duck CASP1 cloned and sequenced from Pekin ducks, human CASP1 (NM_001257118), and mouse CASP1 (NM_009807). Red arrowheads denote CASP1 processing sites conserved in human CASP1 and mouse CASP1. Yellow arrowheads denote CASP1 processing sites conserved in human CASP1. Green arrowheads denote CASP1 in mouse CASP1. Blue arrowheads denote processing sites conserved in human, mouse, chicken, and duck CASP1. B) Phylogenetic tree of the aligned sequences was created using MEGA11 with bootstrap analysis (Neighbour-Joining method, 1000 replicates, Poisson mode). Numbers underneath the branches indicate the distance between each node and the number of substitutions per site. Numbers at the node above the branch indicate bootstrap values.

A

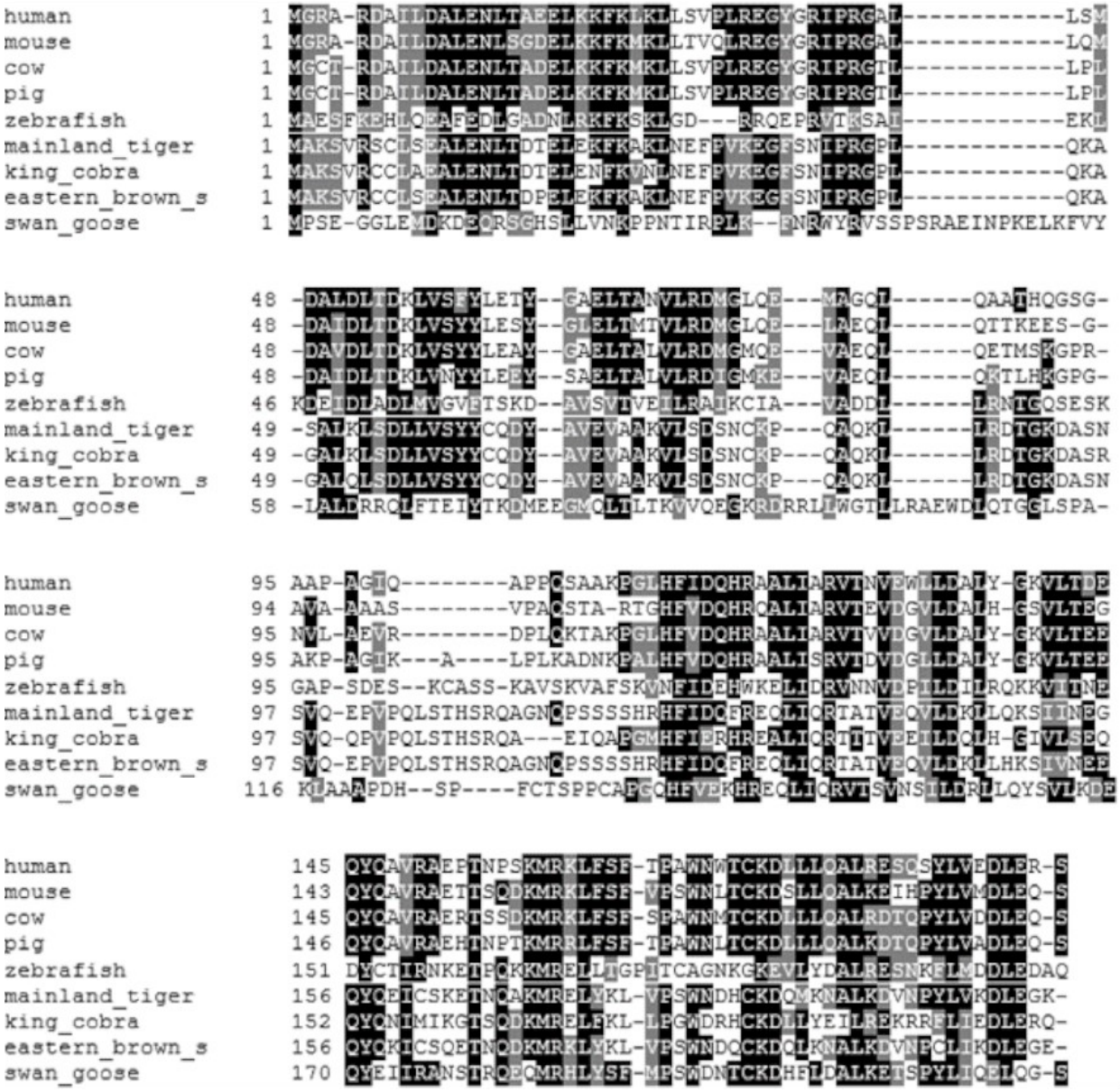
human
mouse
cow
pig
zebrafish
mainland_tiger
king_cobra
eastern_brown_s
swan_goose

B

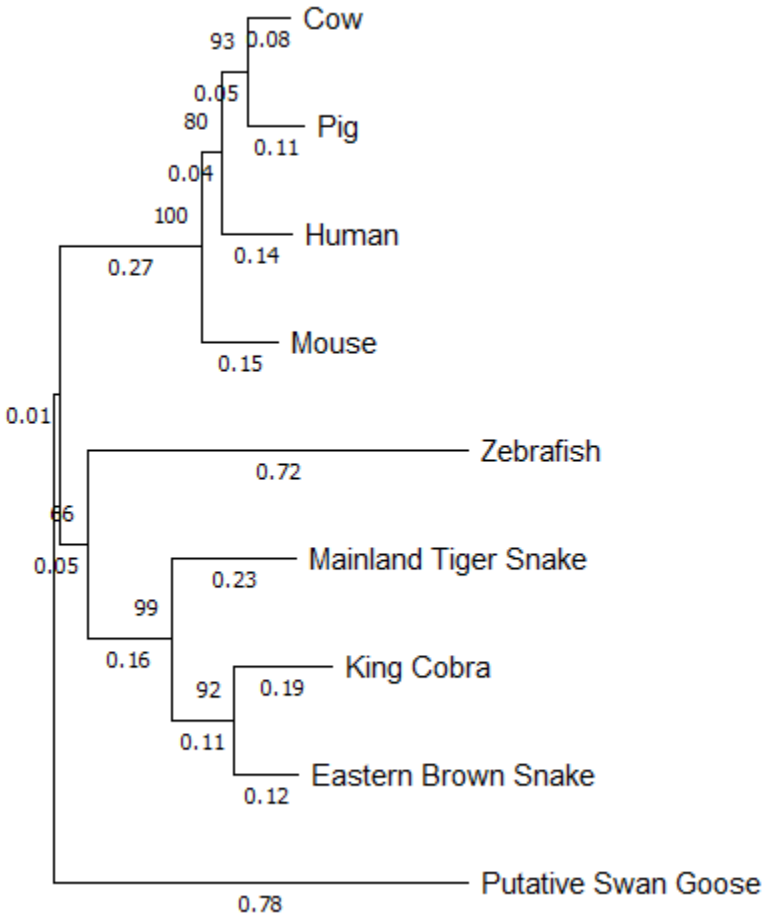

Figure 7. Alignment of ASC protein sequences from different species used in the search for duck ASC. A) Multiple sequence alignment was performed using T-COFFEE and edited using Boxshade. Black shading indicates amino acid conservation and grey shading indicates similarity between the amino acid residues. Human ASC (NP_037390.2), mouse ASC (NP_075747), cow ASC(NP_777155), pig ASC (BAV13623), zebrafish ASC (NP_571570), mainland tiger snake ASC (XP_026539257), king cobra (ETE61892.1), eastern brown snake (XP_026580032), swan goose ASC (XP_013056762) were aligned. B) Phylogenetic tree of the aligned sequences was created using MEGA11 with bootstrap analysis (Neighbour-Joining method, 1000 replicates,

Poisson mode). Numbers underneath the branches indicate the distance between each node and the number of substitutions per site. Numbers at the node above the branch indicate bootstrap values.

A

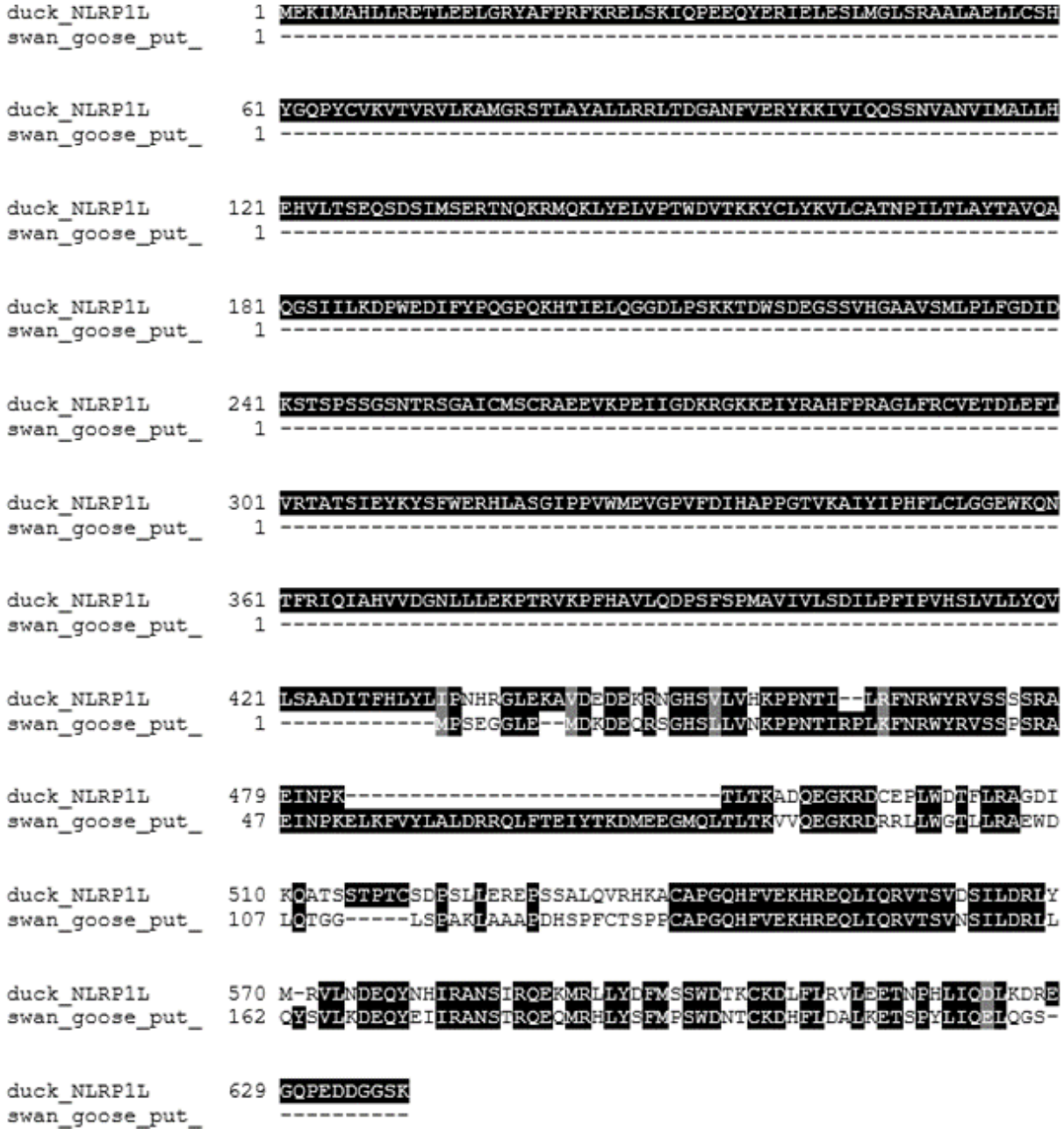
duck_NLRP1L 1 MEKIMAHLLRETLEELGRYAFPRFKRELSKIQPEEQYERIELESLMGLSRAALAELLCSH
swan_goose_put_ 1 ----------
duck_NLRP1L 61 YGQPYCVKVTVRVLKAMGRSTLAYALLRRLTDGANFVERYKKIVIQQSSNVANVIMALLH
swan_goose_put_ 1 ----------
duck_NLRP1L 121 EHVLTSEQSDSIMSERTNQKRMQKLYELVPTWDVTKKYCLYKVLCATNPILTLAYTAVQA
swan_goose_put_ 1 ----------
duck_NLRP1L 181 QGSIILKDPWEDIFYPQGPQKHTIELQGGDLPSKKTDWSDEGSSVHGAAVSMLPLFGDID
swan_goose_put_ 1 ----------
duck_NLRP1L 241 KSTSPSSGSNTRSGAICMSCRAEEVKPEIIGDKRGKKEIYRAHFPRAGLFRCVETDLEFL
swan_goose_put_ 1 ----------
duck_NLRP1L 301 VRTATSIEYKYSFWERHLASGIPPVWMEVGPVFDIHAPPGTVKAIYIPHFLCLGGEWKQN
swan_goose_put_ 1 ----------
duck_NLRP1L 361 TFRIQIAHVVDGNLLLEKPTRVKPFHAVLQDPSFSPMAVIVLSDILPFIPVHSLVLLYQV
swan_goose_put_ 1 ----------
duck_NLRP1L 421 LSAADITFHLYLMPNHRGLEKAVDEDEKRNGHSVLVHKPPNTI--LRFNRWYRVSSSSRA
swan_goose_put_ 1 ----------MESEGGLE--MDKDEQRSGHSLLVNKPPNTIRPLKFNRWYRVSSPSRA
duck_NLRP1L 479 EINPK----------TLTKADQEGKRDCEPLWDTFLRAGDI
swan_goose_put_ 47 EINPKELKFVYLALDRRQLFTEIYTKDMEEGMQLTLTKVVQEGKRDRRLLWGTLLRAEWD
duck_NLRP1L 510 KQATSSTPTCSDESLLEREPSSALQVRHKACAPGQHFVEKHREQLIQRVTSVDSILDRLY
swan_goose_put_ 107 LQTGG-----LSEAKLAAAPDHSPFCTSPPCAPGQHFVEKHREQLIQRVTSVNSILDRLL
duck_NLRP1L 570 M-RVLNDEQYNHIRANSIRQEKMRLLYLFMSSWDTKCKDLFLRVLEETNPHLIQDLKDRE
swan_goose_put_ 162 QYSVLKDEQYEIIRANSTRQEQMRHLYSFMPSWDNTCKDHFLDALKETSPYLIQELQGS-
duck_NLRP1L 629 GQPEDDGGSK
swan_goose_put_ ----------

B

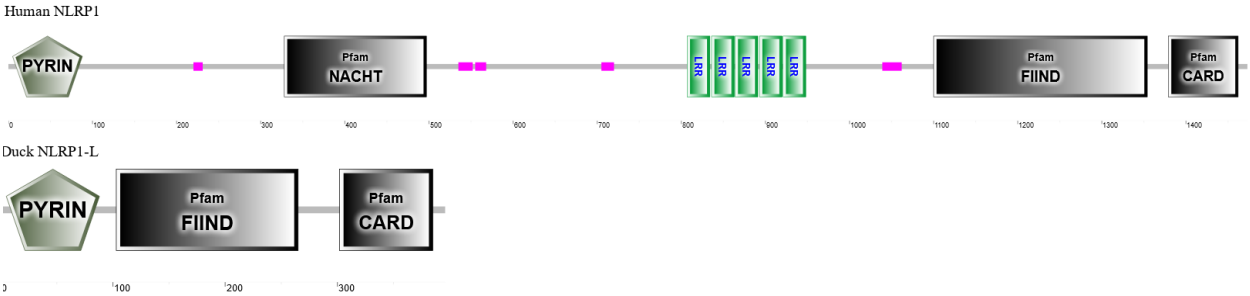
Human NLRP1
PYRIN
Pfam NACHT
LRR
LRR
LRR
LRR
LRR
Pfam FIIND
Pfam CARD
0
100
200
300
400
500
600
700
800
900
1000
1100
1200
1300
1400
Duck NLRP1-L
PYRIN
Pfam FIIND
Pfam CARD
0
100
200
300

Figure 8. Alignment of duck NLRP1-like protein with putative swan goose ASC. A) Alignment of the amino acid sequence of putative swan goose ASC (XM_013201308) and duck NLRP1-L amino acid sequence that I cloned and sequenced. Multiple alignment sequences were made with T-COFFEE, and the alignment was edited using Boxshade. Black shading in both lines indicates amino acid conservation and grey shading indicates similarity between the amino acid residues. B) Protein domain architecture analysis of both human NLRP1 and duck NLRP1-L amino acid sequences were analyzed using SMART.

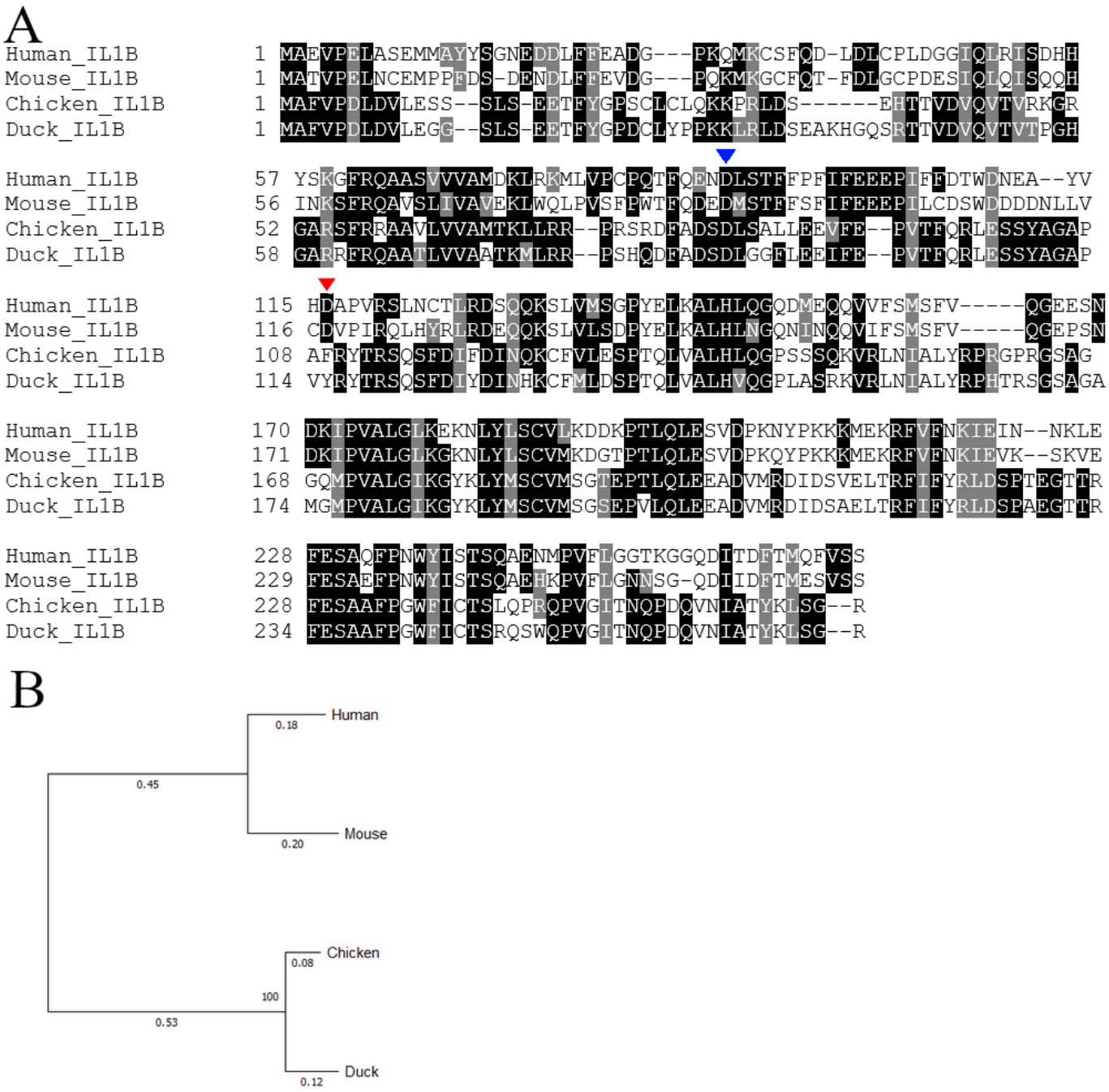

Figure 9. Alignment of IL-1β protein sequences from different species. A) Alignment was created using T-COFFEE and edited using Boxshade. Black shading indicates amino acid conservation and grey shading indicates similarity between the amino acid residues. Human IL-1β,(M15330.1), mouse IL-1β (NM_008361.4), chicken IL-1β (NM_204524.1), and duck IL-1β

were aligned. The blue arrowhead denotes the avian processing site of IL-1β. The red arrowhead denotes the mammalian processing site of IL-1β. B) Phylogenetic tree of the aligned sequences was created using MEGA11 with bootstrap analysis (Neighbour-Joining method, 1000 replicates, Poisson mode). Numbers underneath the branches indicate the distance between each node and the number of substitutions per site. Numbers at the node above the branch indicate bootstrap values.

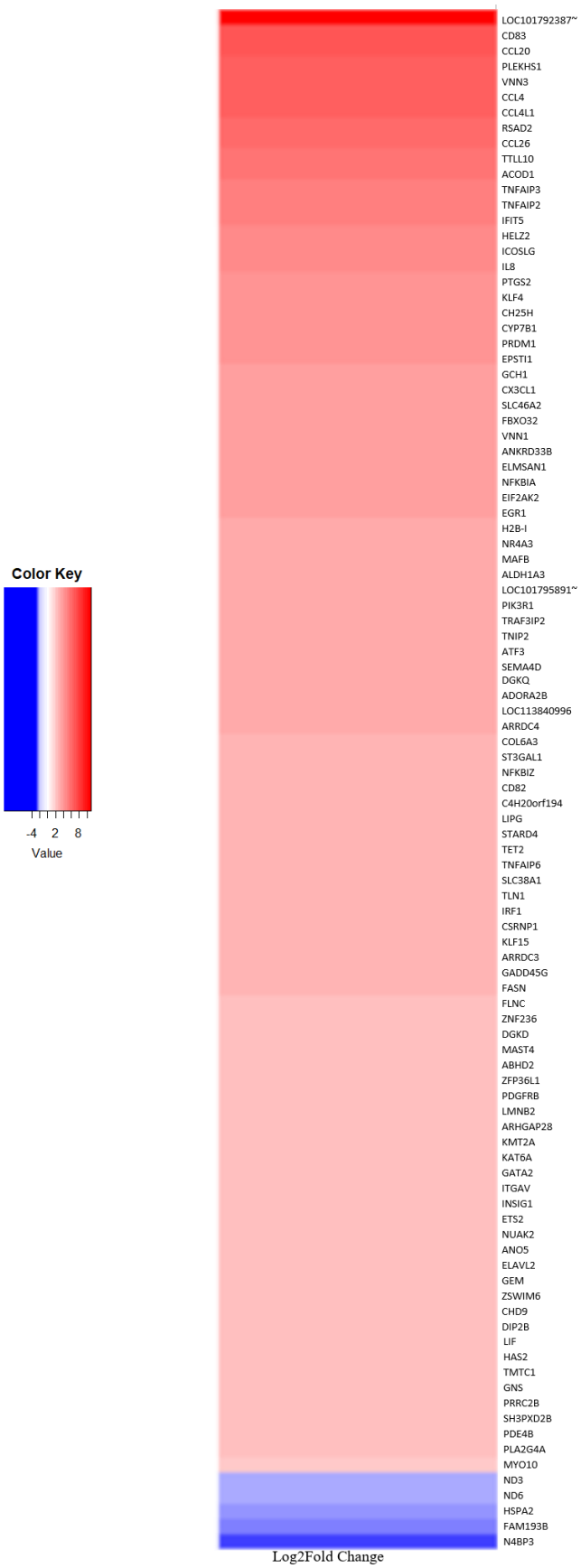
Color Key
-4
2
8
Value
LOC101792387~
CD83
CCL20
PLEKHS1
VNN3
CCL4
CCL4L1
RSAD2
CCL26
TTLL10
ACOD1
TNFAIP3
TNFAIP2
IFIT5
HELZ2
ICOSLG
IL8
PTGS2
KLF4
CH25H
CYP7B1
PRDM1
EPSTI1
GCH1
CX3CL1
SLC46A2
FBXO32
VNN1
ANKRD33B
ELMSAN1
NFKBIA
EIF2AK2
EGR1
H2B-I
NR4A3
MAFB
ALDH1A3
LOC101795891~
PIK3R1
TRAF3IP2
TNIP2
ATF3
SEMA4D
DGKQ
ADORA2B
LOC113840996
ARRDC4
COL6A3
ST3GAL1
NFKBIZ
CD82
C4H20orf194
LIPG
STARD4
TET2
TNFAIP6
SLC38A1
TLN1
IRF1
CSRNP1
KLF15
ARRDC3
GADD45G
FASN
FLNC
ZNF236
DGKD
MAST4
ABHD2
ZFP36L1
PDGFRB
LMNB2
ARHGAP28
KMT2A
KAT6A
GATA2
ITGAV
INSIG1
ETS2
NUAK2
ANO5
ELAVL2
GEM
ZSWIM6
CHD9
DIP2B
LIF
HAS2
TMTC1
GNS
PRRC2B
SH3PXD2B
PDE4B
PLA2G4A
MYO10
ND3
ND6
HSPA2
FAM193B
N4BP3
Log2Fold Change

Figure 10. Genes of the duck NLRP3 inflammasome are not upregulated after treatment with poly I:C and nigericin. The heatmap shows genes with differential expression in the whole transcriptome of duck embryonic fibroblasts primed with poly I:C and then treated with nigericin compared to control duck embryonic fibroblasts. Differential expression greater than 1.5 or less than -1.5 was mapped. Red indicates upregulation while blue indicates down-regulation. Differential expression of CASP1 and IL-1β was not detected. The heatmap is representative of one sample of DEFs treated with poly I:C and nigericin and one sample of untreated DEFs.

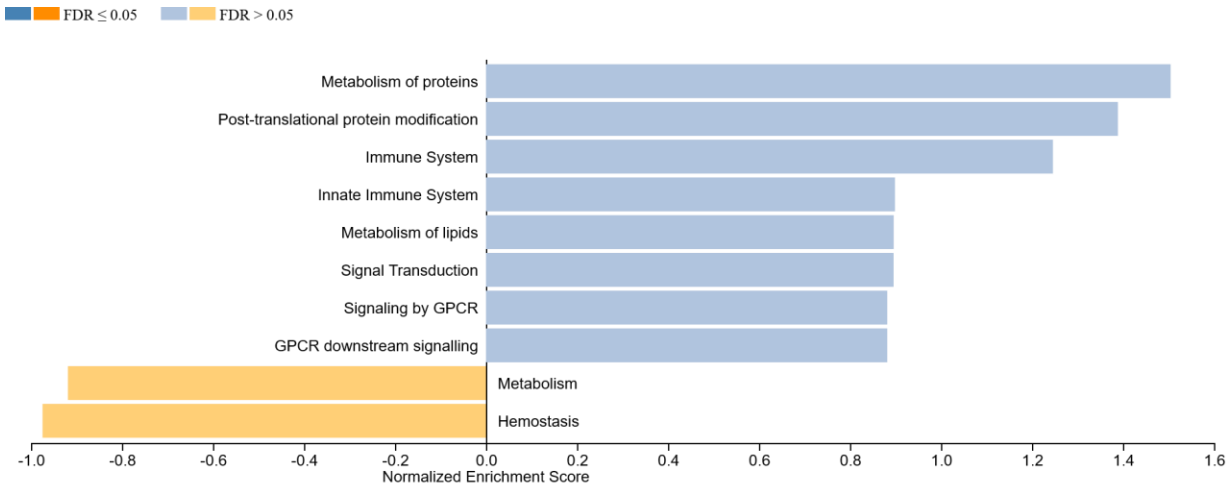

Figure 11. Reactome pathways of genes differentially expressed in DEFs. Analysis of genes that have a differential expression greater than 1.5-fold change or less than a -1.5-fold change using Gene Set Enrichment Analysis of pathways through the Reactome on WEBGESTALT. Pathways shown in blue are upregulated while pathways shown in yellow indicate downregulation. DEFs were treated with poly I:C and nigericin and compared to untreated control DEFs.

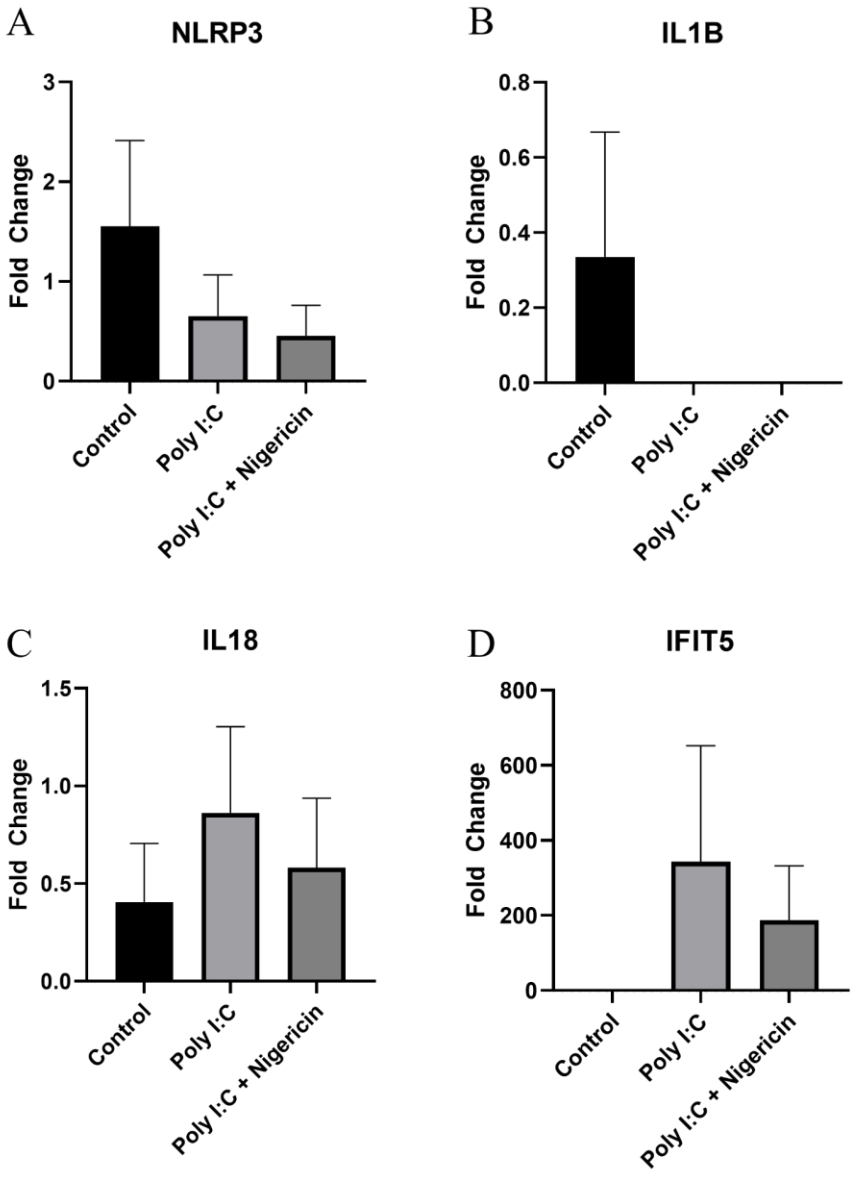

Figure 12. Priming duck embryonic fibroblasts with poly I:C does not upregulate the duck NLRP3 inflammasome. Normalized relative expression of NLRP3 inflammasome genes, *NLRP3*, *IL1B*, and *IL18*, as well as a positive control, *IFIT5*. Duck embryonic fibroblasts treated with poly I:C for 4 hours or with poly I:C for 3 hours and nigericin for 1 hour compared to untreated control. *GAPDH* was used as the endogenous gene for comparison. Treatments were performed in triplicate on DEFs from three individual embryos. Data represents the mean and

standard of error of the mean (SEM) of one qPCR assay on DEFs from 3 different individuals. *NLRP3*, *IL1B*, and *IL18* (A-C) show no upregulation after treatment while *IFIT5* is upregulated (D).

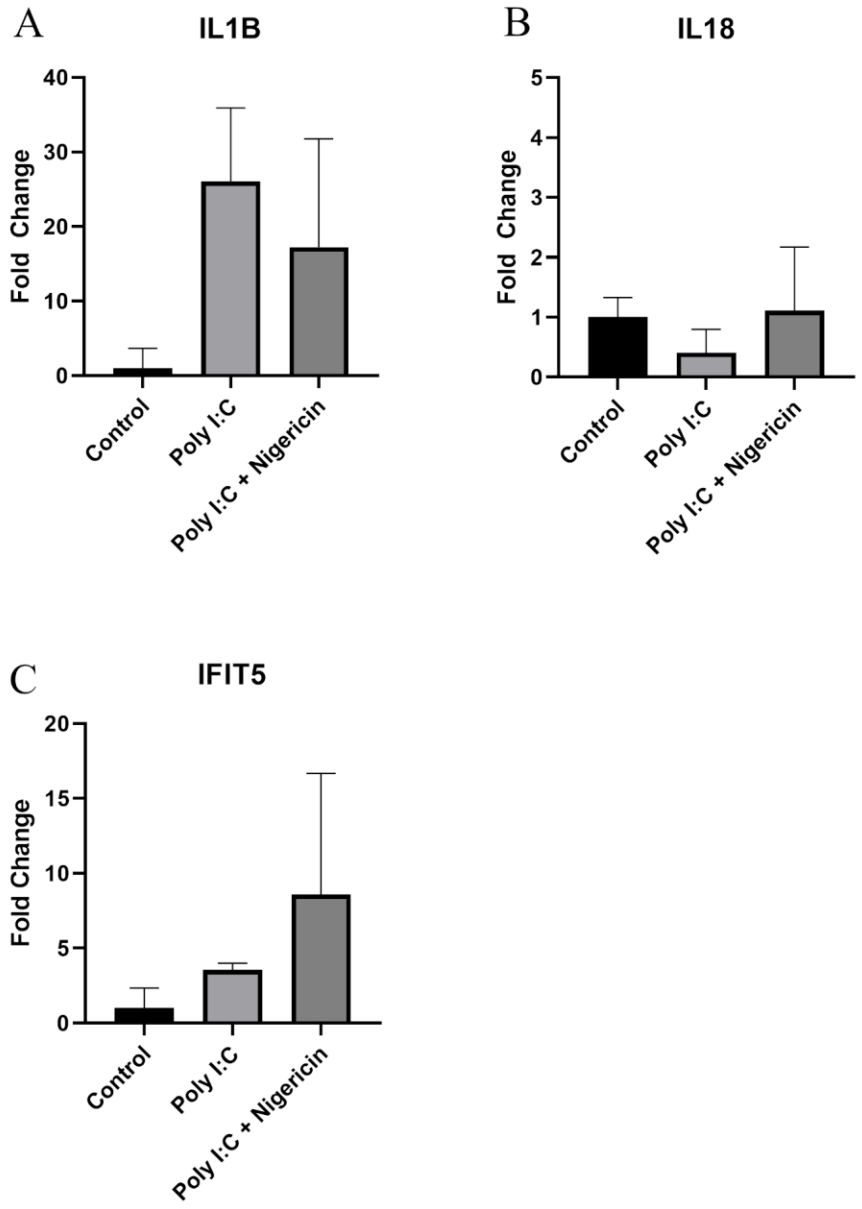

Figure 13. Priming human lung epithelial cells with poly I:C upregulates *IL1B* and *IFIT5* but not *IL18*. Normalized relative expression of NLRP3 inflammasome genes, *IL1B* and *IL18* as well as a positive control, IFIT5. A549 cells were treated with poly I:C for 4 hours or with poly I:C for 3 hours and nigericin for 1 hour compared to untreated control. The experiment was performed in triplicate on A549 cells. The data shown is representative of two replicate qPCR

experiments. *GAPDH* was used as the endogenous gene for comparison. Data represents the fold change and fold change max and min error. *IL1B* and *IFIT5* (A and C) show upregulation after treatment while *IL18* shows no upregulation compared to the untreated controls (B).

A

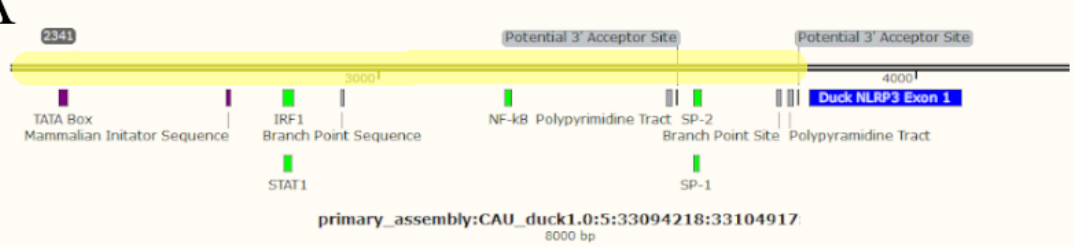
2341
Potential 3' Acceptor Site
Potential 3' Acceptor Site
3000
4000
Duck NLRP3 Exon 1
TATA Box
Mammalian Initator Sequence
IRF1
Branch Point Sequence
NF-kB
Polypyrimidine Tract
SP-2
Branch Point Site
Polypyramidine Tract
STAT1
SP-1
primary_assembly:CAU_duck1.0:5:33094218:33104917
8000 bp

B


TGTTTGCCAGGATTTTCTGTCAGCCTTGCTAATGGATCACAGTGAAAAATCAGGTTTATAATTTCTATAAAAAACAACAACATTGTTTTC
ACAAACGGTCCTAAAAGACAGTCGGAACGATTACCTAGTGTCACTTTTTAGTCCAAATATTAAAGATATTTTTTGTTGTTGTAACAAAAG
TATA Box
AAAATTTCTTGAAAATTTCACTCAGAGCAGTCTCATCTTCTTTAGGACCACACGTATTTGTCCAGAGGACTGGCAGGTGCCATTACTTCA
TTTTAAAGAACTTTTAAAGTGAGTCTCGTCAGAGTAGAAGAAATCCTGGTGTGCATAAACAGGTCTCCTGACCGTCCACGGTAATGAAGT
2447
GCTTTGGTACCAGATTTTCCACCTGGGATTGATCCTCCGAGGATGGCTGTTTCCAGTACTCTGTATCTGTCTTTGTTACAGCTTGTTTCT
CGAAACCATGGTCTAAAAGGTGGACCCTAACTAGGAGGCTCCTACCGACAAAGGTCATGAGACATAGACAGAAACAATGTCGAACAAAGA
GTCATTTGACCCTTTATGATGGCCTTTTCCTGTTTTCTGCATTACTTATACAAAAATCCATCTCTTCTGATGTGCTACCACTACCATTGC
CAGTAAACTGGGAAATACTACCGGAAAAGGACAAAAGACGTAATGAATATGTTTTTAGGTAGAGAAGACTACACGATGGTGATGGTAACG
CATTTCCAGCCACCTCCTATTCCTCTGCTTTGTTGTTTGCCCCCCTCGTTACTGAAAGGTTTCCTCTGCTGCACCTCCCTGCCCAGGAGA
GTAAAGGTCGGTGGAGGATAAGGAGACGAAACAACAAACGGGGGGAGCAATGACTTTCCAAAGGAGACGACGTGGAGGGACGGGTCCTCT
Mammalian Initator Sequence
GTTGTTAGATGAGGACAACAGCTGCTGTTGTTCCCAGTTTCTTTTTCCTTTCTGTCCATACATATCACCCAAATAACCAACTTCCCTAGC
CAACAATCTACTCCTGTTGTCGACGACAACAAGGGTCAAAGAAAAAGGAAAGACAGGTATGTATAGTGGGTTTATTGGTTGAAGGGATCG
IRF1
STAT1
AGCCCCCAGTCTAATTCTCCATTTTGCACAGCTATTTTTACTTTCTCTATCCTAATCTCTTTTGGCAATCATCTAAACTCAGTTTTACAC
TCGGGGGTCAGATTAAGAGGTAAAACGTGTCGATAAAAATGAAAGAGATAGGATTAGAGAAAACCGTTAGTAGATTTGAGTCAAAATGTG
TTCCTGTGATCAGATCCGCCTTGTGAGGTCCCCCTTGCTCCGAGGTGGAAACCGCAGTATGCAGCAGCAACCCCCTGCAGCTTCCTTCTG
AAGGACACTAGTCTAGGCGGAACACTCCAGGGGGAACGAGGCTCCACCTTTGGCGTCATACGTCGTCGTTGGGGGACGTCGAAGGAAGAC
CTTCCAGCTGCTGTGGGGCCAGCACAGAAGCCCCCAGCTGTAGAAGGGGCCAGCAGCAGGGGCCCAGCCCTCCCTGCCCGTGTCCCTGTG
GAAGGTCGACGACACCCCGGTCGTGTCTTCGGGGGTCGACATCTTCCCCGGTCGTCGTCCCCGGGTCGGGAGGGACGGGCACAGGGACAC
TGCAGCCCGGTGCTGGGGCAGGAGGAAGTGTGTGCCGGGTGCGCAGGCGCTGCTCAAAACTGACACCCTGTTTATATGCATCATTGGGCA
ACGTCGGGCCACGACCCCGTCCTCCTTCACACACGGCCCACGCGTCCGCGACGAGTTTTGACTGTGGGACAAATATACGTAGTAACCCGT
NF-kB

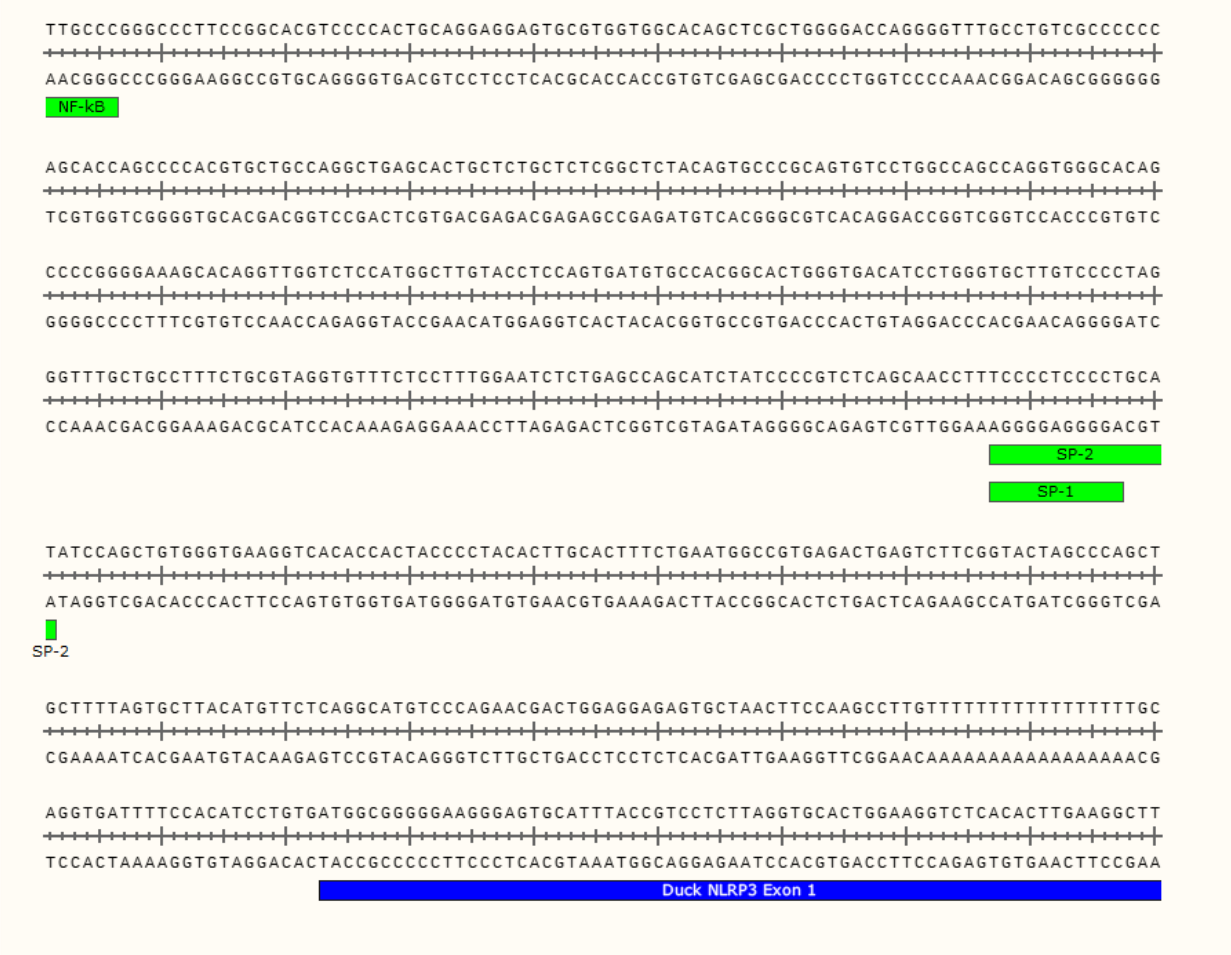

Figure 14. Putative duck NLRP3 gene promoter. A) Map of duck NLRP3 promoter located in the 5′-UTR of duck NLRP3 at 1398 bp upstream of the translational start site of duck NLRP3. Shown is a section of chromosome 5 from bp 33094218- 33104917 obtained from primary assembly CAU-duck 1.0 from Ensembl. Highlighted in yellow is the section shown in B. B) Sequence of the section highlighted in yellow in A. Underlined in purple is the putative TATA box and mammalian initiator sequence. Underlined in green are predicted transcriptional factor binding sites as predicted by JASPAR 2020 online database.

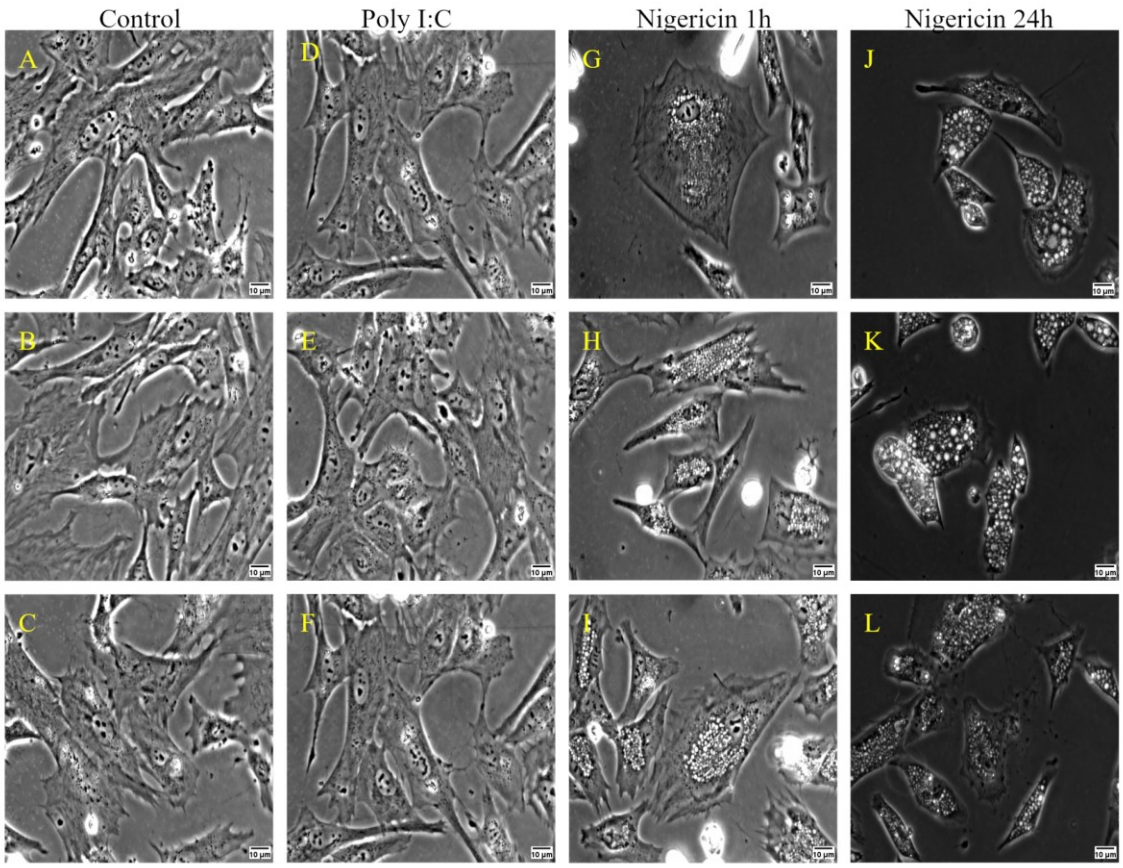

Figure 15. Duck embryonic fibroblasts show a change in cell phenotype after treatment with poly I:C and nigericin. Pekin DEFs seeded and grown in DMEM + 10% FBS for 24 hours. (A-C) Control DEFs. (D-F) DEFs primed with poly I:C for 4 hours. (G-J) DEFs primed with poly I:C for 3 hours and treated with nigericin for 1 hour. (J-K) DEFs primed with poly I:C for 3 hours and treated with nigericin for 24 hours. DEFs treated with nigericin show increased vacuolation compared to control DEFs and DEFs just primed with poly I:C. Images are representative of 3 separate experiments with DEFs collected from 3 different individuals. The scale bar represents 10 µm in each image.

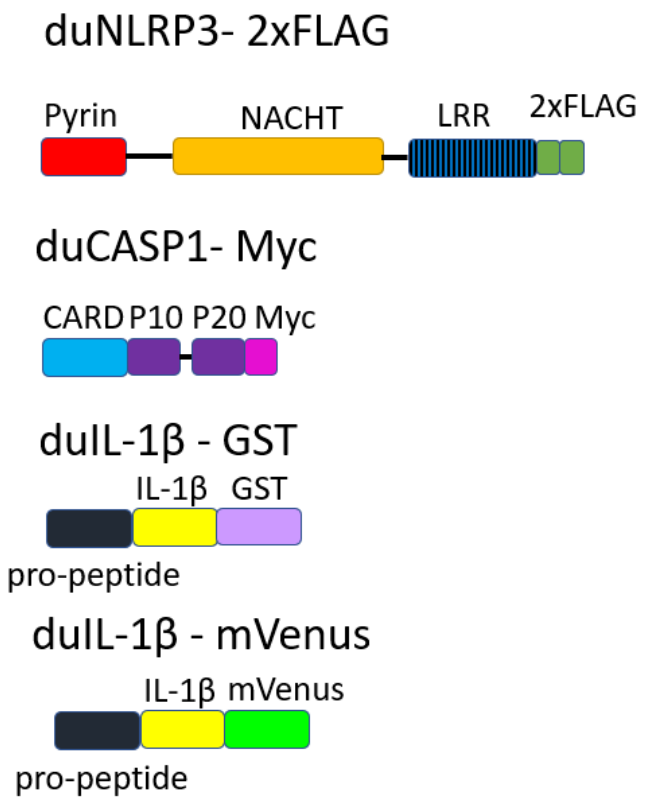

Figure 16. Schematic of recombinant duck NLRP3 inflammasome proteins. Duck NLRP3 is epitope-tagged with a 2xFLAG tag on the C-terminus. Duck CASP1 was epitope-tagged with a Myc tag on the C-terminus. Duck IL-Iβ was epitope-tagged with a GST tag on the C-terminus as well as mVenus on the C-terminus.

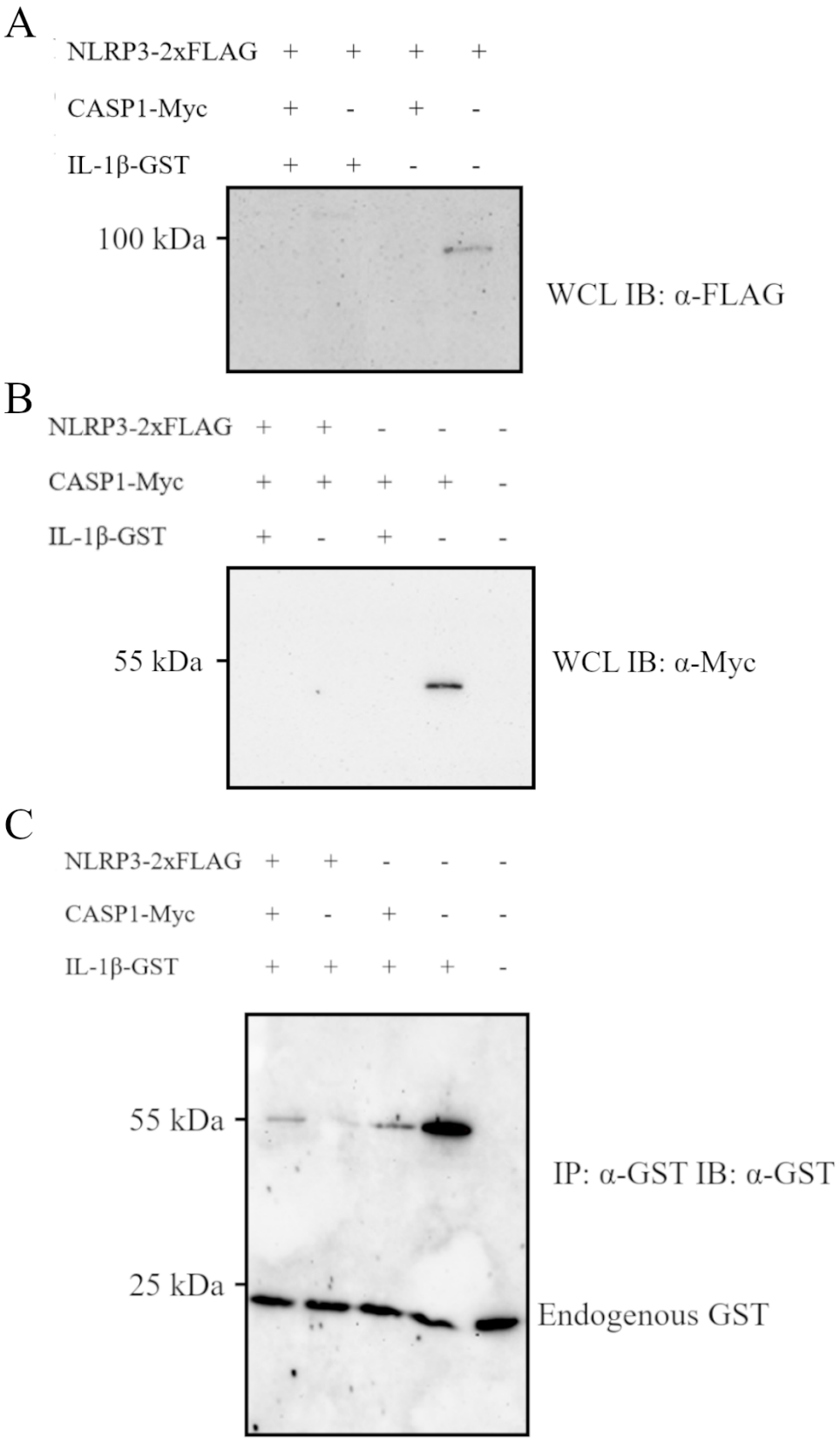
A
NLRP3-2xFLAG + + + +
CASP1-Myc + - + -
IL-1β-GST + + - -
100 kDa
WCL IB: α-FLAG
B
NLRP3-2xFLAG + + - - -
CASP1-Myc + + + + -
IL-1β-GST + - + - -
55 kDa
WCL IB: α-Myc
C
NLRP3-2xFLAG + + - - -
CASP1-Myc + - + - -
IL-1β-GST + + + + -
55 kDa
IP: α-GST IB: α-GST
25 kDa
Endogenous GST

Figure 17. Protein expression of components of the duck NLRP3 inflammasome in DF-1 cells. Protein expression of duck NLRP3 inflammasome components, NLRP3, CASP1, and IL-1β, decreases when co-transfected compared to transfections alone. A) Whole cell lysates from DF-1 cells transfected with NLRP3-2xFLAG, CASP1-Myc, and IL-1β-GST, were analyzed for the presence of NLRP3-2xFLAG using a monoclonal anti-FLAG antibody B) Whole cell lysates from DF-1 cells transfected with NLRP3-2xFLAG, CASP1-Myc, and IL-1β-GST were analyzed for the presence of CASP1-Myc using a monoclonal anti-Myc antibody. C) Lysates from DF-1 cells co-transfected with NLRP3-2xFLAG, CASP1-Myc, and IL-1β-GST, were analyzed using co-IP and detected for the presence of IL-1β-GST through a Western blot using a monoclonal anti-FLAG antibody. Activated duck IL-1β-GST, which would appear as a protein band at about 45 kDa was not detected. Endogenous GST is visible just below 25 kDa. The blots shown are representative of 3 replicates.

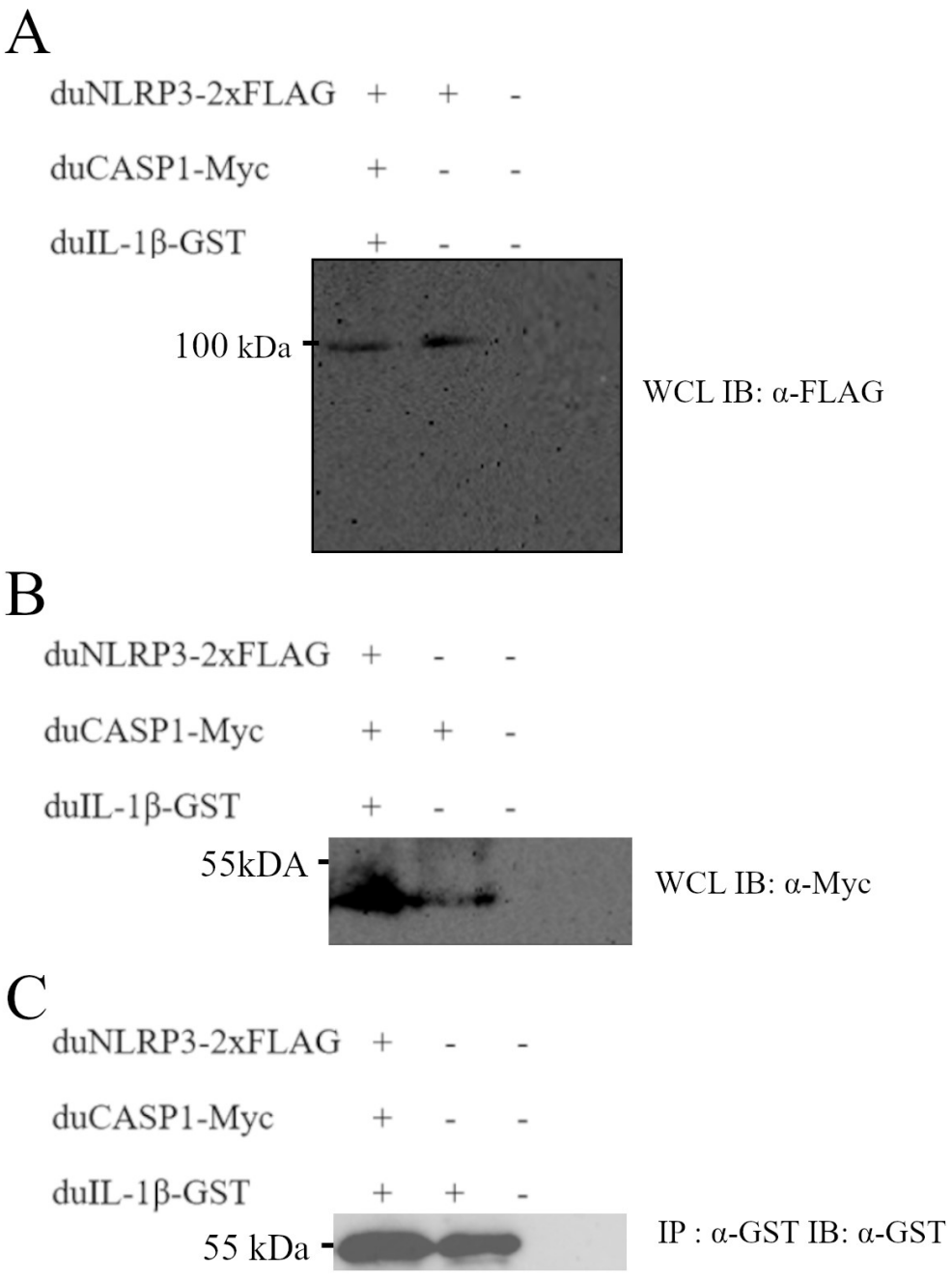

Figure 18. Protein expression of components of the duck NLRP3 inflammasome in HEK293T cells. Expression of the protein does not differ when duck NLRP3 inflammasome components are co-transfected compared to individual transfection. A) Whole cell lysates from

HEK293T transfected with NLRP3-2xFLAG, CASP1-Myc, and IL-1β-GST, were analyzed for the presence of NLRP3-2xFLAG using a monoclonal anti-FLAG antibody B) Whole cell lysates from HKK293T cells transfected with NLRP3-2xFLAG, CASP1-Myc, and IL-1β-GST were analyzed for the presence of CASP1-Myc using a monoclonal anti-Myc antibody. C) Lysates from HKK293T cells transfected with NLRP3-2xFLAG, CASP1-Myc, and IL-1β-GST were analyzed using co-IP and detected for the presence of IL-1β-GST through a Western blot using a monoclonal anti-FLAG antibody. Activated duck IL-1β-GST which would appear as a protein band at about 45 kDa was not detected. The blots shown are representative of two replicates.

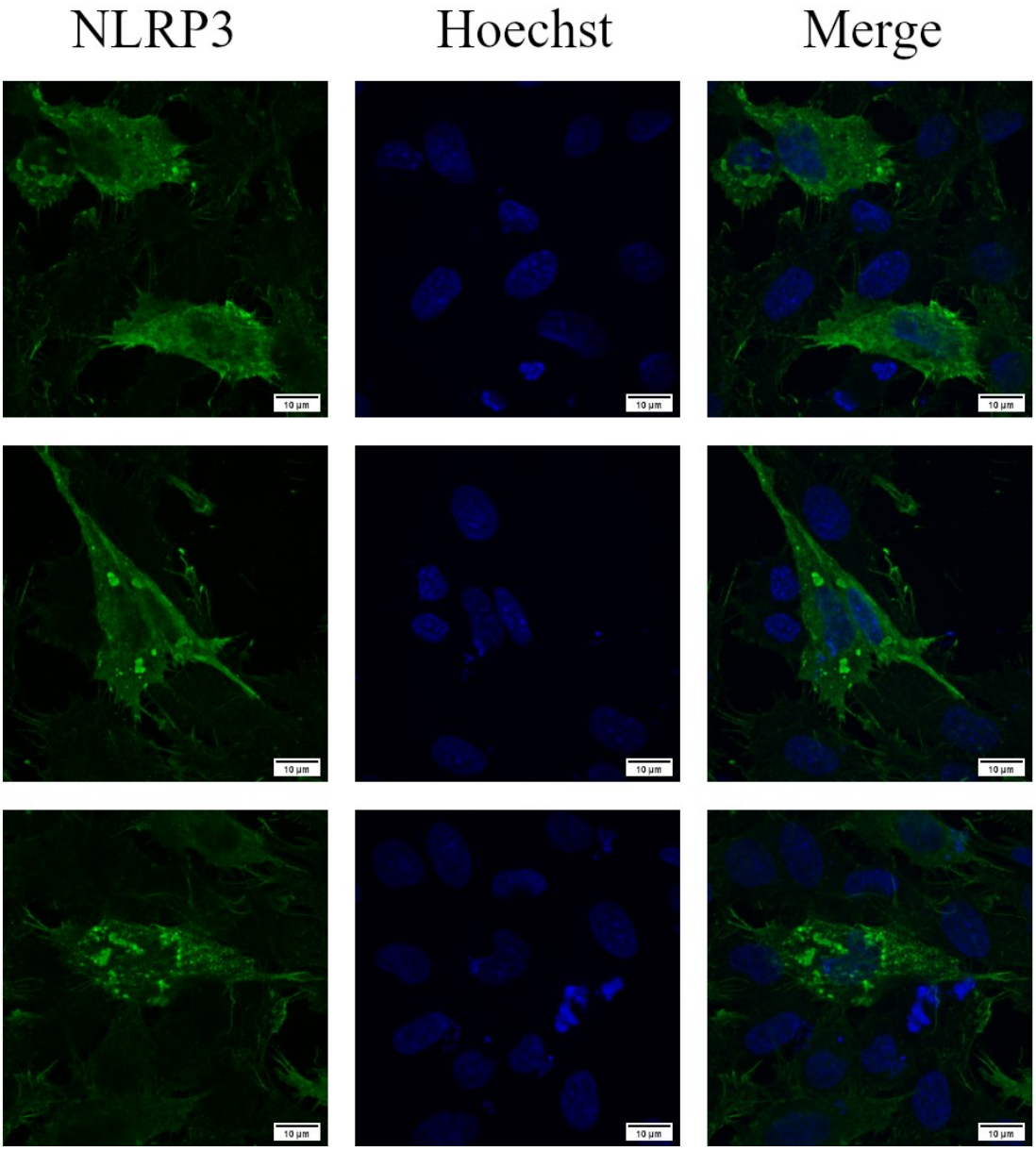

Figure 19. Transfection of duck NLRP3-2xFLAG into DF-1 cells. Duck NLRP-2xFLAG spreads diffusely throughout the cytoplasm of the cell. Some specks are also visible in the cytoplasm. Hoechst stain in blue shows the cell nuclei. Cells are stained with a rabbit anti-FLAG antibody and a goat anti-rabbit antibody conjugated to Alexa Fluor 647. Images are cells from the same slide taken in different fields of view. The scale bar shown represents 10 µm in each image.

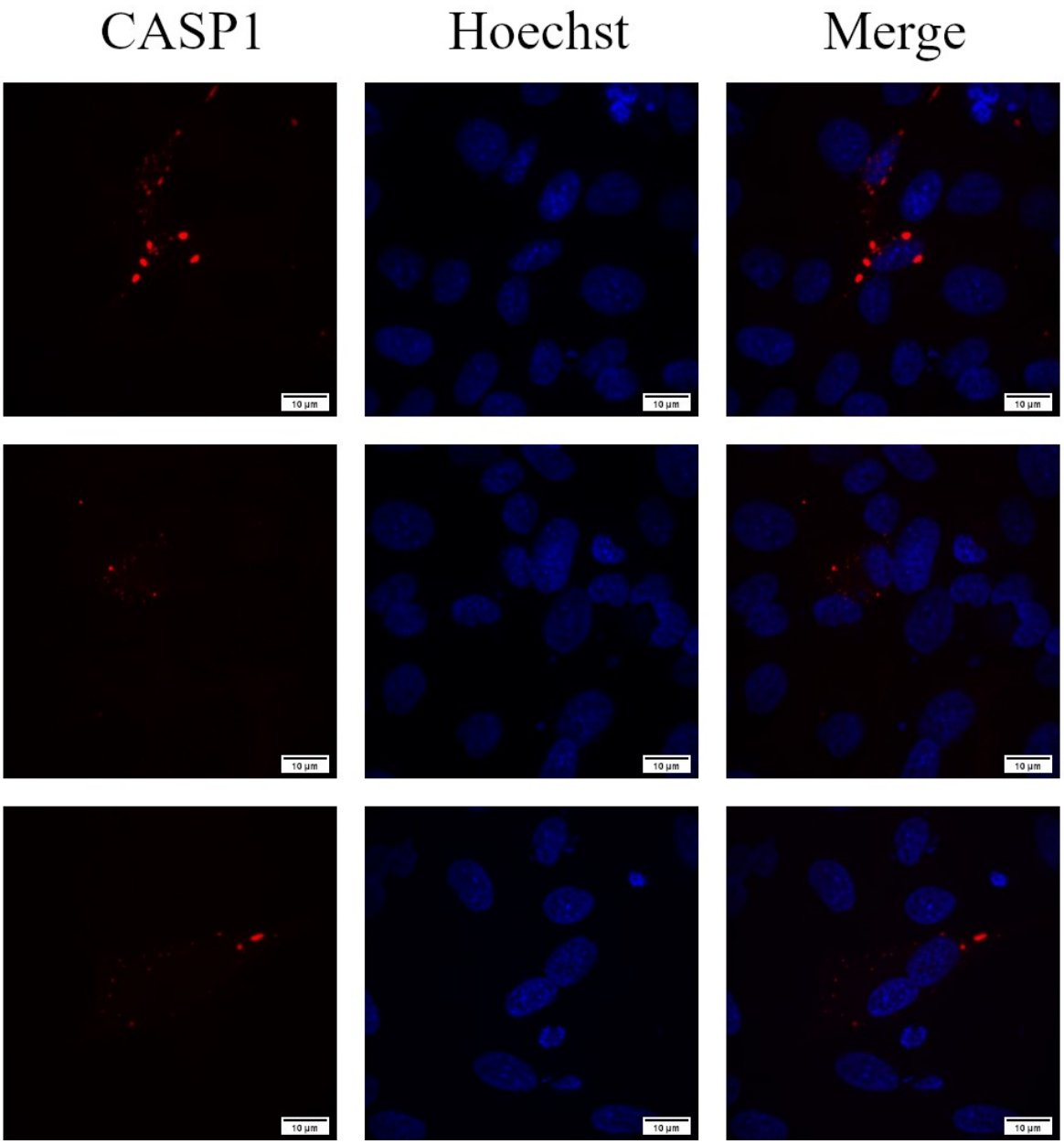

Figure 20. Duck CASP1-Myc transfected into DF-1 cells. Duck CASP1-Myc forms punctate structures in the cytoplasm of the cell (red). Hoechst stain in blue shows the cell nuclei. Cells are stained with mouse anti-Myc antibody and a goat anti-mouse antibody conjugated to Alexa Fluor 549. Images are cells from the same slide taken in different fields of view. The scale bar shown represents 10 µm in each image.

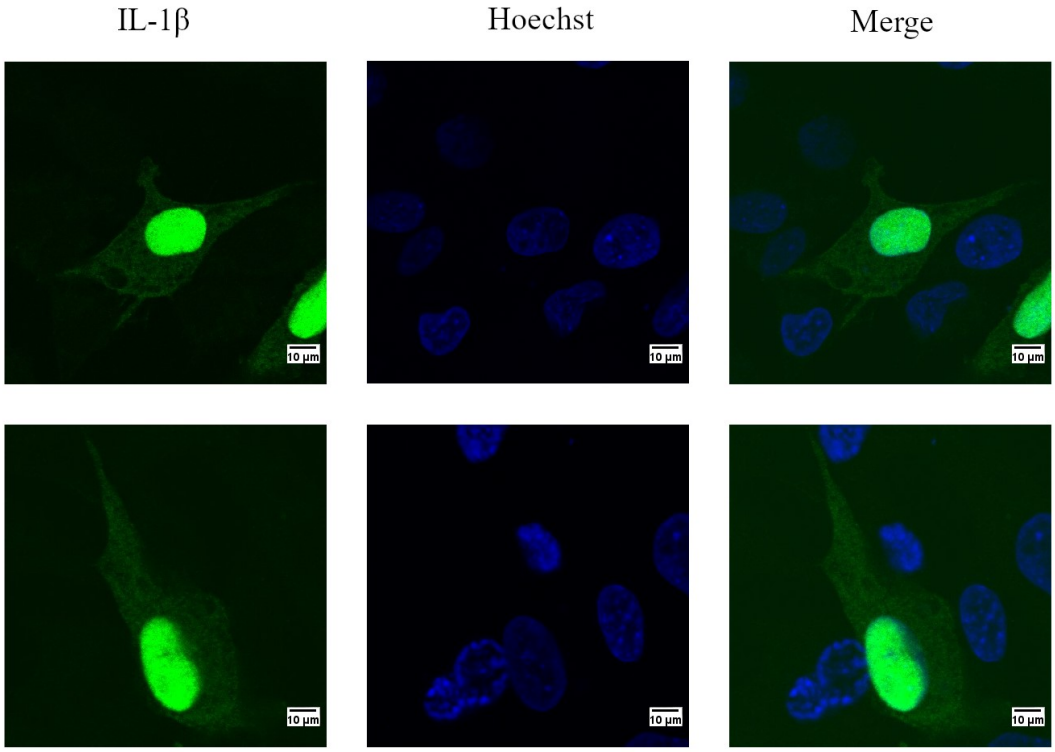

Figure 21. Duck IL-1β-mVenus transfected into DF-1 cells. Duck IL-1β-mVenus localizes heavily to the nucleus of the cell (green). Hoechst stain in blue shows the nuclei of the cell. Images are cells from the same slide taken in different fields of view. The scale bar shown represents 10 µm in each image.

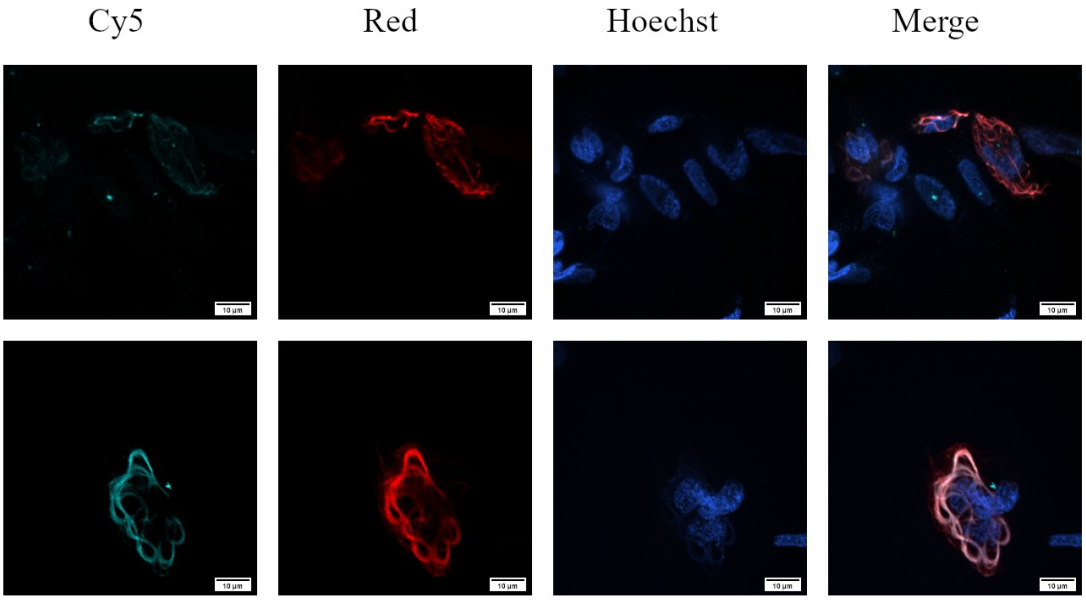

Figure 22. Transfection of duck IL-1β-mVenus into DF-1 cells. Cells were stained sequentially with rabbit anti-FLAG antibodies, mouse anti-Myc antibodies, goat anti-rabbit antibodies conjugated with Alexa Fluor 647, and goat anti-mouse antibodies conjugated with Alexa Fluor 549. Large stringy structures are visible in several different channels including Cy5 (cyan) and the red channel (red) which obscures any other fluorescent signals. Hoechst stain in blue shows the nuclei of the cells. Images are cells from the same slide taken in different fields of view. The scale bar shown represents 10 μm in each image.

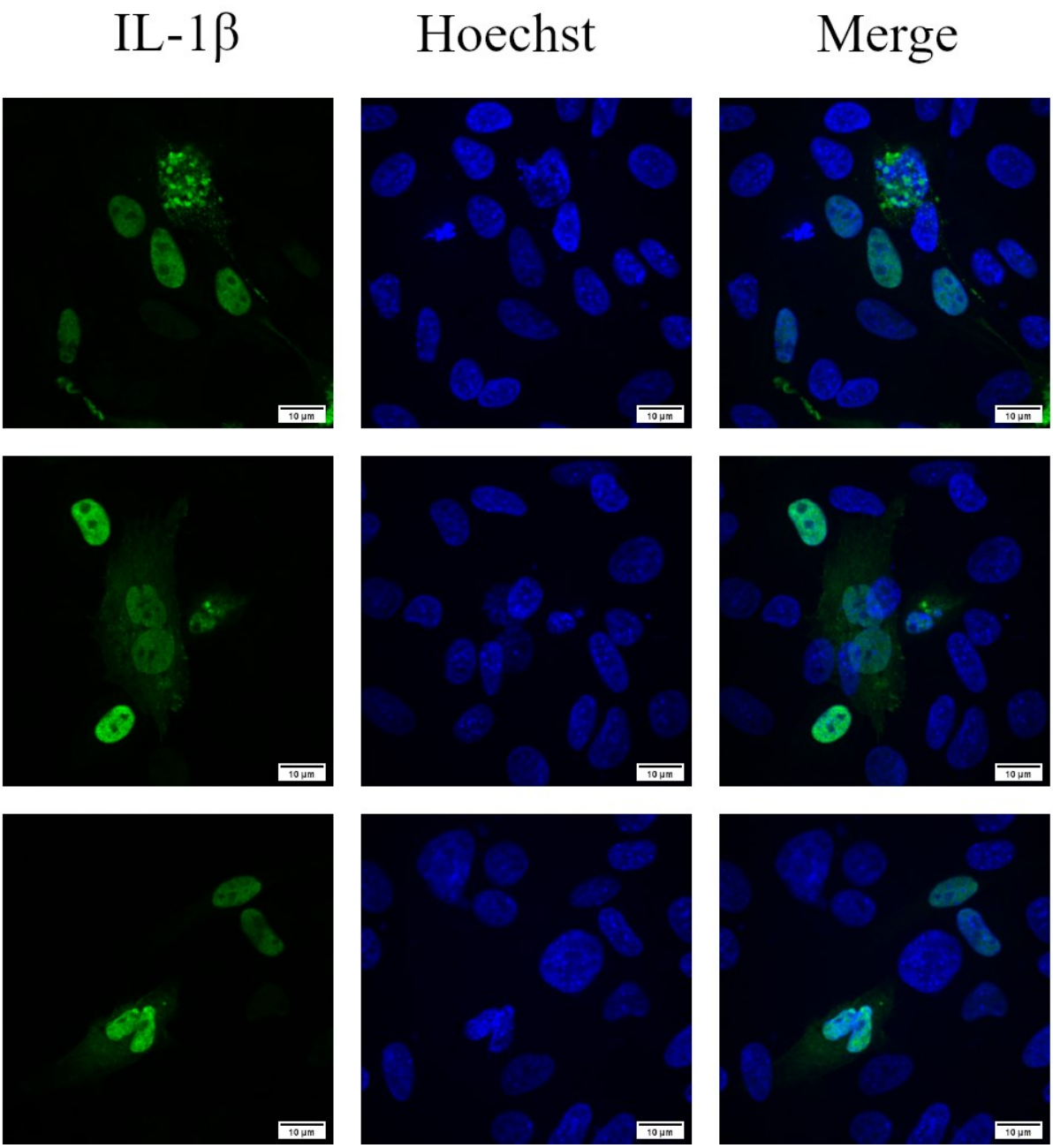

Figure 23. Transfection of duck IL-1β-GST into DF-1 cells. Duck IL-1β-GST transfected into DF-1 cells is abundantly expressed in the nucleus of the cell (green). Hoechst stain showing the nuclei of cells is seen in blue. Cells are stained with rabbit anti-GST antibody conjugated to FITC. Images are cells from the same slide taken in different fields of view. The scale bar shown represents 10 µm in each image.

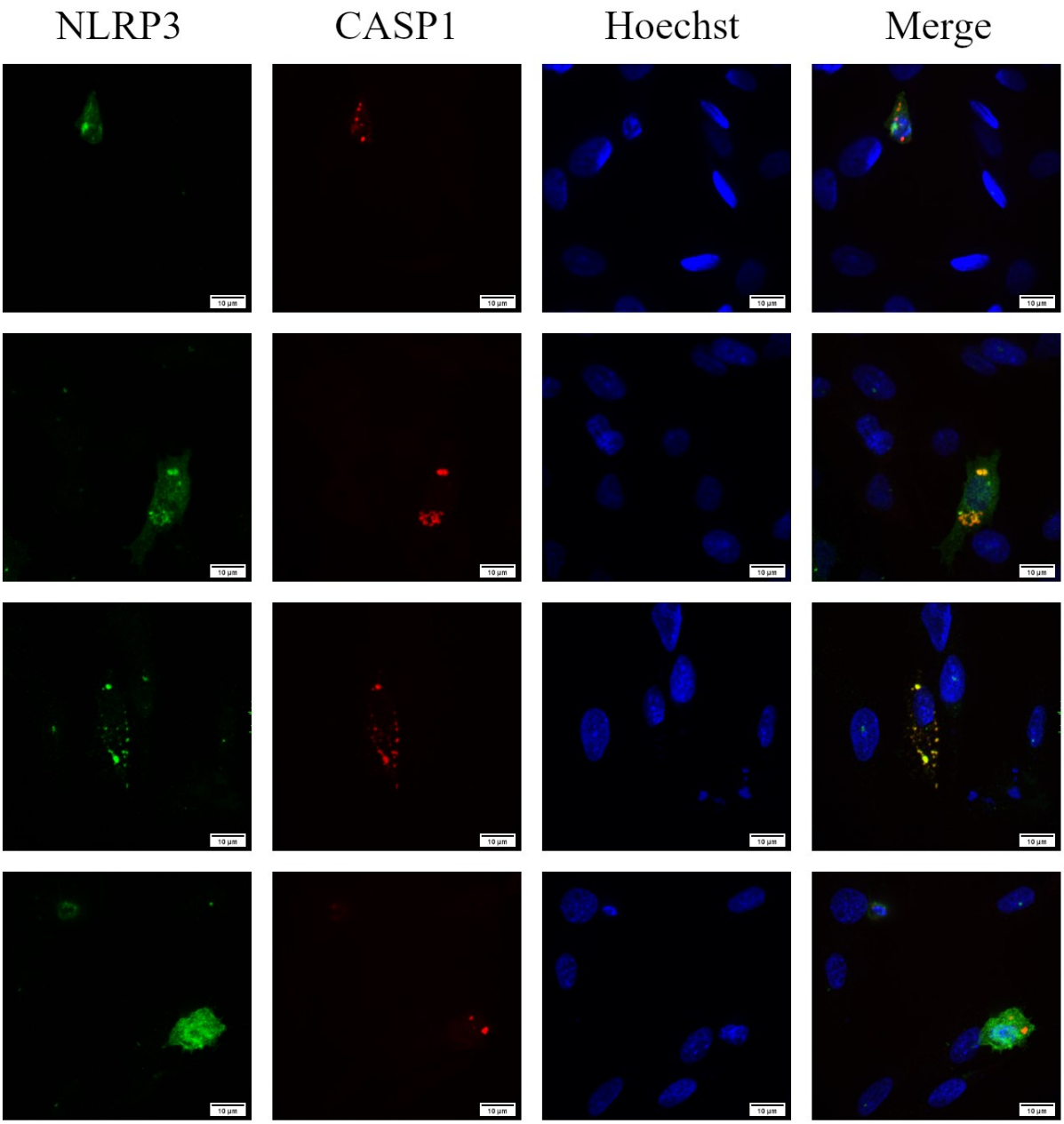

Figure 24. Co-transfection of duck NLRP3-2xFLAG and CASP1-Myc into DF-1 cells. Duck NLRP3-2xFLAG (green) transfected into DF-1 cells with CASP1-Myc (red) shows a more speckled appearance. The recombinant protein does appear to remain cytoplasmic, but more specks do form. CASP1-Myc remains largely cytoplasmic with some punctate forms appearing in the nucleus. Some colocalization is seen in the merged images (seen as yellow). The co-

localization of NLRP3 and CASP1 has a mean Pearson's coefficient of 0.63. Pearson's coefficient for colocalization was calculated using 8 different images, 4 representative images are shown here. Pearson's coefficient was calculated using the Coloc2 tool in ImageJ. Hoechst stain showing the cell nuclei is shown in blue. Cells are stained with rabbit anti-FLAG antibody, mouse anti-Myc antibody, goat anti-rabbit antibody conjugated to Alexa Fluor 647, and goat anti-mouse antibody conjugated to Alexa Fluor 549. Images are cells from the same slide taken in different fields of view. The scale bar represents 10 μm in each image.

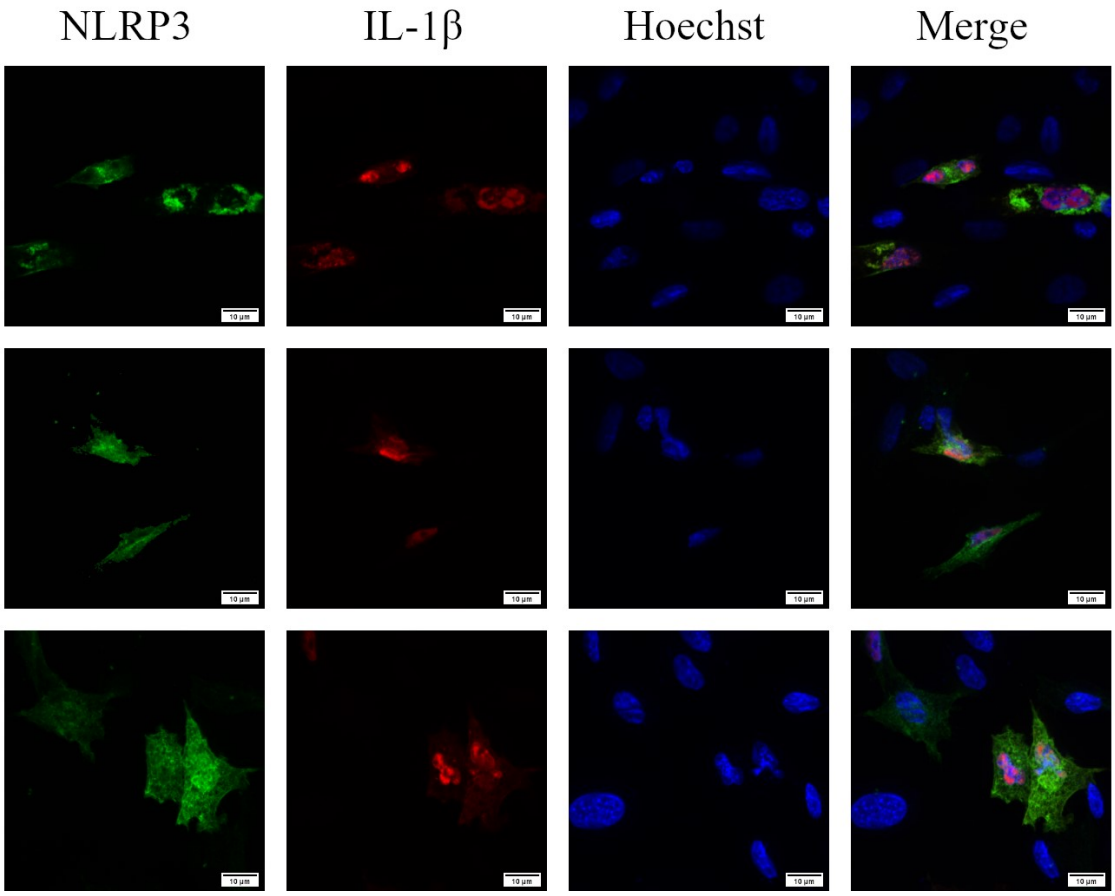

Figure 25. Duck NLRP3-2xFLAG and duck IL-1β-GST co-transfected into DF-1 cells.

Duck NLRP3-2xFLAG appears to be spread throughout the cytoplasm of the cell (green). IL-1β-GST is localized mainly to the nucleus of the cell (red). No co-localization appears to be visible. Hoechst stain showing the cell nuclei is shown in blue. DF-1 cells were stained with rabbit anti-FLAG antibody, goat anti-rabbit antibody conjugated to Alexa Fluor 647, and rabbit anti-GST antibody conjugated to FITC. Images are different fields of view from the same slide. The scale bar represents 10 µm in each image.

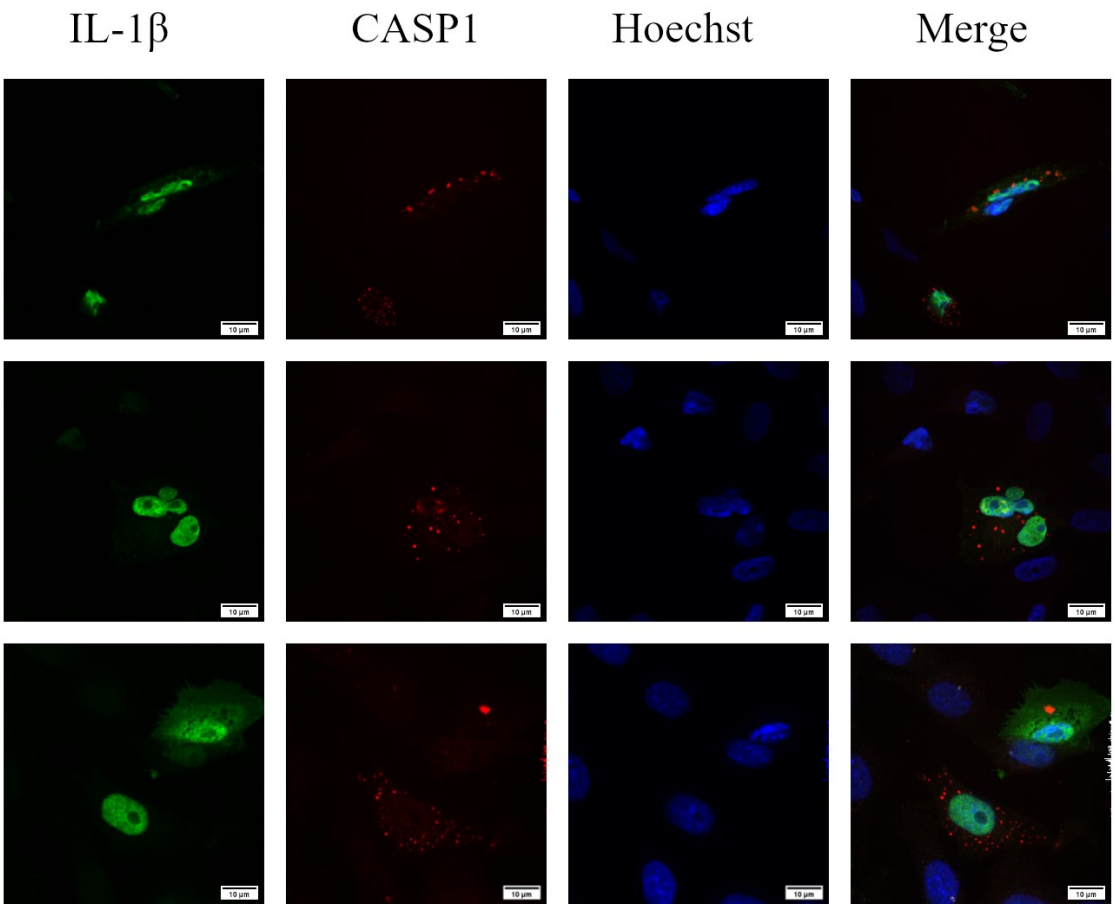

Figure 26. Duck IL-1 β -GST and duck CASP1-Myc co-transfected into DF-1 cells. Duck IL-1β-GST is localized diffusely in the nucleus of the cell mainly with some present in the cytoplasm (green). CASP1 is seen as punctate forms in the cytoplasm in the cell (red). Images are cells from the same slide taken in different fields of view. The scale bar represents 10 μm in each image.

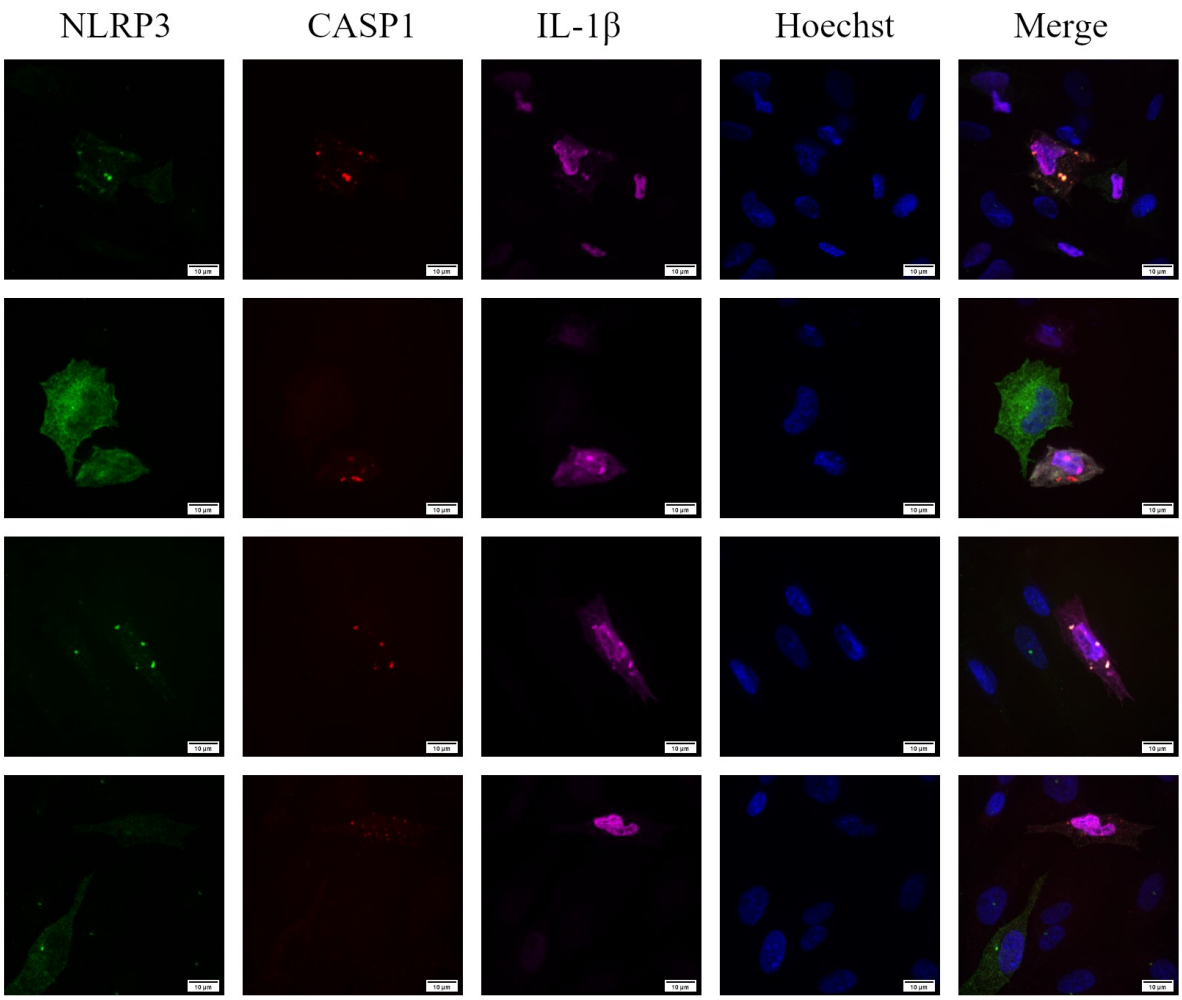

Figure 27. Duck NLRP3-2xFLAG, duck CASP1-Myc, and duck IL-1 β-GST co-transfected into DF-1 cells. Duck NLRP3-2xFLAG is seen in the cytoplasm of the cell (green). Sometimes it is diffuse throughout the cytoplasm and can also form specks in the cytoplasm. Duck CASP1-Myc is seen in the cytoplasm of the cell as punctate structures (red). Duck IL-1β-GST is seen mainly spread throughout the nucleus of the cell (magenta). Co-localization is seen in the merged image as yellow. Hoechst staining of the cell nuclei is shown in blue. Cells are stained with rabbit anti-FLAG antibody, mouse anti-Myc antibody, goat anti-rabbit antibody conjugated to Alexa Fluor 647, goat anti-mouse antibody conjugated to Alexa Fluor 549, and rabbit anti-GST

antibody conjugated to FITC. The co-localization of NLRP3 and CASP1 has a mean Pearson's coefficient of 0.69. Pearson's coefficient for colocalization was calculated using 8 different images, 4 representative images are shown here. Pearson's coefficient was calculated using the Coloc2 tool in ImageJ. Hoechst staining of the cell nuclei is shown in blue. Images are cells from the same slide taken in different fields of view. The scale bar represents 10 μm in each image.

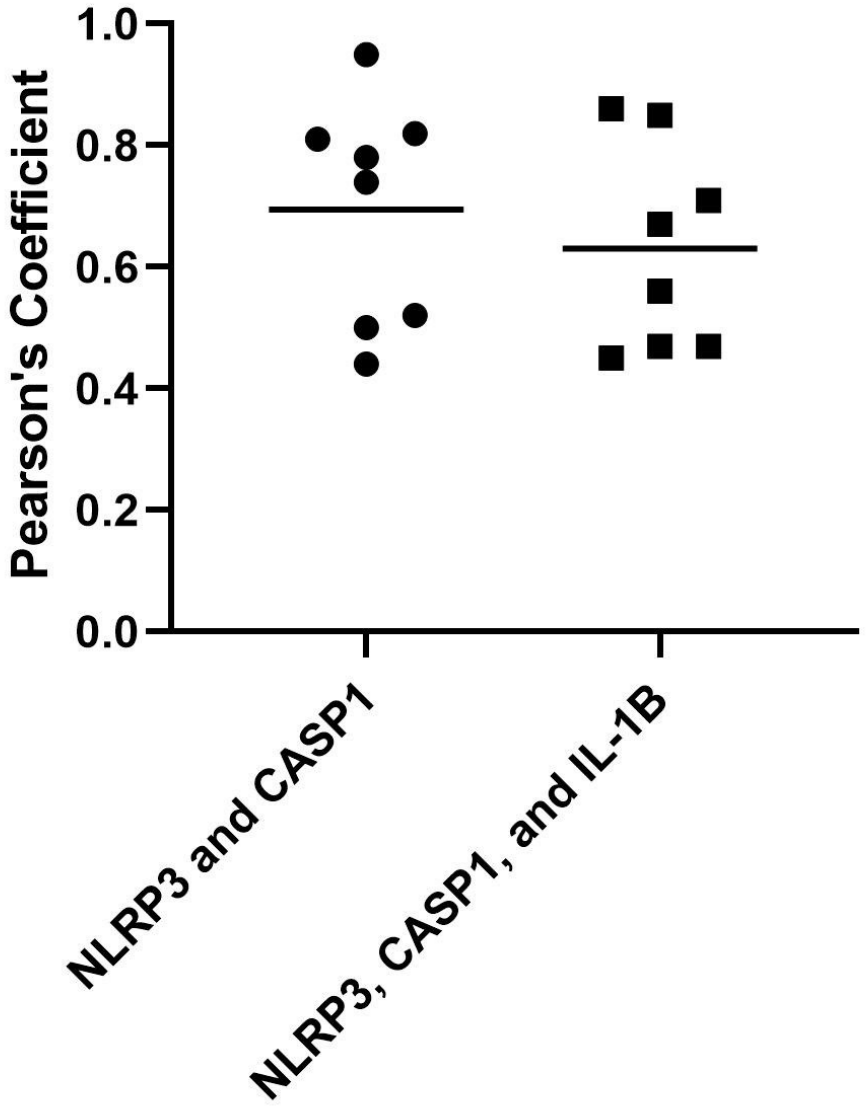

Figure 28. Pearson's coefficient of confocal microscopy images examining the co-localization of NLRP3 and CASP1. DF-1 cells co-transfected with duck NLRP3-2xFLAG, duck CASP1-Myc and duck IL-1β-GST. Co-transfected cells were stained with rabbit anti-FLAG antibody, mouse anti-Myc antibody, goat anti-rabbit antibody conjugated to Alexa Fluor 647, goat anti-mouse antibody conjugated to Alexa Fluor 549, and rabbit anti-GST antibody conjugated to FITC. The Pearson's coefficient for the co-localization of duck NLRP3-2xFLAG

and duck CASP1-Myc was examined using the Coloc2 tool on the ImageJ program. 8 separate images from one slide were analyzed and shown here.

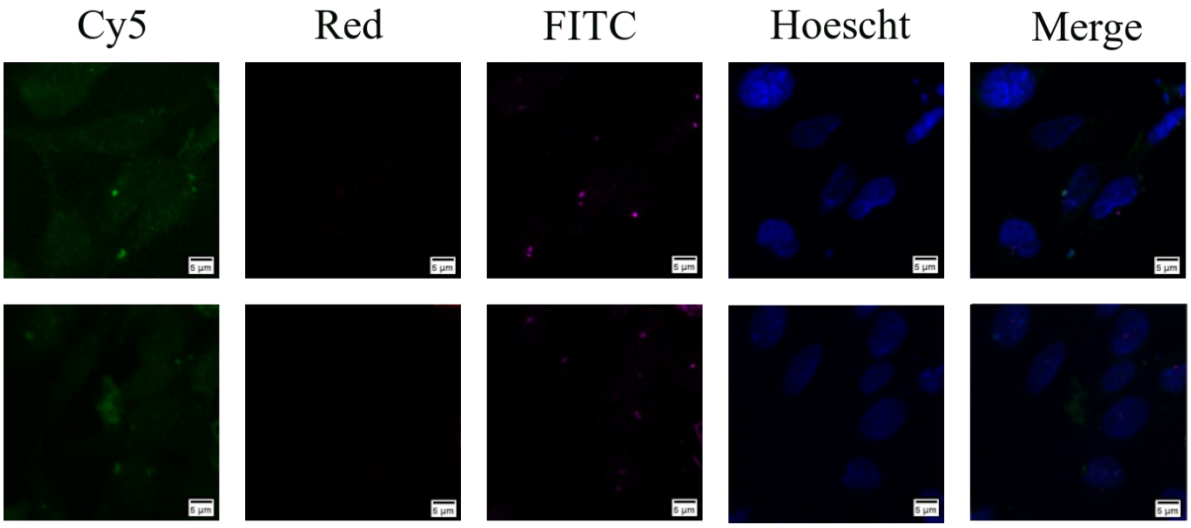

Figure 29. Untransfected DF-1 cells stained with antibodies. Untransfected cells were stained with rabbit anti-FLAG antibody, mouse anti-Myc antibody, goat anti-rabbit antibody conjugated to Alexa Fluor 647, goat anti-mouse antibody conjugated to Alexa Fluor 549, and rabbit anti-GST antibody conjugated to FITC. The nuclei of the cells are shown in blue. The scale bar represents 5 μm in each image.

Chapter 4. Discussion

The NLRP3 inflammasome is a key innate immune complex that induces the secretion of activated pro-inflammatory cytokines necessary for the clearance of pathogens from a host. However, dysregulated activation of the NLRP3 inflammasome is correlated with uncontrolled activation of pro-inflammatory cytokines and can cause pulmonary damage, potentially leading to fatal outcomes for the host (Coates et al. 2018). Many dsRNA viruses lead to the activation of the NLRP3 inflammasome, including IAV. As mentioned before, ducks are the natural reservoir host for IAV and do not exhibit the same hyper-inflammation during IAV infection. It was previously described that ducks have a robust innate immune response (Fleming-Canepa et al. 2019) and since the NLRP3 inflammasome played a key role in the innate immune response in other species (Allen et al. 2009; Thomas et al. 2009), the aim of my project was to characterize the duck NLRP3 inflammasome in the context of an IAV infection.

4.1 Ducks appear to lack a complete classical NLRP3 inflammasome

Classically, the NLRP3 inflammasome consists of three proteins: NLRP3, ASC, and CASP1 (Martinon, Burns, and Tschopp 2002). After examining the duck genome and transcriptome, we were able to identify, clone, and sequence duck NLRP3, duck CASP1, and the pro-inflammatory cytokine, duck IL-1β. However, we were unable to locate duck ASC. The duck genome that is currently available for analysis still has many unscaffolded pieces of gDNA. Our attempts to identify ASC through locating the genes that flank ASC in other species was not possible due to this limitation. Wei *et al.* (2019) examined the response of the duck NLRP3

inflammasome after exposure to cadmium. In their study, they claimed to have located duck ASC based on the putative *A. cygnoides* ASC (XM_013201308.1) that I had also analyzed during my search for duck ASC. Phylogenetic analysis of the putative *A. cygnoides* ASC sequence compared to ASC sequences from other species show that it diverged from a point before the mammalian and reptilian sequences diverged. The qPCR primers that Wei *et al.* (2021) used bound to the 3′ end of ENSAPLG00000026622. ENSAPLG00000026622 is the same gene that I had previously analyzed when I was searching for duck ASC and identified as being a part of duck NLRP1-L. This, coupled with the phylogenetic analysis leads me to believe that their qPCRs performed on duck ASC is detecting upregulation of duNLRP1-L.

To further support my position that the duck NLRP3 inflammasome could be missing the traditional ASC, the other studies on avian NLRP3 inflammasomes that are currently published do not examine avian ASC, only NLRP3, CASP1, and IL-1β (He et al. 2021; R. Li et al. 2018). The lack of research on the activity of one of the major components of the NLRP3 inflammasome in avian NLRP3 inflammasome studies suggests that other groups have encountered similar difficulties in identifying ASC. Additionally, there are no published sequences for ASC that come from studies in any avian species. There are only putative avian sequences. When I use the BLAST tool to search the duck genome on *Ensembl* with these putative avian sequences, the only match is what I have termed duck NLRP1-L. Duck NLRP1-L is also the only match to ASC sequences from other species when searching in the transcriptome. Searches of Genbank with the duck NLRP1-L sequence using the BLAST tool show matches to NLRP1b allele 2-like protein in a few different bird species. There remains the possibility that the duck NLRP1-L sequence that I identified could be alternatively spliced to yield ASC or functions as ASC, but further experiments will be needed to confirm this.

However, we were able to amplify, sequence, and clone duck NLRP3 and CASP1. Like the NLRP3 proteins from other species, duck NLRP3 does not have a CARD domain, therefore an adaptor protein that links duck NLRP3 to duck CASP1 is crucial for the activation of the duck NLRP3 inflammasome. Duck NLRP3 also appeared to lack a small segment between the PYRIN and NACHT domains in the linking region, but PCR analysis of duck gDNA and cDNA showed that this gene does exist this way and was not an artifact of PCR amplification or alternate splicing. Furthermore, in the alignment of different NLRP3 species, chicken NLRP3 also lacked the same segment, suggesting that this could be a difference in avian NLRP3 proteins in general. The pyrin domain had the lowest percent identity when comparing duck NLRP3 and human NLRP3. Subramanian *et al.* (2013) found that the deletions in the pyrin domain of human NLRP3 ablated inflammasome speck formation, suggesting that a functional pyrin domain is crucial in the activation of the NLRP3 inflammasome. The differences in the protein sequence of the duck NLRP3 pyrin domain compared to the mammalian NLRP3 pyrin domains could affect how strongly the duck NLRP3 inflammasome is activated as well as the subsequent inflammatory response.

In addition to the missing segment in duck NLRP3, there are other important differences between the duck NLRP3 amino acid sequence and the mammalian ones. Lu *et al.* (2013) found crucial residues in human NLRP3 that when mutated, would ablate ASC speck formation nucleated by NLRP3. Of the 7 amino acid residues, only three are conserved in duck NLRP3 (E15, E64, and D82). The other 4 (K23, K24, M27, and R43) are not conserved. However, without the sequence of duck ASC or the duck ASC substitute protein, it is difficult to analyze whether lacking these 4 conserved residues would change the way that duck NLRP3 and putative duck ASC would bind or if other residues are critical instead. Stutz *et al.* (2017) identified the

serine-5 in human NLRP3 is dephosphorylated by protein phosphatase 2A and helps with the activation of the NLRP3 inflammasome. Duck NLRP3 does not conserve this serine residue, however, there is a nearby serine residue at position 6 that could function in a similar matter. Song *et al*. (2017) found that serine-198 in human NLRP3 was an important phosphorylation site by JNK1 which would help the NLRP3 inflammasome activate. Analysis of the duck NLRP3 inflammasome shows that there is a glutamine instead of a serine at position 198. However, there is a serine nearby at positions 159 and 221 which could function similarly. Another serine residue that is phosphorylated during post-translational modification in mammalian NLRP3 is S295 (as reviewed in Shim and Lee 2018), which is also not conserved in either avian NLRP3 sequence. There is a serine residue at position 265 that is conserved between the mammalian NLRP3 and avian NLRP3 which could have a similar function. However, S265 has not yet been identified as a residue with a post-translational modification in mammalian NLRP3. Tyrosine-861 has also been identified as an important phosphorylation site that is dephosphorylated by protein tyrosine phosphatase non-receptor 22 to promote NLRP3 inflammasome activation (Spalinger et al. 2016). This tyrosine residue is not conserved in the duck NLRP3 sequence. Han *et al.* (2015) found that lysine-689 is ubiquitinated by F-Box L2 which leads to degradation of the protein, this ubiquitination site is not conserved in ducks. Bae *et al.* (2011) identified important amino acid residues in mammalian NLRP3 that were conserved across many mammalian species: cysteine-8 and cysteine-108. Both cysteine residues are not conserved in chicken and the duck NLRP3 protein sequences, further emphasizing how different the avian and mammalian NLRP3 proteins are. None of the analyzed post-translational modification sites identified in human NLRP3 were conserved in duck NLRP3. Duck CASP1 does not have many of the conserved cleavage sites that are present in mammalian species. Of

the 5 mammalian CASP1 cleavage sites (D109, D119, D297, D315, and D316), only D297 is conserved in duck CASP1 and chicken CASP1. Duck IL-1β, however, retains the avian cleavage site that was discovered in chickens, at aspartate-80 (Reis et al. 2012).

There are many other differences between the duck NLRP3 inflammasome and mammalian NLRP3 inflammasomes that I have observed— aside from differences in amino acid sequences and missing post-translational modification sites when compared to their mammalian counterparts, there is also the lack of an identifiable ASC. To the best of my ability, I have not been able to identify ASC in the duck genome and transcriptome. Further experiments are needed to identify what protein is functioning in place of ASC or whether the protein I have identified as duck NLRP1-L can act as ASC. Furthermore, phylogenetic analysis of the different duck NLRP3 inflammasome components shows that the avian NLRP3 inflammasome sequences are more closely related to each other than they are to the mammalian sequences. The duck NLRP3 inflammasome components cluster together with the chicken NLRP3 inflammasome components during phylogenic analysis. Given the importance of the NLRP3 inflammasome in the innate immune response against IAV infections in other species such as mice (Allen et al. 2009), the resistance that ducks can exhibit against the virus (van den Brand et al. 2018) could be due to these aforementioned differences in the duck NLRP3 inflammasome compared to the mammalian NLRP3 inflammasome.

4.2 The duck NLRP3 inflammasome shows a reduced transcriptional priming response to poly I:C.

The NLRP3 inflammasome requires a priming step before activation (Bauernfeind et al. 2009). Without a priming step, the activation of the NLRP3 inflammasome is ablated. Due to the wide variety of activating signals that the NLRP3 inflammasome responds to, the priming step offers the NLRP3 inflammasome a degree of specificity in what signals it responds to. Only treatments or pathogens able to prime a cell through other PRRs can activate the NLRP3 inflammasome (Bauernfeind et al. 2009). Bauernfeind *et al.* (2009) also showed that the NLRP3 inflammasome could be primed with poly I:C. My aim was to examine the duck NLRP3 inflammasome in the context of an IAV infection. Since IAV is an RNA virus, I used poly I:C as an agonist to mimic an RNA virus infection as well as prime the duck NLRP3 inflammasome. However, I found that treatment of DEFs with poly I:C or poly I:C then followed by nigericin does not result in upregulation of *NLRP3* or *IL1B* and examination of the transcriptome does not show evidence that *NLRP3, IL1B,* or *CASP1* are upregulated under the same conditions. *NLRP3* and *IL1B* are known to be transcriptionally primed by poly I:C in other species and as evidenced by the upregulation of *IL1B* seen in the A549 cells after the same treatment. Interestingly, analysis of our transcriptome from ducks infected with different strains of IAV as well as the transcriptome data from Huang *et al.* (2013) showed that duck NLRP3 is not differentially expressed. Ahn *et al.* (2019) examined the murine NLRP3 inflammasome and found that priming with poly I:C induced significant levels of *IL1B* upregulation. However, the lower levels of *IL1B* upregulation that I observed in the DEFs after treatment was in line with the levels that Saito *et al*. (2018) observed. Ducks infected with different H5N1 strains of IAV exhibited modest levels of upregulation of *IL1B*, only a 3-fold to 6-fold increase at 1-day post-infection (Saito et al. 2018). This modest level of upregulation is different from the much higher level of upregulation in chickens that are infected with various strains of H5N1 (Burggraaf et al. 2014). It is noted that

the ducks and chickens in these two studies were infected with different strains of H5N1 and there are differences in the methodology, but generally, the chickens have a higher level of upregulation of *IL1B* when infected with H5N1. The difference in IL-1β responses to H5N1 between the duck and the chicken could be a mechanism in which the ducks prevent detrimental symptoms as a result of hyperinflammation.

Additionally, chickens have also shown an NLRP3 inflammasome response to other viral infections. He *et al.* (2021) showed that infectious bursal disease virus, which is another RNA virus, induced an NLRP3 inflammasome response in chickens. However, the NLRP3 response exhibited by DF-1 cells against IBDV is lower than what I would have expected. While infection with IBDV resulted in some upregulation of *NLRP3, IL1B,* and *CASP1*, He *et al.* (2021) only saw about 4-fold upregulation of *IL1B* at 50 multiplicity of infection (MOI). An MOI of 50 is very high and is beyond a physiologically relevant level, and I would expect other pathways in the cell to be affected potentially interfering with the accurate measurements of upregulation. Meanwhile, Gao *et al.* (2020) found that DF-1 cells infected with a highly virulent strain of Newcastle disease virus (NDV) showed almost 150-fold upregulation in gene expression of IL-1β. This indicates that DF-1 cells, embryonic fibroblasts, are capable of upregulating IL-1β expression in response to viral infections. However, there is variability to their immune response depending on the virus used for infections.

The decreased response of the duck NLRP3 inflammasome to the priming signal given by poly I:C is similar to the response seen with the bat NLRP3 inflammasome which exhibits reduced transcriptional priming by a wide variety of TLR agonists, including poly I:C (Ahn et al. 2019). Bats are natural reservoir host of many different RNA viruses like Ebola (Leroy et al. 2005), and SARS-like coronaviruses (Li et al. 2005), which can induce hyper-inflammation in

other susceptible hosts. The dampening of the priming response of the bat NLRP3 inflammasome is a mechanism by which bats avoid some of the detrimental side effects induced by hyper-inflammation when infected by certain viruses (Ahn et al. 2019). Ducks, as the natural reservoir host of IAV, are in a similar situation as bats and do not exhibit detrimental side effects in response to being infected with IAV (Taubenberger and Kash 2010; Webster et al. 1992). It would stand to reason that the duck NLRP3 inflammasome, like the bat NLRP3 inflammasome, would also have a dampened transcriptional priming response to avoid damage by hyper-inflammation caused by IAV. Furthermore, poly I:C, the agonist that I used to induce a duck NLRP3 inflammasome priming response, is used to mimic an RNA viral infection.

Despite not appearing to prime the duck NLRP3 inflammasome, poly I:C does exhibit an effect on the DEFs. Examination of the interferon-stimulated gene, *IFIT5*, which is known to be upregulated by poly I:C (Yu et al. 2020), is also highly upregulated in DEFs treated with poly I:C. This further supports that poly I:C is effective and also has specificity in which immune genes it upregulates. Additionally, poly I:C followed by nigericin treatments on DEFs exhibit a phenotypic change which is similar to the phenotypic change seen in HeLa cells under similar nigericin treatment conditions by Chen and Chen (2018). This change in the phenotype of the DEFs also confirms that the nigericin treatment used is effective.

In addition to potentially playing a role in the innate immune response to RNA viruses, R. Li *et al.* (2018) found that the duck NLRP3 inflammasome contributed to the reduction of levels of *Escherichia coli* in ducks during *in vivo* experiments. This suggests that the duck NLRP3 inflammasome could play a role in antibacterial immune responses and still be primed by other pathogens. Taken all together, this suggests that the treatment of the cells using poly I:C only or poly I:C followed by nigericin can upregulate the NLRP3 inflammasome at a

transcriptional level, as evidenced by the upregulation seen in A549 cells. However, the duck NLRP3 inflammasome does not appear to be transcriptionally upregulated after the same treatments, suggesting that the duck NLRP3 inflammasome has a dampened transcriptional priming response when primed through the TLR3 pathway. Instead of a broad dampening of the NLRP3 inflammasome priming response like the mechanism in the bat (Ahn et al. 2019), ducks could have evolved to dampen priming signals from specific pathogens like RNA viruses. This dampening of the priming signal from a specific pathway, in this case, TLR3, would still allow an NLRP3 inflammasome response to other pathogens which would prime the inflammasome through other pathways. Additionally, dampening of the priming response that would be induced through the TLR3 pathway could reduce the overactivation of the NLRP3 inflammasome induced by IAV infections. However, further experiments are needed to determine whether the transcriptional priming step in ducks is broadly dampened or limited to specific pathways and stimuli.

In examining the transcriptional upregulation of the duck NLRP3 inflammasome, I examined the duck NLRP3 promoter. Currently, there is not a published duck NLRP3 promoter sequence. However, I have identified a putative duck NLRP3 promoter sequence and transcriptional factor binding sites for NF-κB, SP-1, SP-2, IRF1, and STAT1 along a 1398 bp sequence immediately upstream of the translational start site of duck NLRP3. The presence of a site for NF-κB and IRF1 in the promoter region suggests duck NLRP3 could be transcriptionally upregulated in response to a priming signal. However, because this putative promoter has not been experimentally examined, I still do not know if this promoter sequence is correct or if the predicted transcriptional factor binding sites are functional. A 5′-RACE of the 5′-UTR of the duck NLRP3 gene to help confirm the promoter sequence could be performed in the future.

Additionally, how different TLR stimuli would affect how the duck NF-κB would bind and its subsequent pathway is also not known. Further experiments to confirm the sequence of the promoter, the function of the promoter, and examination of how the promoter induces NLRP3 expression are needed.

4.3 Activation of duck IL-1β is not detected when duck NLRP3 inflammasome components are overexpressed.

I was not able to observe that duck IL-1β activation on Western blots when the duck NLRP3 inflammasome components were transfected into DF-1 cells. I chose to use DF-1 cells because I was not able to detect any protein expression during the initial transfections using primary DEF, Additionally, the protein sequences of duck NLRP3 and duck CASP1 that I identified have a high percent identity to chicken NLRP3 and CASP1. Additionally, since ASC is crucial to activating CASP1 through the NLRP3 inflammasome, I hypothesized that endogenous ASC or an analogous protein from DF-1 cells would function as the adaptor protein during my co-transfection experiments to induce duck NLRP3 inflammasome activation. Furthermore, DF-1 cells have a higher transfection efficiency than primary DEFs. I had tried co-transfecting the duck NLRP3 inflammasome constructs into primary DEFs and was unable to detect their protein expression with Western blots. After co-transfecting DF-1 cells with my recombinant duck NLRP3 inflammasome constructs, there was no detection of a protein band at about 45 kDa which would be indicative of duck IL-1β -GST being activated. Additionally, due to an inability to detect duck CASP1-Myc on the Western blot during co-transfections in DF-1 cells, I could not determine whether duck CASP1 was activated by duck NLRP3. Activated

CASP1 can be detected from cell lysates on Western blots (Lai et al. 2018). The absence of activated duck IL-1β and duck CASP1 on the Western blot during co-transfections in DF-1 cells would suggest that duck IL-1β and duck CASP1 were not activated by the duck NLRP3 inflammasome. Wang *et al.* (2020) saw the activation of IL-1β and CASP1 when NLRP3 was overexpressed in a murine system on a Western blot. Yu *et al.* (2006) also saw similar activation in a human system. This could suggest that the duck NLRP3 inflammasome could be exhibiting reduced duck IL-1β activation, similar to the bat NLRP3 inflammasome (Goh et al. 2020). Potentially, with decreased IL-1β activation, this would reduce the levels of inflammation seen in the duck during infection which in turn, would reduce the number of detrimental side effects caused by hyper-inflammation experienced by the duck.

However, taking the Western blots from transfected DF-1 cells together with the Western blots from transfected HEK293T cells would suggest that the NLRP3 inflammasome is forming. HEK293T cells do not express endogenous NLRP3 inflammasome components. The lack of decrease in the protein detection on a Western blot when the HEK293T cells were co-transfected with my duck NLRP3 inflammasome components indicates that the duck NLRP3 inflammasome components do not aggregate into insoluble specks on their own. This indicates that other proteins are needed to interact with the duck NLRP3 inflammasome components to cause the aggregation. The lack of ASC in the HEK293T cells is important here because this suggests that ASC is needed to cause the aggregation leading to decreased detection of protein. Additionally, the aggregation into an insoluble speck would be most simply explained by the formation of the duck NLRP3 inflammasome. Active duck CASP1 and duck IL-1β were not detected on the HEK293T cell Western blots when the components of the duck NLRP3 inflammasome were co-transfected together. I did not expect activation of duck CASP1 or duck IL-1β to occur in the

HEK293T cells. This absence of activation would indicate that these components do not spontaneously activate when they are co-expressed without the formation of a proper inflammasome. However, without further experiments, I cannot rule out that the cell lysis process and protein purification caused the aggregation of the duck NLRP3 inflammasome. Protein aggregation caused by the purification process or cell lysis process has been documented and could be a possible explanation (Papanayotou et al. 2010; Stathopulos et al. 2004). However, because the decrease in protein detection only occurred in the DF-1 cells and not the HEK293T cells, this suggests that the duck NLRP3 inflammasome components are activating and forming an insoluble speck.

The lack of detection of the activated forms of duck IL-1β and duck CASP1 does not necessarily mean that the duck NLRP3 inflammasome is not able to activate these proteins. Rather, this could be indicative of the Western blots not being sensitive enough to detect the activated proteins. Additionally, the presence of the epitope tags on duck CASP1 or duck IL-1β could be interfering with their activation. CASP1 has been epitope-tagged with a Myc tag and used in Western blots before (Keller et al. 2008). For IL-1β, the FLAG tag or HA tag is common (Mizushina et al. 2019; Niebler et al. 2013), however, most mammalian studies use a primary antibody against IL-1β and do not use an epitope tag (Park et al. 2018). Vojtech *et al.* (2012) has used the GST tag with zebrafish IL-1β and detected cleavage of zebrafish IL-1β on Western blots. However, I cannot rule out that the Myc epitope tag or the GST epitope tag could be interfering with the cleavage of duck CASP1 or duck IL-1β, respectively, in a manner that is unique to the duck proteins. This interference caused by the epitope tag would affect the detection of these two activated duck proteins on a Western blot. Further studies are needed to

confirm whether the duck NLRP3 inflammasome exhibits reduced activation or if other factors are interfering with the detection of the activated CASP1 and IL-1β proteins.

4.4 The duck NLRP3 inflammasome shows co-localization.

Transfections of the three recombinant duck NLRP3 inflammasome proteins that I created showed that these three proteins localized to different compartments of the DF-1 with a distinct morphology. Some speck-like structures were visible in the cytoplasm, but generally, when duck NLRP3-2xFLAG was transfected into DF-1 cells on its own, it was spread throughout the cytoplasm of the cell. Duck CASP1-Myc formed punctate structures in the cytoplasm of the cell. Duck IL-1β-GST was localized heavily to the nucleus of the cell. When I co-transfected my duck NLRP3 inflammasome recombinant proteins into DF-1 cells, I found that NLRP3-2xFLAG and CASP1-Myc were able to co-localize with each other with or without the presence of duck IL-1β-GST. Without IL-1β-GST, NLRP3 and CASP1 had an average Pearson's correlation coefficient of 0.69 and with IL-1β-GST the Pearson's correlation coefficient was 0.63, indicating that there was co-localization of NLRP3 and CASP1 in both conditions. Yu *et al.* (2006) observed a similar result; over-expression of NLRP3 in a human system led to NLRP3 clustering in speck-like structures which co-localized to ASC specks. They used a fluorescently tagged ASC and saw the localization of ASC in these specks. However, because I was unable to identify duck ASC, I could only see that duck NLRP3-2xFLAG and CASP1-Myc were co-localized together, suggesting the duck NLRP3 inflammasome had formed. IL-1β-GST was also co-localized to these specks in a few instances as well. However, the presence or absence of duck IL-1β-GST did not appear to alter whether duck NLRP3-

2xFLAG and duck CASP1-Myc co-localized in these specks, as suggested by how close the Pearson's colocalization coefficients were (0.69 without IL-1β-GST and 0.63 with IL-1β-GST). While I cannot confirm that ASC is also co-localized to the NLRP3 and CASP1 specks seen in the images, I am also not able to rule out that an analogous protein in the DF-1 cells is present in the specks in place of ASC. Identifying this analogous protein in the duck using co-immunoprecipitation of the NLPR3-ASC complex and then analysis of the protein sequence would be an interesting aspect of future research because many other inflammasomes, like AIM2 or IFI16, also require ASC (Bürckstümmer et al. 2009; Unterholzner et al. 2011).

Additionally, in the co-transfection of duck NLRP3-2xFLAG, duck CASP1, and duck IL-1β-GST, CASP1-Myc specks were visible in the nucleus of the cell. These CASP1-1-Myc specks co-localized with IL-1β -GST in the nucleus. However, duck NLRP3-2xFLAG was not visible as a part of these structures. This could suggest that a speck-like structure formed in the nucleus was nucleated by a different sensor protein. Previous studies have found that CASP1 can enter the nucleus and be a part of an inflammasome structure (Mao et al. 1998; Wang et al. 2016). As mentioned in the introduction, IFI16 is a PRR that recognizes DNA and is located in the nucleus (Unterholzner et al. 2011) which is capable of activating CASP1 through the formation of an inflammasome (Ansari et al. 2013; Kerur et al. 2011). Transfection of the duck NLRP3 inflammasome components into the DF-1 cells could have triggered IFI16 in this particular instance. There are still many other inflammasomes nucleated by other PRRs that have yet to be fully characterized in the duck which may be at work.

4.5 Future Directions

There is still much to characterize with the duck NLRP3 inflammasome. It is still not known what protein could be substituted in place of ASC in the duck NLRP3 inflammasome. Examination of what analogous protein could be taking the place of duck ASC through the use of co-immunoprecipitation and mass spectroscopy would also be very informative. Due to the fact the NLRP3 inflammasome can be activated by so many different stimuli, the priming step offers some specificity to the NLRP3 inflammasome (Bauernfeind et al. 2009). While I have observed a dampened transcriptional priming response to poly I:C through the TLR3 pathway, other TLR pathways may still function to prime the duck NLRP3 inflammasome. Li *et al.* (2019) found that the duck NLRP3 inflammasome had antibacterial effects in live animals infected with *E. coli*. Perhaps only the TLR3 transcriptional priming pathway has been dampened in the ducks and the TLR4 pathway would still be functional. Examination of the other TLR pathways with their respective agonists to assess whether the priming mechanism of the duck NLRP3 inflammasome is similar to the bat NLRP3 inflammasome priming mechanism that Ahn *et al.* (2019) established (i.e., transcriptional priming is dampened broadly across all pathways or if only specific pathways are dampened). Further investigation of the duck NLRP3 promoter is also needed, both to confirm the putative sequence that I have identified as well as to determine the functionality of the transcriptional binding sites. 5′-RACE could be used to confirm the sequence of the NLRP3 promoter. Reduction of transcriptional priming of the NLRP3 inflammasome could be a possible therapeutic target for addressing the hyper-inflammation and cytokine storms in susceptible hosts. Another interesting aspect that has yet to be investigated in ducks is the RIG-I inflammasome. RIG-I is important in the duck innate immune response against IAV (Barber et al. 2010) and whether a RIG-I inflammasome response contributes to the duck immune response to IAV has yet to be investigated.

4.6 Conclusions

In conclusion, I have helped show that the duck NLRP3 inflammasome differs from the inflammasome of other species like humans or mice. The duck NLRP3 inflammasome is different from known NLRP3 inflammasomes and appears to lack the traditional ASC found in the NLRP3 inflammasome of other species. More studies are needed to show what protein the duck NLRP3 inflammasome is using in place of ASC. In addition to this missing protein, the duck NLRP3 inflammasome also exhibits a dampened transcriptional priming response when treated with poly I:C, which would stimulate the TLR3 pathway. I did not observe upregulation of *NLRP3* or *IL1B* in DEFs treated with poly I:C or poly I:C followed by nigericin. Both *NLRP3* and *IL1B* are known to be transcriptionally upregulated as part of the priming response (Bauernfeind et al. 2009). This is in line with generally lower *IL1B* upregulation levels seen in ducks that are infected with a highly pathogenic influenza A virus compared to chickens (Burggraaf et al. 2014; Saito et al. 2018). Despite not seeing upregulation of *NLRP3* or *IL1B,* treatment with poly I:C does induce an immune response from DEFs, as seen in the upregulation of *IFIT5*. Additionally, the absence of an adequate priming response does not change the upregulation of the duck *NLRP3* and *IL1B* when treated with nigericin, an activating signal. Further studies are needed to understand the priming response using other TLR or PRR pathways to investigate how the duck NLRP3 inflammasome responds to different immune challenges. The duck NLRP3 promoter does not have a published sequence. I have identified a putative promoter that has an NF-κB binding site, but further experiments are needed to assess the validity of this sequence. Furthermore, the duck NLRP3 inflammasome does not appear to

activate duck IL-1β when overexpressed, unlike what has been observed in other species (Yu et al. 2006). Unfortunately, I cannot rule out other factors as reasons for why I am unable to detect activated IL-1β. Protein aggregation into an insoluble pellet that cannot be separated on a Western blot, or the epitope tag attached to duck IL-1β interfering with duck IL-1β activation would all prevent detection of duck IL-1β on Western blots. External factors interfering in the detection of duck IL-1β activation by the duck NLRP3 inflammasome is also supported by the co-localization of duck NLRP3 and duck CASP1. This co-localization of duck NLRP3 and duck CASP1 suggests that the duck NLRP3 inflammasome is capable of forming the oligomeric structure that inflammasomes are known for and could be functional. However, the formation of the NLRP3 inflammasome does not determine the strength of the NLRP3 inflammasome response. Determining the level of the duck NLRP3 inflammasome response will require additional research. Understanding how differences in the duck NLRP3 inflammasome could contribute to the natural resistance of the duck against IAV can be crucial in developing a therapeutic approach to limit damaging effects in susceptible hosts.

Works Cited

Ahn, M., Anderson, D.E., Zhang, Q., Tan, C.W., Lim, B.L., Luko, K., Wen, M., Chia, W.N., Mani, S., Wang, L.C., Ng, J.H.J., Sobota, R.M., Dutertre, C.-A., Ginhoux, F., Shi, Z.-L., Irving, A.T., Wang, L.-F., 2019. Dampened NLRP3-Mediated Inflammation in Bats and Implications for a Special Viral Reservoir Host. Nat. Microbiol. 4, 789–799. https://doi.org/10.1038/s41564-019-0371-3

Aliprantis, A.O., 1999. Cell Activation and Apoptosis by Bacterial Lipoproteins through Toll-Like Receptor-2. Science 285, 736–739. https://doi.org/10.1126/science.285.5428.736

Allen, I.C., Scull, M.A., Moore, C.B., Holl, E.K., McElvania-TeKippe, E., Taxman, D.J., Guthrie, E.H., Pickles, R.J., Ting, J.P.-Y., 2009. The NLRP3 Inflammasome Mediates in Vivo Innate Immunity to Influenza A Virus through Recognition of Viral RNA. Immunity 30, 556–565. https://doi.org/10.1016/j.immuni.2009.02.005

Amer, A., Franchi, L., Kanneganti, T.-D., Body-Malapel, M., Özören, N., Brady, G., Meshinchi, S., Jagirdar, R., Gewirtz, A., Akira, S., Núñez, G., 2006. Regulation of Legionella Phagosome Maturation and Infection through Flagellin and Host Ipaf. J. Biol. Chem. 281, 35217–35223. https://doi.org/10.1074/jbc.M604933200

Anderson, J., Mueller, J., Misaghi, A., Anderson, S., Sivagnanam, M., Kolodner, R., Hoffman, H., 2008. Initial Description of the Human NLRP3 Promoter. Genes Immun. 9, 721–726. https://doi.org/10.1038/gene.2008.66

Ansari, M.A., Singh, V.V., Dutta, S., Veettil, M.V., Dutta, D., Chikoti, L., Lu, J., Everly, D., Chandran, B., 2013. Constitutive Interferon-Inducible Protein 16-Inflammasome Activation during Epstein-Barr Virus Latency I, II, and III in B and Epithelial Cells. J. Virol. 87, 8606–8623. https://doi.org/10.1128/JVI.00805-13

Barber, M.R.W., Aldridge, J.R., Webster, R.G., Magor, K.E., 2010. Association of RIG-I with Innate Immunity of Ducks to Influenza. Proc. Natl. Acad. Sci. U. S. A. 107, 5913–5918. https://doi.org/10.1073/pnas.1001755107

Bauer, S., Kirschning, C.J., Häcker, H., Redecke, V., Hausmann, S., Akira, S., Wagner, H., Lipford, G.B., 2001. Human TLR9 Confers Responsiveness to Bacterial DNA via Species-Specific CpG Motif Recognition. Proc. Natl. Acad. Sci. 98, 9237–9242. https://doi.org/10.1073/pnas.161293498

Bauernfeind, F., Horvath, G., Stutz, A., Alnemri, E.S., MacDonald, K., Speert, D., Fernandes-Alnemri, T., Wu, J., Monks, B.G., Fitzgerald, K.A., Hornung, V., Latz, E., 2009. NF-kB Activating Pattern Recognition and Cytokine Receptors License NLRP3 Inflammasome Activation by Regulating NLRP3 Expression. J. Immunol. Baltim. Md 1950 183, 787–791. https://doi.org/10.4049/jimmunol.0901363

Bauernfried, S., Scherr, M.J., Pichlmair, A., Duderstadt, K.E., Hornung, V., 2021. Human NLRP1 Is a Sensor for Double-Stranded RNA. Science 371. https://doi.org/10.1126/science.abd0811

Bell, J.K., Mullen, G.E.D., Leifer, C.A., Mazzoni, A., Davies, D.R., Segal, D.M., 2003. Leucine-Rich Repeats and Pathogen Recognition in Toll-Like Receptors. Trends Immunol. 24, 528–533. https://doi.org/10.1016/S1471-4906(03)00242-4

Benedict, R.G., 1953. Antibiotics Produced by Actinomycetes. Bot. Rev. 19, 229. https://doi.org/10.1007/BF02861819

Bergsbaken, T., Fink, S.L., Cookson, B.T., 2009. Pyroptosis: Host Cell Death and Inflammation. Nat. Rev. Microbiol. 7, 99–109. https://doi.org/10.1038/nrmicro2070

Bi, J., Song, S., Fang, L., Wang, D., Jing, H., Gao, L., Cai, Y., Luo, R., Chen, H., Xiao, S., 2014. Porcine Reproductive and Respiratory Syndrome Virus Induces IL-1β Production Depending on

TLR4/MyD88 Pathway and NLRP3 Inflammasome in Primary Porcine Alveolar Macrophages. Mediators Inflamm. 2014, e403515. https://doi.org/10.1155/2014/403515

Boucher, D., Monteleone, M., Coll, R.C., Chen, K.W., Ross, C.M., Teo, J.L., Gomez, G.A., Holley, C.L., Bierschenk, D., Stacey, K.J., Yap, A.S., Bezbradica, J.S., Schroder, K., 2018. Caspase-1 Self-Cleavage Is an Intrinsic Mechanism to Terminate Inflammasome Activity. J. Exp. Med. 215, 827–840. https://doi.org/10.1084/jem.20172222

Boyd, A.C., Peroval, M.Y., Hammond, J.A., Prickett, M.D., Young, J.R., Smith, A.L., 2012. TLR15 Is Unique to Avian and Reptilian Lineages and Recognizes a Yeast-Derived Agonist. J. Immunol. 189, 4930–4938. https://doi.org/10.4049/jimmunol.1101790

Boyden, E.D., Dietrich, W.F., 2006. Nalp1b Controls Mouse Macrophage Susceptibility to Anthrax Lethal Toxin. Nat. Genet. 38, 240–244. https://doi.org/10.1038/ng1724

Boyle, J.P., Mayle, S., Parkhouse, R., Monie, T.P., 2013. Comparative Genomic and Sequence Analysis Provides Insight into the Molecular Functionality of NOD1 and NOD2. Front. Immunol. 4. https://doi.org/10.3389/fimmu.2013.00317

Brightbill, H.D., 1999. Host Defense Mechanisms Triggered by Microbial Lipoproteins through Toll-Like Receptors. Science 285, 732–736. https://doi.org/10.1126/science.285.5428.732

Bürckstümmer, T., Baumann, C., Blüml, S., Dixit, E., Dürnberger, G., Jahn, H., Planyavsky, M., Bilban, M., Colinge, J., Bennett, K.L., Superti-Furga, G., 2009. An Orthogonal Proteomic-Genomic Screen Identifies AIM2 as a Cytoplasmic DNA Sensor for the Inflammasome. Nat. Immunol. 10, 266–272. https://doi.org/10.1038/ni.1702

Burggraaf, S., Karpala, A.J., Bingham, J., Lowther, S., Selleck, P., Kimpton, W., Bean, A.G.D., 2014. H5N1 Infection Causes Rapid Mortality and High Cytokine Levels in Chickens Compared to Ducks. Virus Res. 185, 23–31. https://doi.org/10.1016/j.virusres.2014.03.012

Calisher, C.H., Childs, J.E., Field, H.E., Holmes, K.V., Schountz, T., 2006. Bats: Important Reservoir Hosts of Emerging Viruses. Clin. Microbiol. Rev. 19, 531–545. https://doi.org/10.1128/CMR.00017-06

Chamaillard, M., Hashimoto, M., Horie, Y., Masumoto, J., Qiu, S., Saab, L., Ogura, Y., Kawasaki, A., Fukase, K., Kusumoto, S., Valvano, M.A., Foster, S.J., Mak, T.W., Nuñez, G., Inohara, N., 2003. An Essential Role for NOD1 in Host Recognition of Bacterial Peptidoglycan Containing Diaminopimelic Acid. Nat. Immunol. 4, 702–707. https://doi.org/10.1038/ni945

Chavarría-Smith, J., Mitchell, P.S., Ho, A.M., Daugherty, M.D., Vance, R.E., 2016. Functional and Evolutionary Analyses Identify Proteolysis as a General Mechanism for NLRP1 Inflammasome Activation. PLOS Pathog. 12, e1006052. https://doi.org/10.1371/journal.ppat.1006052

Chavarría-Smith, J., Vance, R.E., 2013. Direct Proteolytic Cleavage of NLRP1B Is Necessary and Sufficient for Inflammasome Activation by Anthrax Lethal Factor. PLOS Pathog. 9, e1003452. https://doi.org/10.1371/journal.ppat.1003452

Chen, H., Ding, S., Tan, J., Yang, D., Zhang, Y., Liu, Q., 2020. Characterization of the Japanese Flounder NLRP3 Inflammasome in Restricting Edwardsiella Piscicida Colonization in Vivo. Fish Shellfish Immunol. 103, 169–180. https://doi.org/10.1016/j.fsi.2020.04.063

Chen, J., Chen, Z.J., 2018. PtdIns4P on Dispersed Trans-Golgi Network Mediates NLRP3 Inflammasome Activation. Nature 564, 71–76. https://doi.org/10.1038/s41586-018-0761-3

Chothe, S.K., Nissly, R.H., Lim, L., Bhushan, G., Bird, I., Radzio-Basu, J., Jayarao, B.M., Kuchipudi, S.V., 2020. NLRC5 Serves as a Pro-viral Factor During Influenza Virus Infection in Chicken Macrophages. Front. Cell. Infect. Microbiol. 10, 230. https://doi.org/10.3389/fcimb.2020.00230

Chotpitayasunondh, T., Ungchusak, K., Hanshaoworakul, W., Chunsuthiwat, S., Sawanpanyalert, P., Kijphati, R., Lochindarat, S., Srisan, P., Suwan, P., Osotthanakorn, Y., Anantasetagoon, T.,

Kanjanawasri, S., Tanupattarachai, S., Weerakul, J., Chaiwirattana, R., Maneerattanaporn, M., Poolsavatkitikool, R., Chokephaibulkit, K., Apisarnthanarak, A., Dowell, S.F., 2005. Human Disease from Influenza A (H5N1), Thailand, 2004. Emerg. Infect. Dis. 11, 201–209. https://doi.org/10.3201/eid1102.041061

Chousterman, B.G., Swirski, F.K., Weber, G.F., 2017. Cytokine Storm and Sepsis Disease Pathogenesis. Semin. Immunopathol. 39, 517–528. https://doi.org/10.1007/s00281-017-0639-8

Chui, A.J., Okondo, M.C., Rao, S.D., Gai, K., Griswold, A.R., Johnson, D.C., Ball, D.P., Taabazuing, C.Y., Orth, E.L., Vittimberga, B.A., Bachovchin, D.A., 2019. N-terminal Degradation Activates the NLRP1B Inflammasome. Science 364, 82–85. https://doi.org/10.1126/science.aau1208

Coates, B.M., Staricha, K.L., Koch, C.M., Cheng, Y., Shumaker, D.K., Budinger, G.R.S., Perlman, H., Misharin, A.V., Ridge, K.M., 2018. Inflammatory Monocytes Drive Influenza A Virus–Mediated Lung Injury in Juvenile Mice. J. Immunol. 200, 2391–2404. https://doi.org/10.4049/jimmunol.1701543

Cornelissen, J.B.W.J., Vervelde, L., Post, J., Rebel, J.M.J., 2013. Differences in Highly Pathogenic Avian Influenza Viral Pathogenesis and Associated Early Inflammatory Response in Chickens and Ducks. Avian Pathol. 42, 347–364. https://doi.org/10.1080/03079457.2013.807325

Coutinho-Silva, R., Parsons, M., Robson, T., Burnstock, G., 2001. Changes in Expression of P2 Receptors in Rat and Mouse Pancreas during Development and Ageing. Cell Tissue Res. 306, 373–383. https://doi.org/10.1007/s004410100458

de Jong, M.D., Simmons, C.P., Thanh, T.T., Hien, V.M., Smith, G.J.D., Chau, T.N.B., Hoang, D.M., Van Vinh Chau, N., Khanh, T.H., Dong, V.C., Qui, P.T., Van Cam, B., Ha, D.Q., Guan, Y., Peiris, J.S.M., Chinh, N.T., Hien, T.T., Farrar, J., 2006. Fatal outcome of human influenza A

(H5N1) Is Associated with High Viral Load and Hypercytokinemia. Nat. Med. 12, 1203–1207. https://doi.org/10.1038/nm1477

Fajgenbaum, D.C., June, C.H., 2020. Cytokine Storm. N. Engl. J. Med. 383, 2255–2273. https://doi.org/10.1056/NEJMra2026131

Finger, J.N., Lich, J.D., Dare, L.C., Cook, M.N., Brown, K.K., Duraiswami, C., Bertin, J.J., Gough, P.J., 2012. Autolytic Proteolysis within the Function to Find Domain (FIIND) Is Required for NLRP1 Inflammasome Activity. J. Biol. Chem. 287, 25030–25037. https://doi.org/10.1074/jbc.M112.378323

Fleming-Canepa, X., Aldridge, J.R., Canniff, L., Kobewka, M., Jax, E., Webster, R.G., Magor, K.E., 2019. Duck Innate Immune Responses to High and Low Pathogenicity H5 Avian Influenza Viruses. Vet. Microbiol. 228, 101–111. https://doi.org/10.1016/j.vetmic.2018.11.018

Franchi, L., Amer, A., Body-Malapel, M., Kanneganti, T.-D., Özören, N., Jagirdar, R., Inohara, N., Vandenabeele, P., Bertin, J., Coyle, A., Grant, E.P., Núñez, G., 2006. Cytosolic Flagellin Requires Ipaf for Activation of Caspase-1 and Interleukin 1β in Salmonella-Infected Macrophages. Nat. Immunol. 7, 576–582. https://doi.org/10.1038/ni1346

Franchi, L., Eigenbrod, T., Núñez, G., 2009a. Cutting Edge: TNF-α Mediates Sensitization to ATP and Silica via the NLRP3 Inflammasome in the Absence of Microbial Stimulation. J. Immunol. 183, 792–796. https://doi.org/10.4049/jimmunol.0900173

Franchi, L., Park, J.-H., Shaw, M.H., Marina-Garcia, N., Chen, G., Kim, Y.-G., Núñez, G., 2007. Intracellular NOD-Like Receptors in Innate Immunity, Infection and Disease. Cell. Microbiol. 0, 071018055442002-??? https://doi.org/10.1111/j.1462-5822.2007.01059.x

Franchi, L., Warner, N., Viani, K., Nuñez, G., 2009b. Function of Nod-like Receptors in Microbial Recognition and Host Defense. Immunol. Rev. 227, 106–128. https://doi.org/10.1111/j.1600-065X.2008.00734.x

Fu, S., Liu, H., Xu, L., Qiu, Y., Liu, Y., Wu, Z., Ye, C., Hou, Y., Hu, C.-A.A., 2018. Baicalin Modulates NF-κB and NLRP3 Inflammasome Signaling in Porcine Aortic Vascular Endothelial Cells Infected by Haemophilus Parasuis Causing Glässer's Disease. Sci. Rep. 8, 807. https://doi.org/10.1038/s41598-018-19293-2

Girardin, S.E., 2003. Nod1 Detects a Unique Muropeptide from Gram-Negative Bacterial Peptidoglycan. Science 300, 1584–1587. https://doi.org/10.1126/science.1084677

Girardin, S.E., Boneca, I.G., Viala, J., Chamaillard, M., Labigne, A., Thomas, G., Philpott, D.J., Sansonetti, P.J., 2003. Nod2 Is a General Sensor of Peptidoglycan through Muramyl Dipeptide (MDP) Detection. J. Biol. Chem. 278, 8869–8872. https://doi.org/10.1074/jbc.C200651200

Goh, G., Ahn, M., Zhu, F., Lee, L.B., Luo, D., Irving, A.T., Wang, L.-F., 2020. Complementary Regulation of Caspase-1 and IL-1β Reveals Additional Mechanisms of Dampened Inflammation in Bats. Proc. Natl. Acad. Sci. 117, 28939–28949. https://doi.org/10.1073/pnas.2003352117

Hayashi, F., Smith, K.D., Ozinsky, A., Hawn, T.R., Yi, E.C., Goodlett, D.R., Eng, J.K., Akira, S., Underhill, D.M., Aderem, A., 2001. The Innate Immune Response to Bacterial Flagellin Is Mediated by Toll-Like Receptor 5. Nature 410, 1099–1103. https://doi.org/10.1038/35074106

He, Z., Ma, Y., Wu, D., Feng, W., Xiao, J., 2021. Protective Effects of the NLRP3 Inflammasome against Infectious Bursal Disease Virus Replication in DF-1 Cells. Arch. Virol. 166, 1943–1950. https://doi.org/10.1007/s00705-021-05099-7

Heil, F., Hemmi, H., Hochrein, H., Ampenberger, F., Kirschning, C., Akira, S., Lipford, G., Wagner, H., Bauer, S., 2004. Species-Specific Recognition of Single-Stranded RNA via Toll-like Receptor 7 and 8. Science 303, 1526–1529. https://doi.org/10.1126/science.1093620

Hemmi, H., Kaisho, T., Takeuchi, O., Sato, S., Sanjo, H., Hoshino, K., Horiuchi, T., Tomizawa, H., Takeda, K., Akira, S., 2002. Small Anti-Viral Compounds Activate Immune cells via the TLR7 MyD88–Dependent Signaling Pathway. Nat. Immunol. 3, 196–200. https://doi.org/10.1038/ni758

Hornung, V., Ablasser, A., Charrel-Dennis, M., Bauernfeind, F., Horvath, G., Caffrey, D.R., Latz, E., Fitzgerald, K.A., 2009. AIM2 Recognizes Cytosolic dsDNA and Dorms a Caspase-1 Activating Inflammasome with ASC. Nature 458, 514–518. https://doi.org/10.1038/nature07725

Hornung, V., Ellegast, J., Kim, S., Brzózka, K., Jung, A., Kato, H., Poeck, H., Akira, S., Conzelmann, K.-K., Schlee, M., Endres, S., Hartmann, G., 2006. 5’-Triphosphate RNA Is the Ligand for RIG-I. Science 314, 994–997. https://doi.org/10.1126/science.1132505

Hoss, F., Mueller, J.L., Rojas Ringeling, F., Rodriguez-Alcazar, J.F., Brinkschulte, R., Seifert, G., Stahl, R., Broderick, L., Putnam, C.D., Kolodner, R.D., Canzar, S., Geyer, M., Hoffman, H.M., Latz, E., 2019. Alternative Splicing Regulates Stochastic NLRP3 Activity. Nat. Commun. 10, 3238. https://doi.org/10.1038/s41467-019-11076-1

Huang, Y., Li, Y., Burt, D.W., Chen, H., Zhang, Y., Qian, W., Kim, H., Gan, S., Zhao, Yiqiang, Li, J., Yi, K., Feng, H., Zhu, P., Li, B., Liu, Q., Fairley, S., Magor, K.E., Du, Z., Hu, X., Goodman, L., Tafer, H., Vignal, A., Lee, T., Kim, K.-W., Sheng, Z., An, Y., Searle, S., Herrero, J., Groenen, M.A.M., Crooijmans, R.P.M.A., Faraut, T., Cai, Q., Webster, R.G., Aldridge, J.R., Warren, W.C., Bartschat, S., Kehr, S., Marz, M., Stadler, P.F., Smith, J., Kraus, R.H.S., Zhao, Yaofeng, Ren, L., Fei, J., Morisson, M., Kaiser, P., Griffin, D.K., Rao, M., Pitel, F., Wang, J., Li, N., 2013.

The Duck Genome and Transcriptome Provide Insight into an Avian Influenza Virus Reservoir Species. Nat. Genet. 45, 776–783. https://doi.org/10.1038/ng.2657

Inoue, M., Shinohara, M.L., 2013. NLRP3 Inflammasome and MS/EAE. Autoimmune Dis. 2013. https://doi.org/10.1155/2013/859145

Jin, M.S., Kim, S.E., Heo, J.Y., Lee, M.E., Kim, H.M., Paik, S.-G., Lee, H., Lee, J.-O., 2007. Crystal Structure of the TLR1-TLR2 Heterodimer Induced by Binding of a Tri-Acylated Lipopeptide. Cell 130, 1071–1082. https://doi.org/10.1016/j.cell.2007.09.008

Jorgensen, I., Miao, E.A., 2015. Pyroptotic Dell Death Defends Against Intracellular Pathogens. Immunol. Rev. 265, 130–142. https://doi.org/10.1111/imr.12287

Juliana, C., Fernandes-Alnemri, T., Kang, S., Farias, A., Qin, F., Alnemri, E.S., 2012. Non-Transcriptional Priming and Deubiquitination Regulate NLRP3 Inflammasome Activation. J. Biol. Chem. 287, 36617–36622. https://doi.org/10.1074/jbc.M112.407130

Kang, J.Y., Nan, X., Jin, M.S., Youn, S.-J., Ryu, Y.H., Mah, S., Han, S.H., Lee, H., Paik, S.-G., Lee, J.-O., 2009. Recognition of Lipopeptide Patterns by Toll-like Receptor 2-Toll-like Receptor 6 Heterodimer. Immunity 31, 873–884. https://doi.org/10.1016/j.immuni.2009.09.018

Kankkunen, P., Teirilä, L., Rintahaka, J., Alenius, H., Wolff, H., Matikainen, S., 2010. (1,3)-β-Glucans Activate both Dectin-1 and NLRP3 Inflammasome in Human Macrophages. J. Immunol. 184, 6335–6342. https://doi.org/10.4049/jimmunol.0903019

Kanneganti, T.-D., Body-Malapel, M., Amer, A., Park, J.-H., Whitfield, J., Franchi, L., Taraporewala, Z.F., Miller, D., Patton, J.T., Inohara, N., Núñez, G., 2006. Critical Role for Cryopyrin/NALP3 in Activation of Caspase-1 in Response to Viral Infection and Double-Stranded RNA. J. Biol. Chem. 281, 36560–36568. https://doi.org/10.1074/jbc.M607594200

Karpala, A.J., Lowenthal, J.W., Bean, A.G., 2008. Activation of the TLR3 Pathway Regulates IFNβ Production in Chickens. Dev. Comp. Immunol. 32, 435–444. https://doi.org/10.1016/j.dci.2007.08.004

Karpala, A.J., Stewart, C., McKay, J., Lowenthal, J.W., Bean, A.G.D., 2011. Characterization of Chicken Mda5 Activity: Regulation of IFN-β in the Absence of RIG-I Functionality. J. Immunol. 186, 5397–5405. https://doi.org/10.4049/jimmunol.1003712

Katsnelson, M.A., Rucker, L.G., Russo, H.M., Dubyak, G.R., 2015. K+ Efflux Agonists Induce NLRP3 Inflammasome Activation Independently of Ca2+ Signaling. J. Immunol. Baltim. Md 1950 194, 3937–3952. https://doi.org/10.4049/jimmunol.1402658

Kawaguchi, M., Takahashi, M., Hata, T., Kashima, Y., Usui, F., Morimoto, H., Izawa, A., Takahashi, Y., Masumoto, J., Koyama, J., Hongo, M., Noda, T., Nakayama, J., Sagara, J., Taniguchi, S., Ikeda, U., 2011. Inflammasome Activation of Cardiac Fibroblasts Is Essential for Myocardial Ischemia/Reperfusion Injury. Circulation 123, 594–604. https://doi.org/10.1161/CIRCULATIONAHA.110.982777

Kawasaki, T., Kawai, T., 2014. Toll-Like Receptor Signaling Pathways. Front. Immunol. 0. https://doi.org/10.3389/fimmu.2014.00461

Keestra, A.M., Zoete, M.R. de, Bouwman, L.I., Putten, J.P.M. van, 2010. Chicken TLR21 Is an Innate CpG DNA Receptor Distinct from Mammalian TLR9. J. Immunol. 185, 460–467. https://doi.org/10.4049/jimmunol.0901921

Keller, M., Rüegg, A., Werner, S., Beer, H.-D., 2008. Active caspase-1 Is a Regulator of Unconventional Protein Secretion. Cell 132, 818–831. https://doi.org/10.1016/j.cell.2007.12.040

Kerur, N., Veettil, M.V., Sharma-Walia, N., Bottero, V., Sadagopan, S., Otageri, P., Chandran, B., 2011. IFI16 Acts as a nuclear Pathogen Sensor to Induce the Inflammasome in Response to Kaposi

Sarcoma Associated Herpesvirus Infection. Cell Host Microbe 9, 363–375. https://doi.org/10.1016/j.chom.2011.04.008

Kida, H., Yanagawa, R., Matsuoka, Y., 1980. Duck Influenza Lacking Evidence of Disease Signs and Immune Response. Infect. Immun. 30, 547–553.

Kim, H.M., Park, B.S., Kim, J.-I., Kim, S.E., Lee, J., Oh, S.C., Enkhbayar, P., Matsushima, N., Lee, H., Yoo, O.J., Lee, J.-O., 2007. Crystal Structure of the TLR4-MD-2 Complex with Bound Endotoxin Antagonist Eritoran. Cell 130, 906–917. https://doi.org/10.1016/j.cell.2007.08.002

Kim, J., Ahn, H., Woo, H.-M., Lee, E., Lee, G.-S., 2014. Characterization of Porcine NLRP3 Inflammasome Activation and its Upstream Mechanism. Vet. Res. Commun. 38, 193–200. https://doi.org/10.1007/s11259-014-9602-5

Kobasa, D., Jones, S.M., Shinya, K., Kash, J.C., Copps, J., Ebihara, H., Hatta, Y., Hyun Kim, J., Halfmann, P., Hatta, M., Feldmann, F., Alimonti, J.B., Fernando, L., Li, Y., Katze, M.G., Feldmann, H., Kawaoka, Y., 2007. Aberrant Innate Immune Response in Lethal Infection of Macaques with the 1918 Influenza Virus. Nature 445, 319–323. https://doi.org/10.1038/nature05495

Kobayashi, K.S., van den Elsen, P.J., 2012. NLRC5: a key regulator of MHC class I-dependent immune responses. Nat. Rev. Immunol. 12, 813–820. https://doi.org/10.1038/nri3339

Kofoed, E.M., Vance, R.E., 2011. Innate Immune Recognition of Bacterial ligands by NAIPs Dictates Inflammasome Specificity. Nature 477, 592–595. https://doi.org/10.1038/nature10394

Kortmann, J., Brubaker, S.W., Monack, D.M., 2015. Cutting Edge: Inflammasome Activation in Primary Human Macrophages Is Dependent on Flagellin. J. Immunol. Author Choice 195, 815–819. https://doi.org/10.4049/jimmunol.1403100

Kuchipudi, S.V., Tellabati, M., Sebastian, S., Londt, B.Z., Jansen, C., Vervelde, L., Brookes, S.M., Brown, I.H., Dunham, S.P., Chang, K.-C., 2014. Highly Pathogenic Avian Influenza Virus Infection in Chickens but not Ducks Is Associated with Elevated Host Immune and Pro-Inflammatory Responses. Vet. Res. 45, 118. https://doi.org/10.1186/s13567-014-0118-3

Lai, M., Yao, H., Shah, S.Z.A., Wu, W., Wang, D., Zhao, Y., Wang, L., Zhou, X., Zhao, D., Yang, L., 2018. The NLRP3-Caspase 1 Inflammasome Negatively Regulates Autophagy via TLR4-TRIF in Prion Peptide-Infected Microglia. Front. Aging Neurosci. 10, 116. https://doi.org/10.3389/fnagi.2018.00116

Leroy, E.M., Kumulungui, B., Pourrut, X., Rouquet, P., Hassanin, A., Yaba, P., Délicat, A., Paweska, J.T., Gonzalez, J.-P., Swanepoel, R., 2005. Fruit Bats as Reservoirs of Ebola Virus. Nature 438, 575–576. https://doi.org/10.1038/438575a

Li, H., Jin, H., Li, Y., Liu, D., Foda, M.F., Jiang, Y., Luo, R., 2017. Molecular Cloning and Functional Characterization of Duck Nucleotide-Binding Oligomerization Domain 1 (NOD1). Dev. Comp. Immunol. 74, 82–89. https://doi.org/10.1016/j.dci.2017.04.012

Li, J.-Y., Wang, Y.-Y., Shao, T., Fan, D.-D., Lin, A.-F., Xiang, L.-X., Shao, J.-Z., 2020. The Zebrafish NLRP3 Inflammasome Has Functional Roles in ASC-Dependent Interleukin-1β Maturation and Gasdermin E–Mediated Pyroptosis. J. Biol. Chem. 295, 1120–1141. https://doi.org/10.1074/jbc.RA119.011751

Li, R., Lin, J., Hou, X., Han, S., Weng, H., Xu, T., Li, N., Chai, T., Wei, L., 2018. Characterization and Roles of Cherry Valley Duck NLRP3 in Innate Immunity During Avian Pathogenic Escherichia Coli Infection. Front. Immunol. 9. https://doi.org/10.3389/fimmu.2018.02300

Li, W., Shi, Z., Yu, M., Ren, W., Smith, C., Epstein, J.H., Wang, H., Crameri, G., Hu, Z., Zhang, H., Zhang, J., McEachern, J., Field, H., Daszak, P., Eaton, B.T., Zhang, S., Wang, L.-F., 2005. Bats

Are Natural Reservoirs of SARS-Like Coronaviruses. Science 310, 676–679. https://doi.org/10.1126/science.1118391

Li, Y., Huang, Y., Cao, X., Yin, X., Jin, X., Liu, S., Jiang, J., Jiang, W., Xiao, T.S., Zhou, R., Cai, G., Hu, B., Jin, T., 2018. Functional and Structural Characterization of Zebrafish ASC. FEBS J. 285, 2691–2707. https://doi.org/10.1111/febs.14514

Lian, L., Ciraci, C., Chang, G., Hu, J., Lamont, S.J., 2012. NLRC5 Knockdown in Chicken Macrophages Alters Response to LPS and poly (I:C) Stimulation. BMC Vet. Res. 8, 23. https://doi.org/10.1186/1746-6148-8-23

Liao, K.-C., Mogridge, J., 2013. Activation of the NLRP1B Inflammasome by Reduction of Cytosolic ATP. Infect. Immun. 81, 570–579. https://doi.org/10.1128/IAI.01003-12

Lin, L., Xu, L., Lv, W., Han, L., Xiang, Y., Fu, L., Jin, M., Zhou, R., Chen, H., Zhang, A., 2019. An NLRP3 Inflammasome-Triggered Cytokine Storm Contributes to Streptococcal Toxic Shock-Like Syndrome (STSLS). PLOS Pathog. 15, e1007795. https://doi.org/10.1371/journal.ppat.1007795

Liniger, M., Summerfield, A., Zimmer, G., McCullough, K.C., Ruggli, N., 2012. Chicken Cells Sense Influenza A Virus Infection through MDA5 and CARDIF Signaling Involving LGP2. J. Virol. 86, 705–717. https://doi.org/10.1128/JVI.00742-11

Liu, L., Botos, I., Wang, Y., Leonard, J.N., Shiloach, J., Segal, D.M., Davies, D.R., 2008. Structural Basis of Toll-Like Receptor 3 Signaling with Double-Stranded RNA. Science 320, 379–381. https://doi.org/10.1126/science.1155406

Lu, A., Magupalli, V., Ruan, J., Yin, Q., Atianand, M.K., Vos, M., Schröder, G.F., Fitzgerald, K.A., Wu, H., Egelman, E.H., 2014. Unified Polymerization Mechanism for the Assembly of ASC-dependent Inflammasomes. Cell 156, 1193–1206. https://doi.org/10.1016/j.cell.2014.02.008

MacDonald, M.R.W., Veniamin, S.M., Guo, X., Xia, J., Moon, D.A., Magor, K.E., 2007. Genomics of Antiviral Defenses in the Duck, a Natural Host of Influenza and Hepatitis B Viruses. Cytogenet. Genome Res. 117, 195–206. https://doi.org/10.1159/000103180

Mao, P.-L., Jiang, Y., Wee, B.Y., Porter, A.G., 1998. Activation of Caspase-1 in the Nucleus Requires Nuclear Translocation of Pro-Caspase-1 Mediated by its Prodomain. J. Biol. Chem. 273, 23621–23624. https://doi.org/10.1074/jbc.273.37.23621

Mariathasan, S., Weiss, D.S., Newton, K., McBride, J., O'Rourke, K., Roose-Girma, M., Lee, W.P., Weinrauch, Y., Monack, D.M., Dixit, V.M., 2006. Cryopyrin Activates the Inflammasome in Response to Toxins and ATP. Nature 440, 228–232. https://doi.org/10.1038/nature04515

Martinon, F., Burns, K., Tschopp, J., 2002. The Inflammasome: A Molecular Platform Triggering Activation of Inflammatory Caspases and Processing of proIL-β. Mol. Cell 10, 417–426. https://doi.org/10.1016/S1097-2765(02)00599-3

Martinon, F., Pétrilli, V., Mayor, A., Tardivel, A., Tschopp, J., 2006. Gout-Associated Uric Acid Crystals Activate the NALP3 Inflammasome. Nature 440, 237–241. https://doi.org/10.1038/nature04516

Masters, S.L., Dunne, A., Subramanian, S.L., Hull, R.L., Tannahill, G.M., Sharp, F.A., Becker, C., Franchi, L., Yoshihara, E., Chen, Z., Mullooly, N., Mielke, L.A., Harris, J., Coll, R.C., Mills, K.H.G., Mok, K.H., Newsholme, P., Nuñez, G., Yodoi, J., Kahn, S.E., Lavelle, E.C., O'Neill, L.A.J., 2010. Activation of the Nlrp3 Inflammasome by Islet Amyloid Polypeptide Provides a Mechanism for Enhanced IL-1β in type 2 Diabetes. Nat. Immunol. 11, 897–904. https://doi.org/10.1038/ni.1935

Merkl, P.E., Knipe, D.M., 2019. Role for a Filamentous Nuclear Assembly of IFI16, DNA, and Host Factors in Restriction of Herpesviral Infection. mBio 10, e02621-18. https://doi.org/10.1128/mBio.02621-18

Mizushina, Y., Karasawa, T., Aizawa, K., Kimura, H., Watanabe, S., Kamata, R., Komada, T., Mato, N., Kasahara, T., Koyama, S., Bando, M., Hagiwara, K., Takahashi, M., 2019. Inflammasome-Independent and Atypical Processing of IL-1β Contributes to Acid Aspiration–Induced Acute Lung Injury. J. Immunol. 203, 236–246. https://doi.org/10.4049/jimmunol.1900168

Mogensen, T.H., 2009. Pathogen Recognition and Inflammatory Signaling in Innate Immune Defenses. Clin. Microbiol. Rev. 22, 240–273. https://doi.org/10.1128/CMR.00046-08

Moore, C.B., Bergstralh, D.T., Duncan, J.A., Lei, Y., Morrison, T.E., Zimmermann, A.G., Accavitti-Loper, M.A., Madden, V.J., Sun, L., Ye, Z., Lich, J.D., Heise, M.T., Chen, Z., Ting, J.P.-Y., 2008. NLRX1 Is a Regulator of Mitochondrial Antiviral Immunity. Nature 451, 573–577. https://doi.org/10.1038/nature06501

Muñoz-Planillo, R., Kuffa, P., Martínez-Colón, G., Smith, B.L., Rajendiran, T.M., Núñez, G., 2013. K+ Efflux Is the Common Trigger of NLRP3 Inflammasome Activation by Bacterial Toxins and Particulate Matter. Immunity 38, 1142–1153. https://doi.org/10.1016/j.immuni.2013.05.016

Muruve, D.A., Pétrilli, V., Zaiss, A.K., White, L.R., Clark, S.A., Ross, P.J., Parks, R.J., Tschopp, J., 2008. The Inflammasome Recognizes Cytosolic Microbial and Host DNA and Triggers an Innate Immune Response. Nature 452, 103–107. https://doi.org/10.1038/nature06664

Nakahira, K., Haspel, J.A., Rathinam, V.A., Lee, S.-J., Dolinay, T., Lam, H.C., Englert, J.A., Rabinovitch, M., Cernadas, M., Kim, H.P., Fitzgerald, K.A., Ryter, S.W., Choi, A.M., 2011. Autophagy Proteins Regulate Innate Immune Response by Inhibiting NALP3 Inflammasome-

Mediated Mitochondrial DNA Release. Nat. Immunol. 12, 222–230. https://doi.org/10.1038/ni.1980

Nakanishi, K., Yoshimoto, T., Tsutsui, H., Okamura, H., 2001. Interleukin-18 Regulates both Th1 and Th2 Responses. Annu. Rev. Immunol. 19, 423–474. https://doi.org/10.1146/annurev.immunol.19.1.423

Niebler, M., Qian, X., Höfler, D., Kogosov, V., Kaewprag, J., Kaufmann, A.M., Ly, R., Böhmer, G., Zawatzky, R., Rösl, F., Rincon-Orozco, B., 2013. Post-Translational Control of IL-1β via the Human Papillomavirus Type 16 E6 Oncoprotein: A Novel Mechanism of Innate Immune Escape Mediated by the E3-Ubiquitin Ligase E6-AP and p53. PLoS Pathog. 9, e1003536. https://doi.org/10.1371/journal.ppat.1003536

Okamura, H., Tsutsui, H., Komatsu, T., Yutsudo, M., Hakura, A., Tanimoto, T., Torigoe, K., Okura, T., Nukada, Y., Hattori, K., Akita, K., Namba, M., Tanabe, F., Konishi, K., Fukuda, S., Kurimoto, M., 1995. Cloning of a New Cytokine that Induces IFN-γ Production by T Cells. Nature 378, 88–91. https://doi.org/10.1038/378088a0

Onoguchi, K., Yoneyama, M., Fujita, T., 2011. Retinoic Acid-Inducible Gene-I-Like Receptors. J. Interferon Cytokine Res. 31, 27–31. https://doi.org/10.1089/jir.2010.0057

Pal, Aruna, Pal, Abantika, Baviskar, P., 2020. Molecular Characterization of RIGI, TLR7 and TLR3 as Immune Response Gene of Indigenous Ducks in Response to Avian Influenza. https://doi.org/10.1101/2020.09.28.316687

Papanayotou, I., Sun, B., Roth, A.F., Davis, N.G., 2010. Protein Aggregation Induced During Glass Bead lysis of Yeast. Yeast Chichester Engl. 27, 10.1002/yea.1771. https://doi.org/10.1002/yea.1771

Park, H.-S., Liu, G., Thulasi Raman, S.N., Landreth, S.L., Liu, Q., Zhou, Y., 2018. NS1 Protein of 2009 Pandemic Influenza a Virus Inhibits Porcine NLRP3 Inflammasome-Mediated Interleukin-1 Beta Production by Suppressing ASC Ubiquitination. J. Virol. 92. https://doi.org/10.1128/JVI.00022-18

Peiris, J., Hui, K.P., Yen, H.-L., 2010. Host Response to Influenza Virus: Protection Versus Immunopathology. Curr. Opin. Immunol. 22, 475–481. https://doi.org/10.1016/j.coi.2010.06.003

Pelegrin, P., Surprenant, A., 2006. Pannexin-1 Mediates Large Pore Formation and Interleukin-1β Release by the ATP-Gated P2X7 Receptor. EMBO J. 25, 5071–5082. https://doi.org/10.1038/sj.emboj.7601378

Perregaux, D., Gabel, C.A., 1994. Interleukin-1 Beta Maturation and Release in Response to ATP and Nigericin. Evidence that Potassium Depletion Mediated by These Agents Is a Necessary and Common Feature of Their Activity. J. Biol. Chem. 269, 15195–15203.

Perrone, L.A., Plowden, J.K., García-Sastre, A., Katz, J.M., Tumpey, T.M., 2008. H5N1 and 1918 Pandemic Influenza Virus Infection Results in Early and Excessive Infiltration of Macrophages and Neutrophils in the Lungs of Mice. PLoS Pathog. 4. https://doi.org/10.1371/journal.ppat.1000115

Pétrilli, V., Papin, S., Dostert, C., Mayor, A., Martinon, F., Tschopp, J., 2007. Activation of the NALP3 Inflammasome Is Triggered by Low Intracellular Potassium Concentration. Cell Death Differ. 14, 1583–1589. https://doi.org/10.1038/sj.cdd.4402195

Philbin, V.J., Iqbal, M., Boyd, Y., Goodchild, M.J., Beal, R.K., Bumstead, N., Young, J., Smith, A.L., 2005. Identification and Characterization of a Functional, Alternatively Spliced Toll-Like Receptor 7 (TLR7) and Genomic Disruption of TLR8 in Chickens. Immunology 114, 507–521. https://doi.org/10.1111/j.1365-2567.2005.02125.x

Poeck, H., Bscheider, M., Gross, O., Finger, K., Roth, S., Rebsamen, M., Hannesschläger, N., Schlee, M., Rothenfusser, S., Barchet, W., Kato, H., Akira, S., Inoue, S., Endres, S., Peschel, C., Hartmann, G., Hornung, V., Ruland, J., 2010. Recognition of RNA Virus by RIG-I Results in Activation of CARD9 and Inflammasome Signaling for Interleukin 1β Production. Nat. Immunol. 11, 63–69. https://doi.org/10.1038/ni.1824

Pothlichet, J., Meunier, I., Davis, B.K., Ting, J.P.-Y., Skamene, E., Messling, V. von, Vidal, S.M., 2013. Type I IFN Triggers RIG-I/TLR3/NLRP3-Dependent Inflammasome Activation in Influenza A Virus Infected Cells. PLOS Pathog. 9, e1003256. https://doi.org/10.1371/journal.ppat.1003256

Poyet, J.-L., Srinivasula, S.M., Tnani, M., Razmara, M., Fernandes-Alnemri, T., Alnemri, E.S., 2001. Identification of Ipaf, a Human Caspase-1-Activating Protein Related to Apaf-1. J. Biol. Chem. 276, 28309–28313. https://doi.org/10.1074/jbc.C100250200

Qu, Y., Misaghi, S., Newton, K., Gilmour, L.L., Louie, S., Cupp, J.E., Dubyak, G.R., Hackos, D., Dixit, V.M., 2011. Pannexin-1 Is Required for ATP Release during Apoptosis but not for Inflammasome Activation. J. Immunol. 186, 6553–6561. https://doi.org/10.4049/jimmunol.1100478

Rehwinkel, J., Gack, M.U., 2020. RIG-I-Like Receptors: Their Regulation and Roles in RNA Sensing. Nat. Rev. Immunol. 20, 537–551. https://doi.org/10.1038/s41577-020-0288-3

Ryan, G.B., Majno, G., 1977. Acute Onflammation. A review. Am. J. Pathol. 86, 183–276.

Saito, L.B., Diaz-Satizabal, L., Evseev, D., Fleming-Canepa, X., Mao, S., Webster, R.G., Magor, K.E.Y. 2018, 2018. IFN and Cytokine Responses in Ducks to Genetically Similar H5N1 Influenza A Viruses of Varying Pathogenicity. J. Gen. Virol. 99, 464–474. https://doi.org/10.1099/jgv.0.001015

Saito, T., Hirai, R., Loo, Y.-M., Owen, D., Johnson, C.L., Sinha, S.C., Akira, S., Fujita, T., Gale, M., 2007. Regulation of Innate Antiviral Defenses through a Shared Repressor Domain in RIG-I and LGP2. Proc. Natl. Acad. Sci. U. S. A. 104, 582–587. https://doi.org/10.1073/pnas.0606699104

Sandstrom, A., Mitchell, P.S., Goers, L., Mu, E.W., Lesser, C.F., Vance, R.E., 2019. Functional Degradation: A Mechanism of NLRP1 Inflammasome Activation by Diverse Pathogen Enzymes. Science 364. https://doi.org/10.1126/science.aau1330

Satoh, T., Kato, H., Kumagai, Y., Yoneyama, M., Sato, S., Matsushita, K., Tsujimura, T., Fujita, T., Akira, S., Takeuchi, O., 2010. LGP2 Is a Positive Regulator of RIG-I– and MDA5-Mediated Antiviral Responses. Proc. Natl. Acad. Sci. 107, 1512–1517. https://doi.org/10.1073/pnas.0912986107

Schaefer-Klein, J., Givol, I., Barsov, E.V., Whitcomb, J.M., VanBrocklin, M., Foster, D.N., Federspiel, M.J., Hughes, S.H., 1998. The EV-O-Derived Cell Line DF-1 Supports the Efficient Replication of Avian Leukosis-Sarcoma Viruses and Vectors. Virology 248, 305–311. https://doi.org/10.1006/viro.1998.9291

Schroder, K., Sagulenko, V., Zamoshnikova, A., Richards, A.A., Cridland, J.A., Irvine, K.M., Stacey, K.J., Sweet, M.J., 2012. Acute Lipopolysaccharide Priming Boosts Inflammasome Activation Independently of Inflammasome Sensor Induction. Immunobiology 217, 1325–1329. https://doi.org/10.1016/j.imbio.2012.07.020

Schroder, K., Zhou, R., Tschopp, J., 2010. The NLRP3 Inflammasome: A Sensor for Metabolic Danger? Science 327, 296–300. https://doi.org/10.1126/science.1184003

Seregin, S.S., Golovchenko, N., Schaf, B., Chen, J., Eaton, K.A., Chen, G.Y., 2017. NLRP6 Function in Inflammatory Monocytes Reduces Susceptibility to Chemically-Induced Intestinal Injury. Mucosal Immunol. 10, 434–445. https://doi.org/10.1038/mi.2016.55

Shim, D.-W., Lee, K.-H., 2018. Posttranslational Regulation of the NLR Family Pyrin Domain-Containing 3 Inflammasome. Front. Immunol. 9, 1054. https://doi.org/10.3389/fimmu.2018.01054

Singer, D.S., Devaiah, B.N., 2013. CIITA and Its Dual Roles in MHC Gene Transcription. Front. Immunol. 4. https://doi.org/10.3389/fimmu.2013.00476

Song, N., Liu, Z.-S., Xue, W., Bai, Z.-F., Wang, Q.-Y., Dai, J., Liu, X., Huang, Y.-J., Cai, H., Zhan, X.-Y., Han, Q.-Y., Wang, H., Chen, Y., Li, H.-Y., Li, A.-L., Zhang, X.-M., Zhou, T., Li, T., 2017. NLRP3 Phosphorylation Is an Essential Priming Event for Inflammasome Activation. Mol. Cell 68, 185-197.e6. https://doi.org/10.1016/j.molcel.2017.08.017

Spalinger, M.R., Kasper, S., Gottier, C., Lang, S., Atrott, K., Vavricka, S.R., Scharl, S., Gutte, P.M., Grütter, M.G., Beer, H.-D., Contassot, E., Chan, A.C., Dai, X., Rawlings, D.J., Mair, F., Becher, B., Falk, W., Fried, M., Rogler, G., Scharl, M., 2016. NLRP3 Tyrosine Phosphorylation Is Controlled by Protein Tyrosine Phosphatase PTPN22. J. Clin. Invest. 126, 1783–1800. https://doi.org/10.1172/JCI83669

Stathopulos, P.B., Scholz, G.A., Hwang, Y.-M., Rumfeldt, J.A.O., Lepock, J.R., Meiering, E.M., 2004. Sonication of Proteins Causes Formation of Aggregates that Resemble Amyloid. Protein Sci. Publ. Protein Soc. 13, 3017–3027. https://doi.org/10.1110/ps.04831804

Stutz, A., Kolbe, C.-C., Stahl, R., Horvath, G.L., Franklin, B.S., van Ray, O., Brinkschulte, R., Geyer, M., Meissner, F., Latz, E., 2017. NLRP3 Inflammasome Assembly Is Regulated by Phosphorylation of the Pyrin Domain. J. Exp. Med. 214, 1725–1736. https://doi.org/10.1084/jem.20160933

Subramanian, N., Natarajan, K., Clatworthy, M.R., Wang, Z., Germain, R.N., 2013. The Adaptor MAVS Promotes NLRP3 Mitochondrial Localization and Inflammasome Activation. Cell 153, 348–361. https://doi.org/10.1016/j.cell.2013.02.054

Surprenant, A., Rassendren, F., Kawashima, E., North, R.A., Buell, G., 1996. The Cytolytic P2Z Receptor for Extracellular ATP Identified as a P2X Receptor (P2X7). Science 272, 735–738. https://doi.org/10.1126/science.272.5262.735

Suzuki, S., Mimuro, H., Kim, M., Ogawa, M., Ashida, H., Toyotome, T., Franchi, L., Suzuki, M., Sanada, T., Suzuki, T., Tsutsui, H., Núñez, G., Sasakawa, C., 2014. Shigella IpaH7.8 E3 Ubiquitin Ligase Targets Glomulin and Activates Inflammasomes to Demolish Macrophages. Proc. Natl. Acad. Sci. 111, E4254–E4263. https://doi.org/10.1073/pnas.1324021111

Suzuki, T., Franchi, L., Toma, C., Ashida, H., Ogawa, M., Yoshikawa, Y., Mimuro, H., Inohara, N., Sasakawa, C., Nuñez, G., 2007. Differential Regulation of Caspase-1 Activation, Pyroptosis, and Autophagy via Ipaf and ASC in Shigella-Infected Macrophages. PLoS Pathog. 3. https://doi.org/10.1371/journal.ppat.0030111

Taubenberger, J.K., Kash, J.C., 2010. Influenza Virus Evolution, Host Adaptation and Pandemic Formation. Cell Host Microbe 7, 440–451. https://doi.org/10.1016/j.chom.2010.05.009

Thomas, P.G., Dash, P., Aldridge, J.R., Ellebedy, A.H., Reynolds, C., Funk, A.J., Martin, W.J., Lamkanfi, M., Webby, R.J., Boyd, K.L., Doherty, P.C., Kanneganti, T.-D., 2009. The Intracellular Sensor NLRP3 Mediates Key Innate and Healing Responses to Influenza A Virus via the Regulation of Caspase-1. Immunity 30, 566–575. https://doi.org/10.1016/j.immuni.2009.02.006

Thornberry, N.A., Bull, H.G., Calaycay, J.R., Chapman, K.T., Howard, A.D., Kostura, M.J., Miller, D.K., Molineaux, S.M., Weidner, J.R., Aunins, J., Elliston, K.O., Ayala, J.M., Casano, F.J.,

Chin, J., Ding, G.J.-F., Egger, L.A., Gaffney, E.P., Limjuco, G., Palyha, O.C., Raju, S.M., Rolando, A.M., Salley, J.P., Yamin, T.-T., Lee, T.D., Shively, J.E., MacCross, M., Mumford, R.A., Schmidt, J.A., Tocci, M.J., 1992. A Novel Heterodimeric Cysteine Protease Is Required for Interleukin-1βprocessing in Monocytes. Nature 356, 768–774. https://doi.org/10.1038/356768a0

Tisoncik, J.R., Korth, M.J., Simmons, C.P., Farrar, J., Martin, T.R., Katze, M.G., 2012. Into the Eye of the Cytokine Storm. Microbiol. Mol. Biol. Rev. MMBR 76, 16–32. https://doi.org/10.1128/MMBR.05015-11

To, K.K.W., Hung, I.F.N., Li, I.W.S., Lee, K.-L., Koo, C.-K., Yan, W.-W., Liu, R., Ho, K.-Y., Chu, K.-H., Watt, C.-L., Luk, W.-K., Lai, K.-Y., Chow, F.-L., Mok, T., Buckley, T., Chan, J.F.W., Wong, S.S.Y., Zheng, B., Chen, H., Lau, C.C.Y., Tse, H., Cheng, V.C.C., Chan, K.-H., Yuen, K.-Y., 2010. Delayed Clearance of Viral Load and Marked Cytokine Activation in Severe Cases of Pandemic H1N1 2009 Influenza Virus Infection. Clin. Infect. Dis. Off. Publ. Infect. Dis. Soc. Am. 50, 850–859. https://doi.org/10.1086/650581

Unterholzner, L., Keating, S.E., Baran, M., Horan, K.A., Jensen, S.B., Sharma, S., Sirois, C.M., Jin, T., Xiao, T., Fitzgerald, K.A., Paludan, S.R., Bowie, A.G., 2010. IFI16 Is an Innate Immune Sensor for Intracellular DNA. Nat. Immunol. 11, 997–1004. https://doi.org/10.1038/ni.1932

van den Brand, J.M.A., Verhagen, J.H., Veldhuis Kroeze, E.J.B., van de Bildt, M.W.G., Bodewes, R., Herfst, S., Richard, M., Lexmond, P., Bestebroer, T.M., Fouchier, R.A.M., Kuiken, T., 2018. Wild Ducks Excrete Highly Pathogenic Avian Influenza Virus H5N8 (2014–2015) Without Clinical or Pathological Evidence of Disease. Emerg. Microbes Infect. 7. https://doi.org/10.1038/s41426-018-0070-9

van der Veen, A.G., Maillard, P.V., Schmidt, J.M., Lee, S.A., Deddouche-Grass, S., Borg, A., Kjær, S., Snijders, A.P., Reis e Sousa, C., 2018. The RIG-I-Like Receptor LGP2 Inhibits Dicer-Dependent Processing of Long Double-Stranded RNA and Blocks RNA Interference in Mammalian Cells. EMBO J. 37, e97479. https://doi.org/10.15252/embj.201797479

Vanderven, H.A., Petkau, K., Ryan-Jean, K.E.E., Aldridge, J.R., Webster, R.G., Magor, K.E., 2012. Avian Influenza Rapidly Induces Antiviral Genes in Duck Lung and Intestine. Mol. Immunol. 51, 316–324. https://doi.org/10.1016/j.molimm.2012.03.034

Venkataraman, T., Valdes, M., Elsby, R., Kakuta, S., Caceres, G., Saijo, S., Iwakura, Y., Barber, G.N., 2007. Loss of DExD/H Box RNA Helicase LGP2 Manifests Disparate Antiviral Responses. J. Immunol. 178, 6444–6455. https://doi.org/10.4049/jimmunol.178.10.6444

Vojtech, L.N., Scharping, N., Woodson, J.C., Hansen, J.D., 2012. Roles of Inflammatory Caspases during Processing of Zebrafish Interleukin-1β in Francisella Noatunensis Infection. Infect. Immun. 80, 2878–2885. https://doi.org/10.1128/IAI.00543-12

Walev, I., Klein, J., Husmann, M., Valeva, A., Strauch, S., Wirtz, H., Weichel, O., Bhakdi, S., 2000. Potassium Regulates IL-1β Processing Via Calcium-Independent Phospholipase A2. J. Immunol. 164, 5120–5124. https://doi.org/10.4049/jimmunol.164.10.5120

Walev, I., Reske, K., Palmer, M., Valeva, A., Bhakdi, S., 1995. Potassium-Inhibited Processing of IL-1 Beta in Human Monocytes. EMBO J. 14, 1607–1614.

Wang, D., Weng, Y., Zhang, Y., Wang, R., Wang, T., Zhou, J., Shen, S., Wang, H., Wang, Y., 2020. Exposure to Hyperandrogen Drives Ovarian Dysfunction and Fibrosis by Activating the NLRP3 Inflammasome in Mice. Sci. Total Environ. 745, 141049. https://doi.org/10.1016/j.scitotenv.2020.141049

Wang, L., Fu, H., Nanayakkara, G., Li, Y., Shao, Y., Johnson, C., Cheng, J., Yang, W.Y., Yang, F., Lavallee, M., Xu, Y., Cheng, X., Xi, H., Yi, J., Yu, J., Choi, E.T., Wang, H., Yang, X., 2016. Novel Extracellular and Nuclear Caspase-1 and Inflammasomes Propagate Inflammation and Regulate Gene Expression: A Comprehensive Database Mining Study. J. Hematol. Oncol.J Hematol Oncol 9, 122. https://doi.org/10.1186/s13045-016-0351-5

Wang, X., Feuerstein, G.Z., Gu, J.L., Lysko, P.G., Yue, T.L., 1995. Interleukin-1 Beta Induces Expression of Adhesion Molecules in Human Vascular Smooth Muscle Cells and Enhances Adhesion of Leukocytes to Smooth Muscle Cells. Atherosclerosis 115, 89–98. https://doi.org/10.1016/0021-9150(94)05503-b

Wang, Y., Goossens, E., Eeckhaut, V., Pérez Calvo, E., Lopez-Ulibarri, R., Eising, I., Klausen, M., Debunne, N., De Spiegeleer, B., Ducatelle, R., Van Immerseel, F., 2021. Dietary Muramidase Degrades Bacterial Peptidoglycan to NOD-Activating Muramyl Dipeptides and Reduces Duodenal Inflammation in Broiler Chickens. Br. J. Nutr. 126, 641–651. https://doi.org/10.1017/S0007114520004493

Webster, R.G., Bean, W.J., Gorman, O.T., Chambers, T.M., Kawaoka, Y., 1992. Evolution and Ecology of Influenza A viruses. Microbiol. Rev. 56, 152–179.

Wei, Z., Nie, G., Yang, F., Pi, S., Wang, C., Cao, H., Guo, X., Liu, P., Li, G., Hu, G., Zhang, C., 2021. Inhibition of ROS/NLRP3/Caspase-1 Mediated Pyroptosis Attenuates Cadmium-Induced Apoptosis in Duck Renal Tubular Epithelial Cells. Environ. Pollut. 273, 115919. https://doi.org/10.1016/j.envpol.2020.115919

Wickliffe, K.E., Leppla, S.H., Moayeri, M., 2008. Killing of Macrophages by Anthrax Lethal Toxin: Involvement of the N-end rule pathway. Cell. Microbiol. 10, 1352–1362. https://doi.org/10.1111/j.1462-5822.2008.01131.x

Xiao, Y., Reeves, M.B., Caulfield, A.F., Evseev, D., Magor, K.E., 2018. The Core Promoter Controls Basal and Inducible Expression of Duck Retinoic Acid Inducible Gene-I (RIG-I). Mol. Immunol. 103, 156–165. https://doi.org/10.1016/j.molimm.2018.09.002

Yang, C., Bolotin, E., Jiang, T., Sladek, F.M., Martinez, E., 2007. Prevalence of the Initiator over the TATA Box in Human and Yeast Genes and Identification of DNA Motifs Enriched in Human TATA-Less Core Promoters. Gene 389, 52–65. https://doi.org/10.1016/j.gene.2006.09.029

Yang, J., Zhao, Y., Shi, J., Shao, F., 2013. Human NAIP and Mouse NAIP1 Recognize Bacterial Type III Secretion Needle Protein for Inflammasome Activation. Proc. Natl. Acad. Sci. U. S. A. 110, 14408–14413. https://doi.org/10.1073/pnas.1306376110

Ye, J., Yu, M., Zhang, K., Liu, J., Wang, Q., Tao, P., Jia, K., Liao, M., Ning, Z., 2015. Tissue-Specific Expression Pattern and Histological Distribution of NLRP3 in Chinese Yellow Chicken. Vet. Res. Commun. 39, 171–177. https://doi.org/10.1007/s11259-015-9641-6

Yu, J.-W., Wu, J., Zhang, Z., Datta, P., Ibrahimi, I., Taniguchi, S., Sagara, J., Fernandes-Alnemri, T., Alnemri, E.S., 2006a. Cryopyrin and Pyrin Activate Caspase-1, but not NF-kappaB, via ASC Oligomerization. Cell Death Differ. 13, 236–249. https://doi.org/10.1038/sj.cdd.4401734

Yu, J.-W., Wu, J., Zhang, Z., Datta, P., Ibrahimi, I., Taniguchi, S., Sagara, J., Fernandes-Alnemri, T., Alnemri, E.S., 2006b. Cryopyrin and Pyrin Activate Caspase-1, but not NF- κ B, via ASC Oligomerization. Cell Death Differ. 13, 236–249. https://doi.org/10.1038/sj.cdd.4401734

Yu, S., Mao, H., Jin, M., Lin, X., 2020. Transcriptomic Analysis of the Chicken MDA5 Response Genes. Genes 11, 308. https://doi.org/10.3390/genes11030308

Yuen, K., Chan, P., Peiris, M., Tsang, D., Que, T., Shortridge, K., Cheung, P., To, W., Ho, E., Sung, R., Cheng, A., 1998. Clinical Features and Rapid Viral Diagnosis of Human Disease Associated

with Avian Influenza A H5N1 virus. The Lancet 351, 467–471. https://doi.org/10.1016/S0140-6736(98)01182-9

Zhang, B., Liu, X., Chen, W., Chen, L., 2013. IFIT5 Potentiates Anti-Viral Response through Enhancing Innate Immune Signaling Pathways. Acta Biochim. Biophys. Sin. 45, 867–874. https://doi.org/10.1093/abbs/gmt088

Zhang, M., Song, K., Li, C., Chen, Z., Ding, C., Liu, G., 2015. Molecular Cloning of Peking Duck Toll-Like Receptor 3 (duTLR3) Gene and Its Responses to Reovirus Infection. Virol. J. 12, 207. https://doi.org/10.1186/s12985-015-0434-x

Zhao, Y., Yang, J., Shi, J., Gong, Y.-N., Lu, Q., Xu, H., Liu, L., Shao, F., 2011. The NLRC4 Inflammasome Receptors for Bacterial Flagellin and Type III Secretion Apparatus. Nature 477, 596–600. https://doi.org/10.1038/nature10510

Zheng, W., Satta, Y., 2018. Functional Evolution of Avian RIG-I-Like Receptors. Genes 9. https://doi.org/10.3390/genes9090456

Zhong, Y., Kinio, A., Saleh, M., 2013. Functions of NOD-Like Receptors in Human Diseases. Front. Immunol. 0. https://doi.org/10.3389/fimmu.2013.00333

Zhong, Z., Liang, S., Sanchez-Lopez, E., He, F., Shalapour, S., Lin, X., Wong, J., Ding, S., Seki, E., Schnabl, B., Hevener, A.L., Greenberg, H.B., Kisseleva, T., Karin, M., 2018. New Mitochondrial DNA Synthesis Enables NLRP3 Inflammasome Activation. Nature 560, 198–203. https://doi.org/10.1038/s41586-018-0372-z

Zhong, Z., Umemura, A., Sanchez-Lopez, E., Liang, S., Shalapour, S., Wong, J., He, F., Boassa, D., Perkins, G., Ali, S.R., McGeough, M.G., Ellisman, M.H., Seki, E., Gustafsson, A.B., Hoffman, H.M., Diaz-Meco, M.T., Moscat, J., Karin, M., 2016. NF-κB Restricts Inflammasome Activation

Via Elimination of Damaged Mitochondria. Cell 164, 896–910. https://doi.org/10.1016/j.cell.2015.12.057

Zhong, Z., Zhai, Y., Liang, S., Mori, Y., Han, R., Sutterwala, F.S., Qiao, L., 2013. TRPM2 Links Oxidative Stress to the NLRP3 Inflammasome Activation. Nat. Commun. 4, 1611. https://doi.org/10.1038/ncomms2608

Zhou, B., Abbott, D.W., 2021. Gasdermin E Permits Interleukin-1 Beta Release in Distinct Sublytic and Pyroptotic Phases. Cell Rep. 35, 108998. https://doi.org/10.1016/j.celrep.2021.108998

Zhu, Q., Kannegant, T.-D., 2017. Distinct Regulatory Mechanisms Control Proinflammatory Cytokines IL-18 and IL-1β. J. Immunol. Baltim. Md 1950 198, 4210–4215. https://doi.org/10.4049/jimmunol.1700352

Zou, Y.-J., Xu, J.-J., Wang, X., Zhu, Y.-H., Wu, Q., Wang, J.-F., 2020. Lactobacillus johnsonii L531 Ameliorates Escherichia Coli-Induced Cell Damage via Inhibiting NLRP3 Inflammasome Activity and Promoting ATG5/ATG16L1-Mediated Autophagy in Porcine Mammary Epithelial Cells. Vet. Sci. 7, 112. https://doi.org/10.3390/vetsci7030112